Detection and inactivation of human norovirus on frozen berries – an approach to reduce health risks for consumers

Inaugural-Dissertation to obtain the academic degree

Doctor rerum naturalium (Dr. rer. nat.)

submitted to the Department of Biology, Chemistry and Pharmacy

of Freie Universität Berlin

by

Christina Bartsch (M.Sc.)

from Aachen

year of submission

2018

Working period: 01.04.2015 - 31.03.2018

This thesis was conducted at the Federal Institute for Risk Assessment under the direction of Prof. Dr. Reimar Johne.

First reviewer:

Prof. Dr. Reimar Johne
Federal Institute for Risk Assessment
Department 4 “Biological Safety”
Diedersdorfer Weg 1
12277 Berlin

Second reviewer:

Prof. Dr. Rupert Mutzel
Freie Universität Berlin
Institute for Biology (Microbiology)
Königin-Luise-Str. 12-16
14195 Berlin

Disputation on: 17.10.2018

Bundesinstitut für Risikobewertung

TABLE OF CONTENT

List of abbreviations

AGE	Acute gastroenteritis
BfR	Bundesinstitut für Risikobewertung; engl.: Federal Institute for Risk Assessment
BHQ	Probe labelled black hole quencher
°C	Degrees in Celsius
cDNA	Complementary deoxyribonucleic acid
conc	concentration
DMEM	Dulbecco's modifies eagle's medium
dPCR	Digital polymerase chain reaction
E.coli	Escherichia coli
EDC	1-Ethyl-3-(3-dimethylaminopropyl)carbodiimide)
Et al.	Latin: et alli (and others)
FAM	Probe labelled 5' 6-carboxyfluorescein
fCV	Feline Calicivirus
Fig.	Figure
FRET	Fluorescence resonance energy transfer
fw	Forward
x g	Centrifugal force
GI	Genogroup 1
GII	Genogroup 2
h	Hour
HAV	Hepatits A virus
HBGA	Histo blood group antigen
HBV	Hepatitis B virus
HCl	Hypochloric acid
HIV	Human immunodeficiency virus
hNV	Human norovirus
IFREMER	Institut français de recherche pour l'exploitation de la mer; engl.: French Scientific Institute for Ocean Usage
ISO	ISO/TS 15216-2
kg	Kilogramm
MEM	Minimum essential medium

MGB-NFQ	Probe labelled minor groove binder/non-fluorescent quencher
min	Minute
mNV	Murine norovirus
mL	Milliliter
NaCl	Sodium cloride
NaOH	Sodium hydroxide
NCBI	Nation Center for Biotechnology Information
NGS	Next generation sequencing
ORF	Open reading frame
PA	Plaque Assay
PBS	Phosphate-buffered saline
PEG	Polyethylene glycol
PES	Polyethersulfone
PFU	Plaque froming units
PGM	Porcine gastric mucine
pH	Negative decadic logarithm of hydrogen concentration
rev	Reverse
RKI	Robert Koch Institute
RNA	Ribonucleic acid
RNase	Ribonuclease
rpm	Revolutions per minute
RR	Recovery rates
RT	Room temperature or reverse transcription
RT-qPCR	Quantitative reverse transcription polymerase chain reaction
sec	Second
ss	Single stranded (RNA)
Tab.	table
TAMRA	Probe labelled 3’ 6-carboxy-tetramethylrhodamine
TGBE	Tris glycin beef extract
TV	Tulane virus
µM	Micromolar
µL	Microliter
USA	United States of America

List of figures

List of tables

1. Summary

Foodborne diseases induced by viruses involving plant-derived food such as berries are increasingly recognized as threat for public health. For example, a large human norovirus (hNV) gastroenteritis outbreak involving >10,000 diseased people occurred in Germany in 2012, which was traced back to contaminated frozen strawberries. To increase food safety for consumers, three areas were identified, which should be addressed in this thesis.

First, different previously described virus extraction methods in combination with quantitative real time PCR (RT-qPCR) were compared using frozen strawberries artificially contaminated with hNV and the recovery rates (RRs) were calculated. Out of five published protocols, the method according to ISO/TS15216-2 revealed the best RRs. Further improvement of RRs from 2.83±2.92% to 15.28±9.73% was achieved by an additional RNA purification using Sephacryl®-based columns. The optimized protocol showed significantly better hNV detection rates by testing of berries originally involved in gastroenteritis outbreaks in 2012 and 2016.

Second, novel methods for virus quantification and broad pathogen identification were tested on strawberries from the outbreak in 2012: Digital PCR (dPCR) and Next Generation Sequencing (NGS). A quantification of the hNV genomes using RT-dPCR confirmed a very low mean virus amount in the berries (185 RNA copies/25g), which was similar to the independently assessed RT-qPCR result (257 RNA copies/25g). By NGS, about 29 mio sequence reads were generated and analyzed by RIEMS 4.0 software. They mainly showed homologies to sequences from the plant matrix and from the bacterial flora. The most abundant virus sequences originated from plant-specific viruses. Two virus reads showed homologies to hNV identical to those derived from gastroenteritis patients and a strawberry sample obtained during the outbreak.

Third, the thermal inactivation kinetics of hNV in strawberry puree was assessed. Due to the lack of a reliable system for hNV infectivity assessment, capsid integrity assays using RNase treatment prior to detection of protected viral RNA were applied. In addition, murine norovirus (mNV) and Tulane virus (TV) served as surrogates and were analyzed by plaque assay and RT-qPCR. Infectious mNV and TV were completely inactivated (>7 $\log_{10}$ reductions) after treatment at 80°C for 8 sec. However, in comparison to hNV, TV showed a markedly lower stability in capsid integrity assays. A

predictive model generated from the data, which covers reduction of hNV capsid-protected RNA between 50-80°C, suggests that temperatures under 70°C are not reliable for inactivation. About 3.5 $\log_{10}$ reductions are achieved by heating at 80°C for 8 sec.

In conclusion, methods for detection, identification and characterization of hNV in berries could be improved. The generated heat inactivation model may help developing efficient heat treatment strategies to prevent hNV infection due to consumption of berries in the future.

2. Zusammenfassung

Mit Viren verunreinigte Lebensmittel stellen eine Gefahr für Verbraucher dar. Bei einem Gastroenteritis-Ausbruch in Deutschland (2012), der durch mit humanem Norovirus (hNV) kontaminierte Tiefkühl-(TK)Erdbeeren verursacht wurde, erkrankten >10.000 Personen. Zur Erhöhung der Lebensmittelsicherheit wurden drei Problemfelder identifiziert und bearbeitet.

Zuerst wurden publizierte Methoden zur Virusdetektion verglichen und optimiert. Dafür wurden verschiedene Virusextraktionsmethoden in Kombination mit quantitativer real time PCR (RT-qPCR) unter Verwendung von artifiziell mit hNV kontaminierten TK-Erdbeeren durch die Berechnung der Wiederfindungsraten (WFR) evaluiert. Von fünf Protokollen wies die ISO-Methode (ISO/TS15216-2) die höchsten WFR auf. Eine WFR-Verbesserung von 2,83±2,92% auf 15,28±9,73% wurde durch eine zusätzliche RNA-Reinigung mit Sephacryl®-Säulen erzielt. Durch das optimierte Protokoll wurde bei Untersuchungen von Ausbruchsmaterial aus 2012 und 2016 signifikant höhere Detektionsraten erreicht.

Anschließend wurden neue Methoden zur Virusquantifizierung und -identifizierung mit Ausbruchsbeeren (2012) getestet: Digitale PCR (dPCR) und Next Generation Sequencing (NGS). Die Quantifizierung der hNV-Genome mittels dPCR ergab eine geringe Menge auf den Beeren (185 RNA-Kopien/25g), die dem RT-qPCR-Ergebnis ähnelte (257 RNA-Kopien/25g). Mittels NGS wurden ca. 29 Mio. Sequenz-Reads generiert und durch RIEMS 4.0 Software analysiert, die hauptsächlich pflanzlichen und bakteriellen Ursprungs waren. Am häufigsten wurden Virus-Sequenzen mit Homologie zu Pflanzen-Viren gefunden. Zwei hNV-Reads wurden detektiert, die identisch mit solchen aus Gastroenteritis-Patienten und Erdbeeren aus dem Ausbruch waren.

Zuletzt wurde die thermale Inaktivierungskinetik von hNV in Erdbeerpüree evaluiert. Aufgrund des Mangels an Infektiositäts-Assays für hNV wurde ein Kapsid-Stabilitäts-Assay (KSA) durch die Zugabe von RNase vor der RNA-Detektion durchgeführt, sodass nur noch RNAs aus intakten Viruspartikeln nachgewiesen wurden. Muriner Norovirus (mNV) und Tulane Virus (TV) als Surrogate verwendet, die mittels Plaque Assay und RT-qPCR untersucht wurden. Infektiöser mNV und TV wurden bei der

Behandlung bei 80°C/ 8 Sek. vollständig inaktiviert (>7 log_{10} Reduktion). Im Vergleich zu hNV zeigte TV eine geringere Stabilität beim KSA. Diese Hitze-Inaktivierungsdaten wurden zur Generierung eines tertiären Vorhersagemodels verwendet, das sich auf die Abnahme von Kapsid-geschützter hNV-RNA (50-80°C) bezieht und indiziert, dass Temperaturen <70°C nicht für eine schnelle hNV-Inaktivierung geeignet sind. Eine Reduzierung von 3,5 log_{10} Stufen hNV wurde durch Erhitzen bei 80°C/8 Sek. erreicht.

Generell konnten Methoden zur Detektion, Identifikation und Charakterisierung von hNV auf Beeren verbessert werden. Das generierte Hitze-Inaktivierungsmodell könnte zukünftig zur Entwicklung von Hitze-Behandlungsstrategien und der Verhinderung von hNV-Infektionen durch Beerenkonsum beitragen.

3. Introduction

3.1. Foodborne outbreaks

Foodborne diseases induced by viral pathogens are increasingly recognized as threat for public health. Particularly, many outbreaks involving plant-derived food such as berries and lettuce or ready-to-eat meals contaminated with hNV or HAV have been described recently (Mäde et al. 2013; Coudray-Meunier et al., 2015). For example, a large hNV gastroenteritis outbreak involving more than 10,000 diseased people occurred in Germany in 2012, which could be traced to contaminated frozen strawberries (Mäde et al. 2013). In Europe and the USA, frozen berries are often processed in yoghurt desserts in canteen kitchens were many people eat every day. Because a high amount of product is needed, the berries are packed in big units up to 10 kilograms hampering the detection of possible contaminants by prior laboratory tests (Mäde et al. 2013). Moreover, hNV outbreaks induced by contaminated frozen raspberries and blackberries (tab.1) were recorded in central school kitchens in Finland in 2009 (Sarvikivi et al. 2012) and in a canteen of a large company in Germany in 2005 (Fell et al. 2007). Also, HAV outbreaks (tabl.1) with severe liver infections caused by imported frozen mixed berries, berry mix cake and pomegranate arils were recognized in Italy, Norway and the USA between 2013 and 2014 (Chiapponi et al., 2014; Guzman-Herrador et al., 2014; Collier et al., 2015).

Table 1: HAV and hNV outbreaks associated with frozen fruits between 2005 and 2014. We listed generic gastroenteritis (hNV) and HAV outbreak worldwide from the last decade. In some cases, HAV-positive patients did not have severe symptoms. In other cases, patients were suffering from fulminant hepatitis.

Reference	Outbreak (year)	Country	Virus	Food	Patients (number)
Fell et al.	2005	Germany	hNV	frozen raspberries	241
Sarvikivi et al.	2009	Finland	hNV	frozen blackberries	>900
Mäde et al.	2012	Germany	hNV	frozen strawberries	>10,000
Collier et al.	2013	USA	HAV	Frozen pomegranate arils	165
Chiapponi et al.	2013 - 2014	Italy	HAV	frozen mixed berries	1803
Guzman-Herrador et al.	2013 - 2014	Norway	HAV	berry mix cake	19

Usually, berries are harvested manually because some berries (e.g. raspberries) are too delicate for mechanical harvesting and washing. Contamination of berries with viruses can accrue at several stages of their production as summarized in fig.1.

A risk for food contamination represent infected (symptomatic as well as asymptomatic) food handlers who shed the virus and can potentially contaminate the fruits without having any symptoms (Barrabeig et al., 2010). Frozen fruits have a lower profit margin than fresh fruits and are more frequently involved in foodborne outbreaks. To ensure customer protection, the diligent compliance of official hygienic standards, e.g. hand washing/sterilization, is essential during food production or packaging process (Codex Alimentarius, 2012). Unfortunately, in many cases contaminated foods are imported from countries with lower hygienic standards and food control mechanisms. Also, the heating regulations in commercial kitchens concerning the usage of frozen fruits in meals are still not elaborated enough and need to be optimized based on scientific analyses. Therefore, the Federal Institute for Risk Assessment (BfR), recommends heating frozen berries to a core temperature of 90°C to completely inactivated possible contaminants (BfR, 2013a). These recommendations especially apply to so-called high-risk groups such as children, elderly and pregnant women who can suffer from a severe course of disease occasionally leading to death (Murata et al., 2007).

virus contamination by

during		
growing	▪ waste water in fertilizers/ irrigation water ▪ human feces on/near fields (absence of sanitary facilities for harvesters)	
manual harvest automated washing	▪ ill harvesters or food handlers (also asymptomatic) ▪ pathogen distribution by washing water	
packaging freezing	▪ ill food handlers (also asymptomatic) ▪ cross-contamination in mixing centers by other compromised batches or devices	
cooking	▪ ill food handlers (also asymptomatic) ▪ cross-contamination by compromised devices	

Figure 1: Potential sources of virus contamination in the strawberry supply chain.

3.2. History

In 1929, hNV-induced gastroenteritis was first recognized by the pediatrician Dr. John Zahorsky, who described it as 'Hyperemesis hiemis or winter vomiting disease' in infants (Zahorsky et al., 1929). However, the aetiological agent was not known until 1972. Then, the disease was linked to the presence of a small non-enveloped icosahedral virus in fecal samples from a gastroenteritis outbreak in an elementary school in Norwalk, Ohio, USA in 1968 (Dolin et al., 1972). Dolin described this virus as *Norwalk virus* and characterized it morphologically by immune electron microscopy. He also found a connection between the virus and the gastroenteritis outbreak during a volunteer study. Briefly, acute infectious non-bacterial gastroenteritis was induced in adult volunteers at the Maryland State House of Correction after ingestion of three serial passages of bacteria-free stool filtrates. Consequently, Dolin concluded that a replicating agent of sub-bacterial size may be responsible for the observed disease. The biophysical properties of the agent were also assayed in other volunteer studies. They matched those of a small virus, most closely related to the parvovirus group among known animal viruses. The acid stable agent appeared to have a diameter less than 36 nm and to lack a lipid-containing envelope. The agent was stable to heating at 60°C for 30 min, appeared to be relatively host-specific for humans and provided them with at least short-term immunity.

Many years after hNV discovery, its importance as enteric pathogen was still underestimated because of inadequate diagnostic tools (Koo et al., 2010). Advances in the understanding of molecular biology and the development of novel diagnostic tools have contributed to the recognition of hNV as one of the most important causes of acute gastroenteritis (AGE) in community settings (de Wit et al., 2001; Phillips et al., 2010) and in foodborne outbreaks worldwide (Atmar et al., 2006).

3.3. Classification and taxonomy

HNVs are members of the *Caliciviridae* family, which derives its name from the Greek word for cup (calyx), referring to cup-like depressions on the surface of the virus particle (Glass et al. 2009). The *Caliciviridae* family contains six genera (norovirus, vesivirus, lagovirus, recovirus, sapovirus, and becovirus) whereof the hNV species is the most common cause of disease in humans. These viruses were previously referred to by other names, such as “small round structured viruses” and “Norwalk-like viruses” (Lambden et al. 1993). Typically, they have an icosahedral capsid with a diameter of 27–37 nm (fig. 2). They are non-enveloped and have a 7.5–7.7-kilobase positive-sense single-stranded (ss-)RNA genome consisting of three open reading frames (ORFs) (Glass et al. 2000; Jiang et al. 1993; Lambden et al. 1993). The icosaedric hNV nucleocapsid consists of capsid proteins with shell (s) and protruding (p) domains (Koromyslova et al., 2015). It is suggested that the viral (p) domains specifically interact with human histo blood group antigens (HBGAs), which are oligosaccharides specific for the individual blood type (Tan et al. 2008; Kato et al. 2015). Using the p-domain, the hNV particles may be able to enter the host cells and accomplish infection. HNVs can be subdivided into seven genogroups, whereby only genogroups (G) I, II and IV are human pathogens (Vinjé et al., 2015). According to a unified proposal for nomenclature, genogroups are further subdivided into at least 38 genetic clusters (genotypes) (Kroneman et al., 2013).

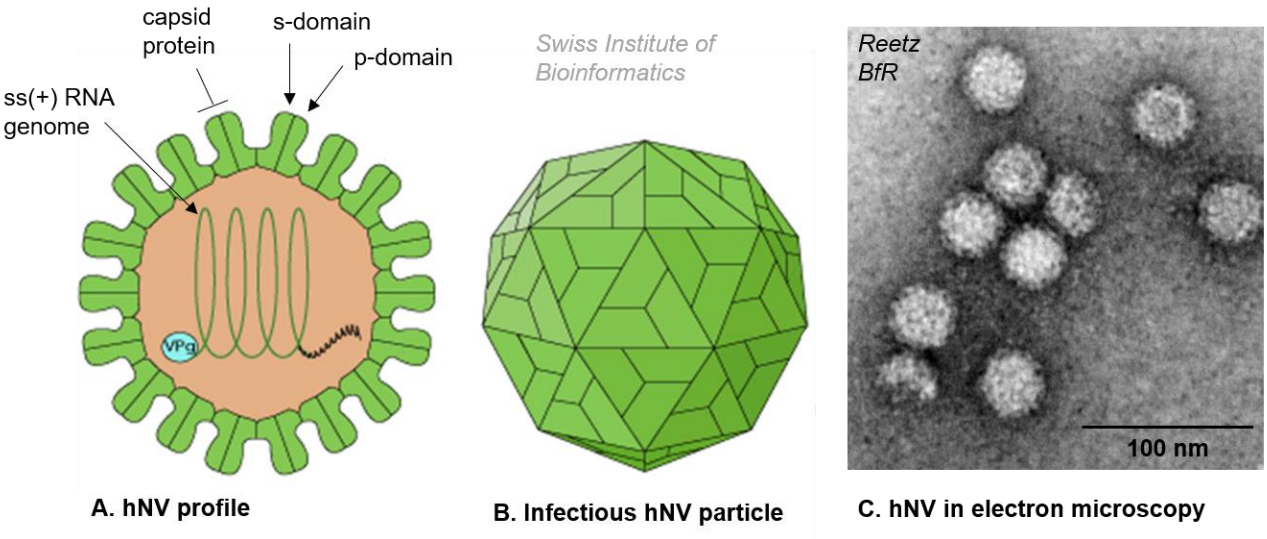

Figure 2: hNV particle. A. Schematic cross section of an hNV particle: The virus particle consists of capsid proteins with a shell (s) and protruding (p) domain interacting with different binding partners during infection. The capsid encloses the single stranded (ss) RNA genome with positive (+) orientation. The VPg protein is attached as a protein primer to the 5’ terminus of the genomic RNA during viral genome replication (Subba-Reddy et al., 2011). **B.** Scheme of intact and infectious icosahedral hNV particle. **C.** Electron microscopy showing hNV particles.

3.4. Transmission pattern and routes of contamination

HNV is transmitted from human-to-human mainly by the fecal–oral route (fig.3). The minimal dose of infection is as low as 10 to 100 virus particles (Caul et al., 1996). In addition, hNV is a highly stable virus, which can survive multiple days up to several months on various surfaces in the environment (Cheesbrough et al. 1997; Sattar et al., 2001). These properties enable indirect transmission through food, water or contact materials contaminated by infected persons or wastewater (Maunula et al. 2013; Brassard et al. 2012). For berries, irrigation water contaminated with human sewage or direct contaminations by infected food handlers have been supposed as described in fig. 1 (Mäde et al., 2013). Also, aerosolized vomitus particles are infectious and are considered to transmit virus particles through air (Lopman, 2011). Additional features of hNV infections contributing to the explosive nature of outbreaks include the prolonged period of virus shedding after symptom resolution and the extremely high amount of virus shed in the stool (Atmar et., 2008). Especially in crowded places where many people come together in a limited space, e.g. cruise ships, schools, hospitals and refugee camps, hNV can spread very fast and infect a high number of people (Mouchtouri et al., 2017; Somura et al., 2017; Fraenkel et al., 2018; Grote et al., 2017). In cruise-ship-related outbreaks, official outbreak management plans dictate information of port public health authorities and placing infected tourists and crew members in quarantine preventing further spreading of the infection on the ship or the harbor town. There are different outbreak management plans which are activated at certain threshold, e.g. after the occurrence of six acute cases within 6 hours, after affection of 1% of passengers on ships with less than 1,000 passengers or after affection of 0.5% passengers on ships with more than 1,000 passengers (Mouchtouri et al., 2017.)

Furthermore, one study highlighted a possible route for indirect zoonotic transmission through the food chain as shown in fig. 3 (Mattison et al., 2007) which might represent a subordinate transmission pattern. They tested 120 swine fecal samples from which 30 were tested positive for partial genomic sequences from NVs by sequence analysis. Three different NV genotypes were detected in Canadian pig samples, belonging to swine GII.11, swine GII.18, and the human GII.4. Furthermore, out of 179 bovine fecal samples tested for NV RNA three were confirmed to contain NV genomes. Two different genotypes of NV were detected in the Canadian dairy farm samples, belonging to bovine GIII.2 and to the human GII.4. All human sequences were not

identical to any other known sequences. Therefore, further studies and investigations with novel methods and specified NV primers are needed to confirm the possible zoonotic potential of NVs.

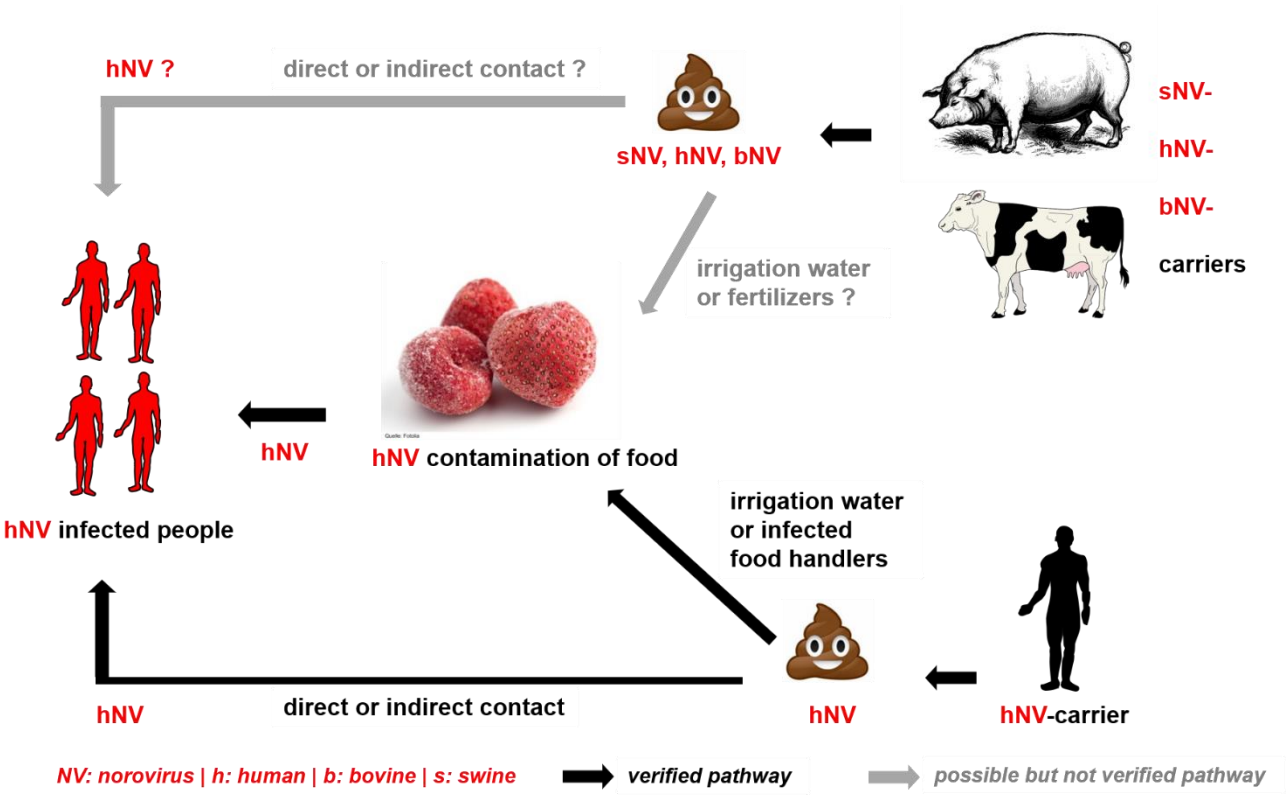

Figure 3: Transmission patterns of hNV. HNV can be transmitted by the fecal-oral route directly or indirectly from human to human. A specific indirect pathway is the contamination of food by hNV containing irrigation water or infected food handlers. A recent study revealed the presence of hNV in animal feces suggesting an additional route of infection and zoonotic potential of NVs in general. Maybe it is possible that people can get infected with hNV by contact with animal feces or also by food contamination mediated by hNV containing irrigation water or fertilizers.

3.5. Disease in humans

In healthy adults and children, infections with hNV can lead to acute gastroenteritis. Generally, the course of disease is rapid, with a short incubation period of 1–2 days followed by severe vomiting and diarrhea for another 1–2 days (Green et al., 2013). Other common symptoms are nausea, abdominal seizures, low-grade fever, and malaise. Infants and young children can experience more severe and prolonged infections lasting up to 6 weeks (Kirkwood et al., 2008), while infections in the elderly can also be quite severe and even fatal (Murata et al., 2007). Additionally, studies suggest that hNV contributes to travelers' diarrhea (Ahn et al., 2011, Chapin et al., 2005). Nevertheless, the pathology of hNV-induced diarrhea is not well understood: According to Schreiber et al., (1973) intestinal biopsies of voluntarily infected patients

also showed abnormal intestinal histology with mucosal inflammation, absorptive cell abnormalities, villous shortening, crypt hypertrophy and increased epithelial-cell mitoses. HNV-induced diarrhea is caused by alterations of secretory and/or absorptive processes but not by structural damage of the intestinal wall. The high frequency of vomiting episodes is typical for hNV infections, but the underlying pathophysiology is also undefined. One study of infected volunteers recognized a notable delay in gastric emptying, possibly due to abnormal gastric motor function (Meeroff et al., 1980). In addition to acute gastroenteritis, hNVs have been associated with more serious intestinal pathologies in premature infants and with persistent even life-threatening infections in immunocompromised and transplant patients (Karst et al., 2015).

3.6. Methods for virus extraction from food

The detection of viruses in food can be difficult and is mainly dependent on the food matrix (Scherer et al., 2010). Particularly berries (i.a. strawberries and raspberries) have a fragile texture and contain various substances, which will hamper various virus detection methods. Since viruses are mainly detected using reverse transcription (RT-) PCR (see chapter 3.7.), PCR-inhibiting substances are the main interference factor. In berries, these substances are mainly phenols and polysaccharides which can cause co-precipitation of nucleic acids, can lead to reduction in the ability to resuspend precipitated RNA or cross-linking with nucleic acids, or which can change the chemical properties of nucleic acids (Schrader et al., 2012). Consequently, RT-PCR detection of viruses in berries is prone to false negative results (Mäde et al., 2013). Therefore, several methods for virus extraction, which should remove RT-PCR inhibitors and concentrate the virus before RNA extraction and real time RT-PCR analysis, have been developed. A protocol using polyethylene glycol (PEG) precipitation has been shown to be suitable for analysis of berries (Butot et al., 2007; Scherer et al., 2010; Mäde et al., 2013; Bartsch et al., 2016). This method has also been implemented in the ISO/TS 15216-2 standard for detection of hNV and HAV in food (ISO, 2013) briefly outlined in fig.4. Another protocol uses porcine gastric mucin (PGM), which shows a similar structure as HBGAs, for binding of hNV particles to magnetic beads (Tian et al., 2005; Tan et al., 2008). In addition, an ultrafiltration method aiming at decreasing the buffer volume and thereby concentrating the viruses has been described (Mäde et al. 2013). Furthermore, Trizol®-based techniques, which release the viral RNA directly from the

food matrix before RNA extraction (Baert et al., 2008a; Szabo et al., 2015) or methods applying a direct RNA extraction from the food (Perrin et al., 2015) have been described recently. However, most of these techniques show variable virus recovery rates and many of the methods are poorly reproducible in other laboratories.

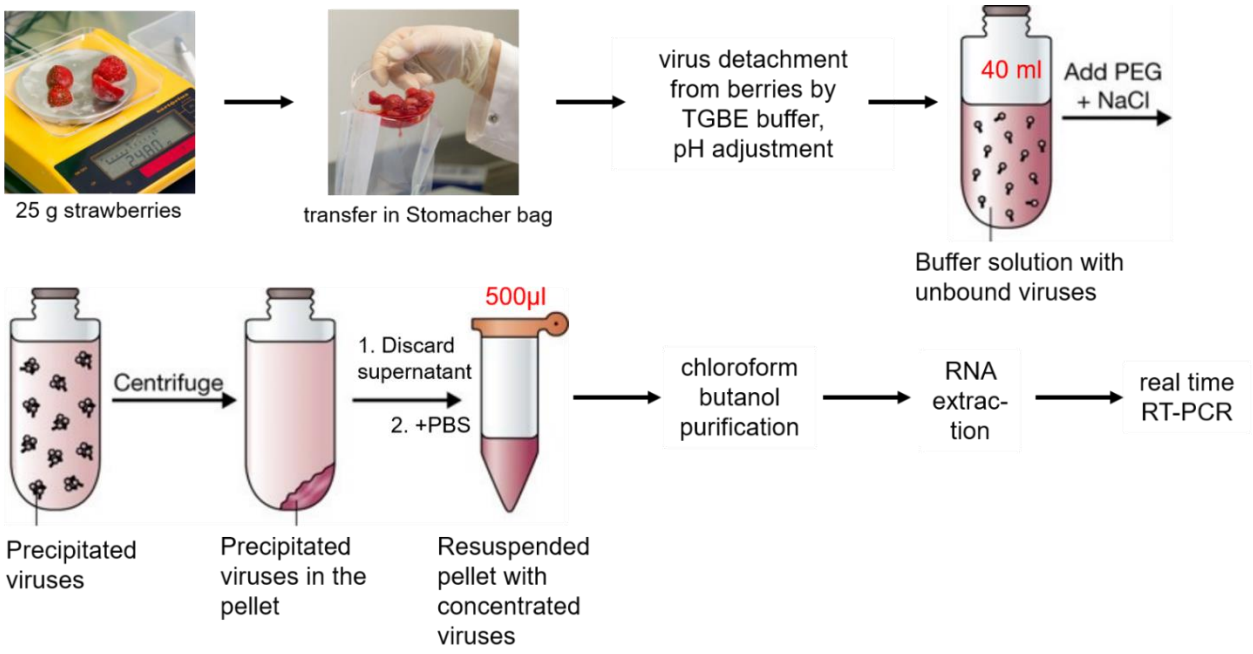

Figure 4: Method scheme of the ISO/TS 15216-2 protocol for detection of viruses in berries. An overview of the most important method steps is shown**.**

3.7. Methods for virus detection and identification

After virus extraction from food, the viruses have to be identified within the extract. Often, methods titrating infectious viruses are very delicate, time consuming and not adapted to food microbiology yet, or the dose of contamination is beyond their detection limit (Ettayebi et al., 2016; Mäde et al., 2013; Gonzalez-Hernandez et al., 2012). For hNV, no suitable cell culture methods for detection of infectious viruses in food are available so far. Therefore, PCR-based analyses of viral nucleic acids are the most important instruments for the identification of contaminated foods as potential outbreak sources. Also, PCR-based methods are useful for quantifying virus material and discovering new viruses in the food chain (Bovo et al., 2017; Boonham et al., 2014; Thompson et al., 2010). There are several established PCR-based methods to identify genetic material from viruses. Real time PCR in general creates and amplifies DNA molecules while detecting and quantifying the generated products (Watzinger et al.,

2006). Before DNA molecules can be produced, the viral RNA is transcribed into DNA by enzyme-mediated reverse transcription (RT). TaqMan® probes are fluorescent dyes which consist of a single-stranded oligonucleotide of the target-specific sequence (fig. 5). This sequence is labelled with a reporter fluorescent dye (fluorophore) at the 5' end, a quencher dye at the 3' end, and located between the used primer pair. Due to the fluorescence resonance energy transfer (FRET), fluorescence is inhibited if reporter and quencher are in close distance. The probe is degraded by the exonuclease activity of the DNA-polymerase during generation of the PCR-product, thus leading to fluorescence emission. Therefore, the intensity of fluorescence is proportional to the amount of PCR-product (Watzinger et al., 2006).

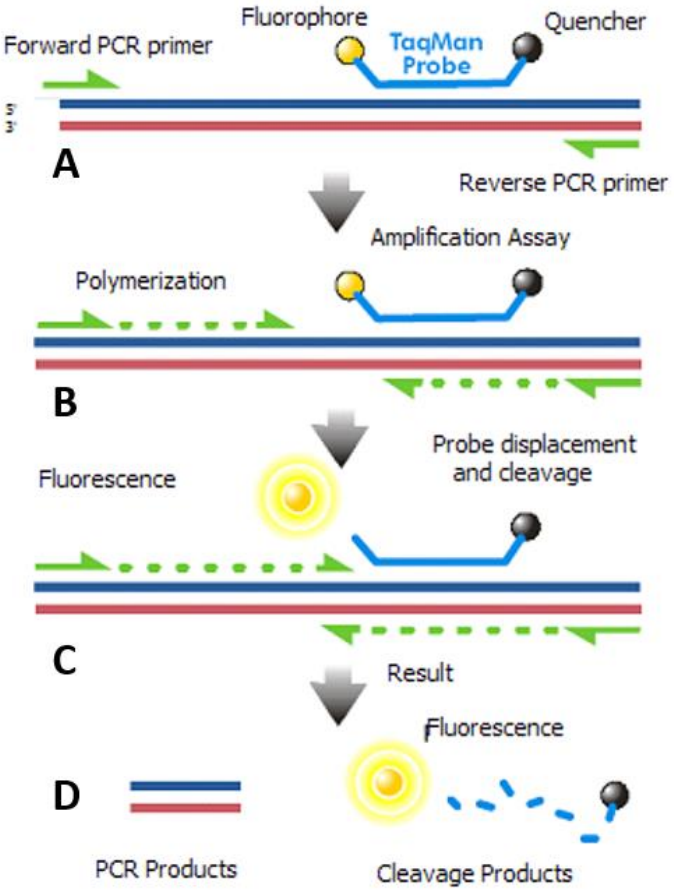

Figure 5: Principle of TaqMan®-based real time PCR. This figure shows one DNA polymerization cycle consisting of annealing and elongation phase. A: Primers and probe bind to cDNA template under annealing conditions after reverse transcription. B: In the elongation phase, DNA-polymerase produces a new DNA strand while approaching the probe. C & D: The polymerase cleaves the probe by 5' to 3' exonuclease activity. The separation between reporter and quencher dye results in a fluorescence signal recognized by detection system.

Figure origin: Wikipedia

A further development of quantitative real time PCR (RT-qPCR) leading to improved quantification is digital PCR (dPCR) (fig.6). The method is based on partitioning the sample into thousands of individual sub-samples each containing a theoretical amount of 1 or no copies of the nucleic acid target. After amplification, the total number of target molecules is calculated by counting the PCR-positive sub-samples in relation to the dilution factor. Therefore, no external reference standards are needed for quantification (Zhang et al., 2016). The dilution of samples into large numbers of subsamples may also decrease the impact of inhibitors associated with matrix-type components. There have been recent efforts to establish dPCR protocols for hNV detection and quantification in water, sediments, lettuce and soft berries (Monteiro et al., 2017; Farkas et al., 2017; Fraisse et al., 2017; Polo et al., 2016; Coudray-Meunier et al., 2015). In all of these studies it was possible to detect hNV with dPCR. However, different detection rates were described depended on the distinct detection system and impact of the matrix.

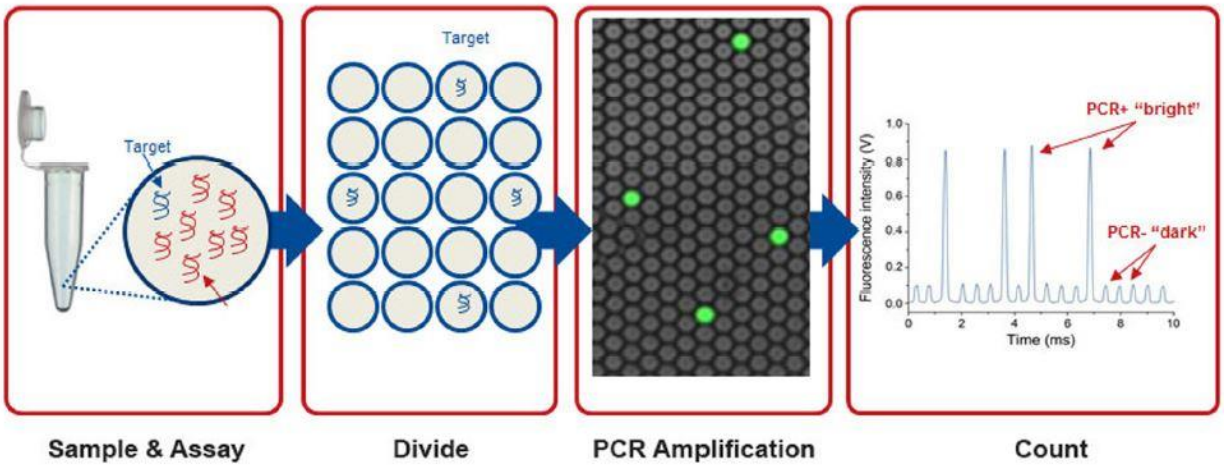

Figure 6: Workflow of dPCR. First, the sample is divided into individual PCRs containing a theoretical amount of 1 or no copies of the nucleic acid target. After amplification, the total number of target molecules is calculated apart from external reference standards. Figure origin: www.idtdna.com

Next generation sequencing (NGS) has recently developed to a promising tool for both detection and identification of foodborne viruses. NGS is a subordinate concept for several technologies: The most frequent analysis concept is Illumina sequencing which can be performed by different machines using diverse PCR and sequencing systems (Kulkarni et al., 2017). All associated methods allow sequence-independent detection and identification of non-culturable viruses and unknown pathogens useful for outbreak investigation. Briefly, the method principle is outlined in fig. 7. After sample preparation, the nucleic acid fragments are combined with priming adapters. These adapters bind to their fixated counterparts on a flow cell device resulting in a bridge-like binding shape of the sequence. After enzymatic synthesis of the complementary strand the double strand dissociates. While one end of a strand is still attached to the same flow cell adapter, the other free end binds to a new flow cell adapter resulting again in a bridge-like state. These cycles repeat a few times until a number of sequences are replicated forming clusters of the same sequence in a certain area of the flow cell. Thereafter, the reverse strands are removed by washing and analysis of the forward strands continues with sequencing by synthesis: Nucleotides with different fluorescent tags compete cycle-wise for binding to the target strand. In case of successful binding they emit a fluorescent signal specific for the nucleotide type. The emitting fluorescent pattern is detected by the machine recognizing the specific nucleotide sequences. The resulting sequence data are analyzed by specific mapping programs comparing them to big sequence data bases. (Meyer and Kirchner, 2010). A problem regarding comparability of these methods is that companies performing NGS analyses on order do not release many method details. Also, technical challenges of NGS analyses of food remain due to anticipated low quantities of viruses present. A recent study identified sequences of rotaviruses and picobirnaviruses on field-harvest and retail lettuce samples (Aw et al., 2016). According to Boonham et al., 2014 metagenomic sequencing is not yet a standard method for evaluating food viromes, viral metagenomic sequencing but could be a promising monitoring tool in the future. The metagenomic detection of hNV and HAV on celery was possible even for a low dose of contamination down to $< 10^3$ RNA copies as well as the NGS detection of hNVGI and hNVGII on Japanese oysters from farms (Yang et al., 2017; Imamura et al., 2017). Also, NGS was used for detection of hNV in clinical fecal samples as well as for identification of inter host nucleotide variations that occur after direct transmission (Joensen et al., 2017; Nasheri et al., 2017).

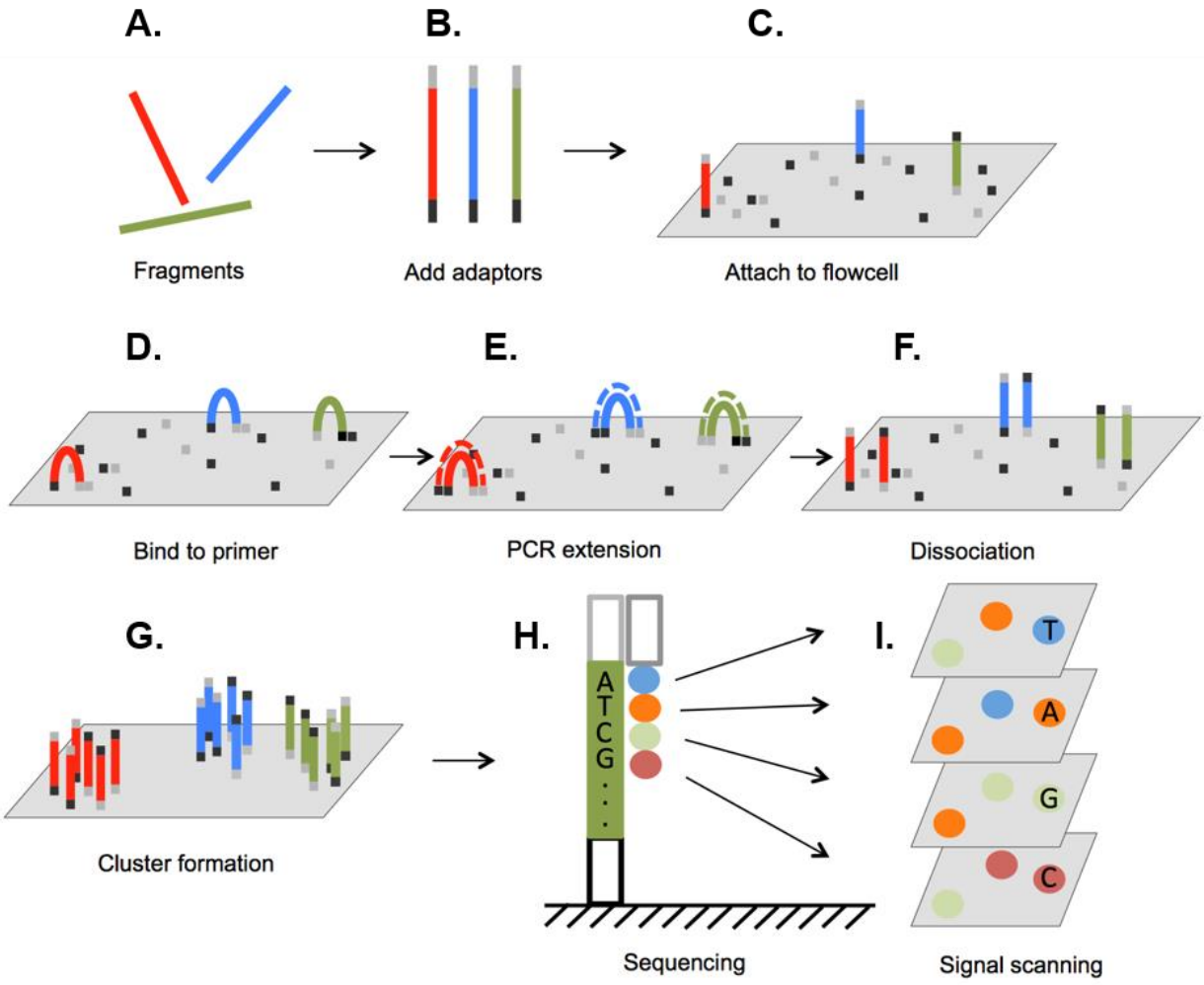

Figure 7: Principle of bridge PCR and sequencing during Illumina sequencing method. A. Nucleic acid fragments from sample. **B.** Adapter Ligation to sample fragments. **C. and D.** Adapter regions on fragment attach to counterparts on flow cell device resulting in a bridge shape of the sequence. **E.** Enzymatic synthesis of the complementary strand. **F.** Dissociation of the double strand, repetition of step D and E. **G.** Cluster formation of specific sequences in certain areas of the flow cell. **H.** Sequencing by synthesis through cycle wise binding of fluorescently tagged nucleotides. **I.** Detection of the fluorescence pattern and identification of the sequence. Figure origin: intechopen.com

3.8. Infectivity and stability assays for human norovirus

The hNV cell culture is not yet adjusted to the needs of microbial food studies and only established in a few facilities (Ettayebi et al., 2016). The method is very delicate and expensive and not elaborated enough for experiment designs involving infectivity assays for food extracts. Further studies will be necessary to analyze the influences of different food extracts on cell viability and to develop respective assays. Consequently, there is still the need for alternative approaches to study viral inactivation behavior in food. Molecular methods to estimate hNV stability have also been applied in different studies. Apart from surrogate viruses these PCR-based stability assays are the best indicator for hNV infectivity. Purification of virus particles by binding to PGM prior to RT-PCR has been used in some virus stability studies to measure only RNA from intact virus particles (Li and Chen, 2015; Huang et al., 2016). It is unclear if the hNV surface structures required for PGM-binding are the same structures needed for cell infection. Therefore, it is uncertain if a PGM-binding assay can monitor infectious hNVs which can only be genuinely confirmed by cell infectivity assays. Another method uses an RNase treatment of virus particles before RT-PCR detection to determine the viral RNA that was protected by the intact capsid (Mormann et al., 2010; Schielke et al., 2011). Nevertheless, it is only possible to distinguish between intact and destroyed virus particles. Intact but non-infectious particles can not be considered by this assay.

3.9. Human norovirus surrogates

HNV surrogates are viruses with similar biophysical properties and genomic structure as hNV and have been frequently used in inactivation studies. The most common surrogates are feline Calicivirus (fCV), murine norovirus (mNV) or Tulane virus (TV) (Cromeans et al., 2014) which can all be cultivated in cell culture systems useful for infectivity assays. Many studies indicated that mNV and TV are the most suitable surrogates for hNVs due to similar thermic and acidic stability as well as their ability to survive in the environment for a longer period (Seo et al., 2012; Bozkurt et al., 2013; Arthur and Gibson, 2015b; Bozkurt et al., 2015a; Drouaz et al., 2015; Bozkurt et al., 2015b). Both surrogates as well as hNV belong to the *Caliciviridae* family and are non-enveloped single positive-stranded RNA viruses with an icosaedric nucleocapsid (tab.2). MNV-1 was the first virus within the genus norovirus reported to be cultivated in cell culture (Wobus et al., 2006), is shed in mouse feces and is commonly

transmitted by the fecal-oral route (Karst et al., 2003). On the one hand, it can cause subclinical chronic infections in adult immunocompetent mice and is endemic in many mouse colonies (Compton 2008). On the other hand, in immunodeficient mice it can cause a lethal disease that presents as hepatitis, pneumonia, or inflammation of the nervous system (Karst et al., 2003). Also, TV was isolated from stool samples of monkeys for the first time in 2008. The clinical consequences of TV infection and its pathogenesis has not been clarified yet (Farkas et al., 2008). While TV could be grown in LLC-MK2 cells (a rhesus macaque kidney cell line), growth attempts in other cell lines failed. Although, TV represents a relatively new Calicivirus genus, *Recovirus* (Farkas et al., 2008), sequence analysis has revealed a close relationship between TV and hNV. Also, a binding of TV to HBGAs like the binding of hNV to HBGAs was confirmed (Farkas et al., 2010). Until hNV cell culture is adjusted to food microbiology, surrogates from the *Caliciviridae* family might give helpful insights into viral inactivation kinetics and help to improve food safety.

Table 2: Taxonomy and properties of hNV, mNV and TV.

Family	Genus	Virus species	Host	Infection	Course of disease
Caliciviridae	Norovirus	hNV	Humans	Asymptomatic up to lethal	Gastroenteritis
		mNV	Mice	Subclinical until lethal	Chronic infection, hepatitis, pneumonia or inflammation of the nervous system
	Recovirus	TV	Apes	Asymptomatic	No or unknown symptoms

3.10. Thermal virus inactivation in berries

In a recent review (Cook et al., 2016) different published methods for virus inactivation on food and contact surfaces were described. The most interesting approaches included application of chemicals, antimicrobial or plant-based disinfectants, solar light, UV or gamma radiation, freezing, high pressure and ozone treatment. Also, several studies have been performed on heat inactivation of viruses in different types of food

such as ready-to-eat meals, soft fruits, mussels, and leafy greens (Arthur and Gibson, 2015a; Araud et al., 2016). The studies showed different results due to the influence of the distinct matrices and foodborne method inhibitors. The comparison of results from different heat inactivation studies is difficult because of the various method protocols and study designs applied. Only a few studies have been performed in berries shown in tab. 3 (Baert et al., 2008b; Verhaelen et al., 2012; Deboosere et al., 2004; Butot et al., 2009). The focus of the study from Deboosere et al. (2004) was directed on the sucrose, pH and calcium dependent inactivation of HAV in strawberry puree at temperatures from 80 to 90°C. Nowadays, pasteurization processes of raspberry puree are limited to short times and rather low temperatures to maintain flavor and nutritional quality. Therefore, Baert et al. (2008b) evaluated three time-temperature combinations regarding inactivation of mNV and *B. fragilis* HSP40 infecting phage B40-8: 4°C/overnight, 65°C/30sec and 75°C/15sec. Butot et al. (2009) investigated the effect of freeze drying and the effect of heating between 80 to 120°C on HAV and hNV inactivation in different berries. Verhaelen et al. (2012) evaluated the influence of storage temperatures between 4 to 21°C, storage times between 1 to 7 days and humidity from 36 to 70% on hNV, mNV and human adenovirus stability on strawberries and raspberries. Unfortunately, the different aims of studies, spiking procedures and virus extraction/detection methods do not allow a direct comparison of their results as meta-analysis regarding hNV and surrogate thermal inactivation kinetics.

Table 3: Summary of heat inactivation studies in berries involving viruses.

Reference	Virus	Temperature range (°C)	Food	Focus of the thermal inactivation study
Deboosere et al., 2004	HAV	80 - 90	Strawberry puree	Influence of sucrose, pH, calcium
Baert et al., 2008	Phage B-40	4, 65, 75	Raspberry puree	Inactivation kinetics for 3 time/ temperature combinations
Butot et al., 2009	HAV, hNV	80 - 120	Blackberries, blueberries, raspberries, strawberries	Influence of freeze drying and heating
Verhaelen et al., 2012	hNV, mNV and human Adenovirus	4 – 21	Strawberries, raspberries	Influence of storage temperatures, storage times and humidity

3.11. Aim of the study

The main purpose of this study was to increase customer safety and reduce risks for public health due to contaminated food. Frozen berries are usually popular and healthy products which can unfortunately be dangerous due to contamination with human pathogens. To increase food safety, three main project areas were identified: In order to reduce health risks originating from contaminated berries, improved methods for detection and inactivation of hNV on berries should be developed during this project. Thereby a sensitive identification and quantification of viruses and other pathogens should be enabled. Also, guidance regarding heating procedures for a save inactivation of hNV should be provided.

1. Optimization of virus detection methods on berries. In the past, the testing during outbreak scenarios was often hampered by false negative results due to insufficient methods. Therefore, hNV detection methods should be compared and optimized. Frozen strawberries should be artificially contaminated with hNVGII and treated with different virus extraction methods. Afterwards the recovered virus amount should be calculated to identify the most effective protocol. The method giving the best results with strawberries containing high amounts of RT-PCR inhibitors should be further optimized and thereafter tested on field samples from original gastroenteritis outbreaks in 2012 and 2016.

2. Testing of the applicability of novel methods for virus identification on berries. Novel virus identification and quantification methods such as NGS and dPCR should be evaluated by the investigation of frozen strawberries from the outbreak in 2012. Therefore, several RNA samples should be prepared from the strawberries according to the optimized method established in the first part of the study. One purpose was to evaluate if detection of hNV and other viruses on strawberries is possible by NGS analysis. Also, results should be analyzed regarding a more comprehensive view on pathogens in the field and plant environment. Furthermore, dPCR and RT-qPCR should be compared regarding application comfort, quality of identified virus material and detection limit during quantification.

3. Testing the efficiency of heat inactivation regimes for virus inactivation on berries. For the development of a reliable heat inactivation model for hNV in strawberry puree, thermal inactivation kinetics should be assessed. In order to enable comparability with other studies in the future, standardized procedures for heat inactivation studies as

suggested by Arthur and Gibson (2015a) were integrated in experimental planning. To this end, methods for comparative testing of the capsid integrity of hNV and surrogate viruses mNV and TV as well as their infectivity should be optimized. The generated data should be used to calculate D and ʒ-values for hNV capsids and surrogates and to generate mathematic models for the prediction of virus inactivation at time-temperature combinations not tested experimentally.

4. Materials

4.1. Commercial material

4.1.1. Strawberries

Sealed 2 – 5 kg batches of fresh and frozen strawberries originating from Germany and Spain were purchased in common food stores in Berlin, Germany, in 2015. After washing and removing the green stem the fresh berries were aliquoted in 25 g portions. After artificially contamination during method optimization they were stored in 50 mL tubes at -20°C until usage. All batches were tested negative for hNV RNA using the ISO/TS 15216-2 method.

4.1.2. Strawberry puree

In March of 2017 2 kg of fresh strawberries from Spain were purchased in a food store in Berlin, Germany. After washing and removing the green stem the strawberries were blended with a hand-held blender to a homogenous mass. The puree was aliquoted in 15 g portions in 50 mL tubes which were stored at -20°C until usage. During the heat inactivation experiments negative controls for hNV, TV and mNV were performed in triplicate.

4.2. Outbreak material

4.2.1. Strawberry field samples

Five sealed 1 kg batches of frozen strawberries from a lot of imported strawberries involved in a large foodborne hNV outbreak in Germany 2012 (Mäde et al., 2013) were kindly provided by D. Mäde (State Office for Consumer Protection, Saxony-Anhalt, Germany). The berries were stored at -20°C until usage.

4.2.2. Raspberry field samples

A sealed 10 kg batch of frozen raspberry mash from a lot of imported raspberry mash involved in a small hNV outbreak in a psychiatric facility in Germany in 2016 (Berg et

al., 2017) was kindly provided by C. Berg (Ministry for Environment, Energy, Nutrition an Forest, Rhineland-Palatinate). The berries were stored at -20°C until usage.

4.3. Virus solutions

4.3.1. Human norovirus

A hNVGII.3-containing stool sample from a child suffering from enteric symptoms was used for the inoculation experiments as described (Scherer et al., 2010). The stool sample was diluted 1:10 in phosphate-buffered saline (PBS), aliquoted and stored at -80 °C in the reference sample deposit of the NRL for monitoring viruses in *bivalve molluscs* (BfR). The stool sample preparation contained 5.4 x 10^6 RNA copies/µl according to quantification by real time RT-PCR as described in the following sections.

4.3.2. Bacteriophage MS2

The bacteriophage MS2, provided by Dr. J. Dreier (Bad Oynhausen, Germany) was used as process control virus as described (Dreier et al., 2005) for method comparison experiments. For every sample, 10µl of a MS2 solution containing 10^4 plaque forming units of the bacteriophage produced by J. Hammerl (BfR, Berlin, Germany) were utilized.

4.3.3. Murine Norovirus

In this study, mNV provided by Dr. E. Schreier (RKI, Berlin, Germany) was propagated in cell culture leading to cell death after successful replication as described in the section below. The mNV containing DMEM was quantified by plaque assay and real time RT-PCR as described in the section below. In thermal inactivation experiments, 450µl were used for every sample containing 4.12 x 10^9 plaque forming units (PFU) and 2.12 x 10^{12} RNA copies in total.

4.3.4. Tulane Virus

Also, TV provided by Prof. S. Le Guyader (IFREMER, Nantes Cedex, France) in cooperation with Dr. J. Jiang (Cincinnati Children's Hospital, Cincinnati, OH, USA) was propagated in cell culture leading to cell death after successful reproduction as described in the section below. The TV containing M199 media was quantified by plaque assay and real time RT-PCR as described in the section below. In our thermal

inactivation experiments, 450µl were used for every sample containing 6.66 x 10^8 PFU in total and 4.87 x 10^{10} RNA copies.

4.4. Primers

The virus sequence priming oligonucleotides (primer) and TAMRA and BHQ labelled probes were ordered from TIB MOLBIOL (Syntheselabor GmbH, Berlin, Germany). Probes labelled with MGB-NQ were ordered from Applied Biosystems (Fisher Scientific GmbH, Schwerte, Germany). The lyophilized oligonucleotides were diluted in nuclease-free water to a 100µM stock solution and stored at -20°C or 4°C (MGB-NQ). These stock solutions were used to make the respective working solution as listed in tab.4.

Table 4: Primers and probes. In this table the origin of the target sequences (virus), the function of the oligonucleotides with the respective names, their specific sequence codes, working concentration and original developers are listed. FAM: Probe labelled 5' 6-carboxyfluorescein; TAMRA: Probe labelled 3' 6-carboxy-tetramethylrhodamine; MGB-NFQ: Probe labelled minor groove binder/non-fluorescent quencher; BHQ: Probe labelled black hole quencher.

Virus	Function	Name	5' – Sequence – 3'	Working conc.
hNVI	fw primer	QNIF4	CGC TGG ATG CGN TTC CAT	40µM
	rev primer	NV1LCR	CCT TAG ACG CCA TCA TCA TTT AC	40µM
	probe	TM9	FAM - TGG ACA GGA GAT CGC – MGB-NFQ	40µM
Hoehne & Schreier, 2006; da Silva et al., 2007; Svraka et al., 2007				
hNVII	fw primer	QNIF2	ATG TTC AGR TGG ATG AGR TTC TCW GA	40µM
	rev primer	COG2R	TCG ACG CCA TCT TCA TTC ACA	40µM
	probe	QNIFS	FAM - AGC ACG TGG GAG GGC GAT CG - TAMRA	40µM
Kageyama et al., 2003; Loisy et al., 2005				
mNV	fw primer	MNV-S	CCG CAG GAA CGC TCA GCA G	40µM
	rev primer	MNV-AS	GGY TGA ATG GGG ACG GCC TG	40µM
	probe	MNV-TP	FAM – ATG AGT GAT GGC GCA - MGB-NFQ	40µM
Kitajima et al., 2010				
TV	fw primer	TV fw	TGA CGA TGA CCT TGC GTG	20µM
	rev primer	TV rev	TGG GAT TCA ACC ATG ATA CAG TC	20µM
	probe	TV probe	FAM - ACC CCA AAG CCC CAG AGT TGA T - BHQ	20µM
Xu et al., 2015				
MS2	fw primer	MS2-TM3-F	GGC TGC TCG CGG ATA CCC	20µM
	rev primer	MS2-TM3-R	TGA GGG AAT GTG GGA ACC G	20µM
	probe	MS2-TM2	FAM – ACC TCG GGT TTC CGT CTT GCT CGT - BHQ	10µM
Dreier et al., 2005				

4.5. Cell lines

For mNV propagation, the murine *(Mus musculus)* macrophage cell line RAW 264.7 (strain Berlin/06/06/DE isolate S99, kindly provided by Dr. E. Schreier, RKI, Berlin, Germany) was used (Gonzalez-Herdandez et al., 2012). It was derived from Abelson murine leukemia virus-induced tumor cells in 1978 (Raschke et al., 1978) and was provided by Dr. E. Schreier (RKI) in 2009. For TV propagation, the rhesus monkey *(Macaca mulatta)* epithelial cell line LLC-MK2 was used (Farkas et al., 2008). This cell line represents normal cells derived from a monkey kidney in 1962 (Hull et al., 1962) and was ordered from ATCC (LGC Standards GmbH, Wesel, Germany). Low passages of both permanent cell lines were stored as cell stock in liquid nitrogen. They are adherent cells and can be passaged up to 25 times (see cultivating details under 3.3.3.).

4.6. Kits, devices, supplies, media and buffers

In the following tables all kits (tab.5), devices (tab.6), supplies (tab.7), chemicals and reagents (tab.8), ready-to-use buffers and media (tab.9) and self-made buffers and media (tab.10) used in this study are listed.

Table 5: Kits.

Kits	Manufacturer
High Pure RNA Isolation Kit	Roche, Mannheim, Germany
MEGAscript T7 Kit	Applied Biosystems, Darmstadt, Germany
QIAamp® Long Range PCR Kit	Qiagen, Hilden, Germany
Qiagen One Step RT-PCR Kit	Qiagen, Hilden, Germany
Qiagen Plasmid Mini Kit	Qiagen, Hilden, Germany
QIAquick Gel Extraction Kit	Qiagen, Hilden, Germany
QuantiTect Probe RT-PCR Kit	Qiagen, Hilden, Germany
RNA Ultrasense One Step qRT-PCR System	Thermo Fisher Scientific, Schwerte, Germany
TOPO TA Cloning® Kit for Sequencing	Thermo Fisher Scientific, Schwerte, Germany

Table 6: Devices.

Device	Manufacturer
ABI Prism 7500 Sequence Detection	Applied Biosystems, Foster City, CA, USA
Biological safety cabinet Antair BSK-4	Anthos, Siegburg, Germany
Biological safety cabinet HS 12	Heraeus, Hanau, Germany
Biological safety cabinet HSP 19	Heraeus, Hanau, Germany
Centrifuge Heraeus-Multifuge 1 S-R	Heraeus, Hanau, Germany
Cooling centrifuge 5402	Eppendorf, Hamburg, Germany
CO_2-incubator (incubator Steri-Cult 3308)	Thermo Electron Corporation, Marietta, Ohio, USA
Electrophoresis Power supply EPS 500/400	Pharmacia Fine Chemicals, Upssala, Sweden
Fridge	Liebherr, Ochsenhausen, Germany
Freezer Labstar -20°C	National Lab, Mölln, Germany
Freezer SANYO -80°C	Sanyo Sales & Marketing Europe GmbH, Munich, Germany
Gel documentation device Gene Flash	Syngene Bio Imaging, Cambride, UK
Gel electrophoresis horizontal	Life Technologies GmbH, Darmstadt, Germany
Hand held blender	BRAUN GmbH, Kronberg, Germany
Incubation shaker MAXQ 4450	Thermo Fisher Scientific, Schwerte, Germany
Incubator WTB BINDER (37°C)	Binder, Tuttingen, Germany
LED Light Box (DINA5)	Shenzhen Huion Animation Technology Co, Shenzhen, China
Magnetic separation rack, 50 mL	New England Biolabs, Frankfurt am Main, Germany
Meat thermometer	ATP Messtechnik GmbH, Ettenheim, Germany
Micro scales PT 120	Sartorius. Göttingen, Germany
Microscope Axiovert 25	Zeiss, Jena, Germany
Microwave	Privileg, Stuttgart, Germany
Multi-channel pipet (8 channels)	Eppendorf, Hamburg, Germany
Multipet stream	Eppendorf, Hamburg, Germany
Nitrogen tank ARPEGE 70 Natal 40	Air Liquide GmbH, Düsseldorf, Germany
NucliSENS® easyMAG system	BioMérieux, Marcy l´Etoile, France
Over-head rotator Sunlab®	Sunlab GmbH, Aschaffenburg, Germany
Pipet boy Accu-jet	Brand GmbH, Wertheim, Germany
Pipets Eppendorf Research	Eppendorf, Hamburg, Germany
Quarz Timer	Oregon Scientific, Neu-Isenburg, Germany
Rocking shaker	neoLab Migge GmbH, Heidelberg, Germany
Spectrometer NanoDrop	Thermo Fisher Scientific, Schwerte, Germany
Table centrifuge Pico 21	Thermo Fisher Scientific, Schwerte, Germany
Thermocycler Gene Amp PCR System 2400	Perkin Elmer, Waltham, Massachusetts, USA
Thermomixer comfort	Eppendorf, Hamburg, Germany

Tweezers, sterile	Altmann Analytik GmbH & Co. KG, Gablingen, Germany
Ultracentrifuge LE 80	Beckmann Instruments, Palo Alto, California, USA
Vortex mixer	Lab4you GmbH, Berlin, Germany
Water bath WS-5	Fried Electric, Haifa, Israel

Table 7: Supplies.

Supply	Manufacturer
Autoclaving bag (20cm x 30cm)	neoLab Migge GmbH, Heidelberg, Germany
Cell culture flasks (25cm^2; 75cm^2)	neoLab Migge GmbH, Heidelberg, Germany
Cell culture plates (6 well)	neoLab Migge GmbH, Heidelberg, Germany
Centrifuge tube, konic, 50mL	neoLab Migge GmbH, Heidelberg, Germany
Cryo vials	neoLab Migge GmbH, Heidelberg, Germany
Eppendorf tube (0.5mL; 1.5mL; 2mL)	Eppendorf, Hamburg, Germany
Gloves, latex	Süd-Laborbedarf GmbH, Gauting, Germany
Gloves, nitrile	IGEFA Handelsgesellschaft GmbH & Co. KG, Ahrensfelde, Germany
MobiSpin columns S-400	MoBiTec, Güttingen, Germany
NucliSENS easyMAG Disposables	BioMérieux, Marcy l´Etoile, France
PCR tubes	Eppendorf, Hamburg, Germany
Petri dishes, Ø 9mm	neoLab Migge GmbH, Heidelberg, Germany
Polyethersulfone syringe filter membrane, PES, 0.22µm	SARSTED, Nümbrecht, Germany
Polyethersulfone syringe filter membrane, PES, 0.45µm	SARSTED, Nümbrecht, Germany
Pipets, serological (5mL, 10mL, 20mL, 50mL)	neoLab Migge GmbH, Heidelberg, Germany
Pipet tips with filter, sterile (10µl, 100µl, 1000µl)	Axygen Inc, Union City, California, USA
Real time RT-PCR tubes, Microamp optical 8-tube strip	Applied Biosystems, Foster City, CA, USA
Real time RT-PCR lids, Microamp optical 8-cap strips	Applied Biosystems, Foster City, CA, USA
Scalpel, sterile	Aesculap AG, Tuttingen, Germany
Stomacher filter bag	VWR International GmbH, Dresden, Germany
Syringe 20 mL	neoLab Migge GmbH, Heidelberg, Germany
Vivaspin 20 ultrafiltration device, 50.000 MWC	Sartorius, Göttingen, Germany

Table 8: Chemicals and reagents.

Chemical / reagent	Manufacturer
Agarose for gel electrophoresis	Serva, Heidelberg, Germany
Agarose low melting temperature for PA	Sigma-Aldrich Co., Darmstadt, Germany
Aqua distilled, dest.	BfR, Berlin, Germany
Ampicillin sodium salt	Sigma-Aldrich Co., Darmstadt, Germany
Blue DNA loading dye, 5x	Qiagen, Hilden, Germany
Butanol	Carl Roth GmbH + Co. KG, Karlsruhe, Germany
Chloroform	Fluka Chemie AG, Buchs, Schweiz
DNA Hyperladder II and IV	Bioline, Luckenwalde, Germany
DNase I, recombinant, RNase free	Roche, Mannheim, Germany
1-Ethyl-3-(3-dimethylaminopropyl)carbodiimide), EDC	Sigma-Aldrich Co., Darmstadt, Germany
Ethanol absolute	Carl Roth GmbH + Co. KG, Karlsruhe, Germany
Ethidiumbromid	Merck, Darmstadt, Germany
Etylendiamintetraacetat, EDTA	Merck, Darmstadt, Germany
Fetal calf serum, FCS	PAN^{TM} Biotech GmBH, Aidenbach, Germany
Gentamycin 10mg/mL, liquid	PAN^{TM} Biotech GmBH, Aidenbach, Germany
Glycine	Carl Roth GmbH + Co. KG, Karlsruhe, Germany
Isopropanol	Merck, Darmstadt, Germany
L-Glutamine 200mM, liquid	PAN^{TM} Biotech GmBH, Aidenbach, Germany
MagnaBind Carboxyl Derivatized Beads	Thermo Fisher Scientific, Schwerte, Germany
Meat extract	Merck, Darmstadt, Germany
Muriatic acid, 37%, liquid, HCl	Merck, Darmstadt, Germany
Neutral red	Merck, Darmstadt, Germany
Non-essential amino acids, NEAA, 100x, liquid	PAN^{TM} Biotech GmBH, Aidenbach, Germany
Nuclease free water	Qiagen, Hilden, Germany
Pectinase (*A. aculeatus*)	Sigma-Aldrich Co., Darmstadt, Germany
pH meter	Testo SE & Co. KG, Lenzkirch, Germany
Polyethylene glycol 8,000, PEG	Sigma-Aldrich Co., Darmstadt, Germany
Porcine gastric mucine (Typ III PGM), PGM	Sigma-Aldrich Co., Darmstadt, Germany
Protector RNase Inhibitor	Sigma-Aldrich Co., Darmstadt, Germany
QIAGEN RNase Inhibitor	Qiagen, Hilden, Germany
RNAse A	Qiagen, Hilden, Germany
Sodium chloride, NaCl	Sigma-Aldrich Co., Darmstadt, Germany
Sodium hydroxide, NaOH	Merck, Darmstadt, Germany
Tris(hydroxymethyl)aminomethane)	Carl Roth GmbH + Co. KG, Karlsruhe, Germany
TRI® Reagent	Life Technologies GmBH, Darmstadt, Germany
Typsine/EDTA solution, 0.25%/0.1%	PAN^{TM} Biotech GmBH, Aidenbach, Germany
Water, sterile	PAN^{TM} Biotech GmBH, Aidenbach, Germany

Table 9: Ready-to-use buffers and media.

Buffer / medium	Manufacturer
2 x MEM, liquid	Lonza AG, Basel, Schweiz
DMEM, liquid	PAN^{TM} Biotech GmBH, Aidenbach, Germany
Gibco™ Antibiotic-Antimycotic, 100 x	Thermo Fisher Scientific, Schwerte, Germany
Luria-Bertani (LB)-agar	Oxoid, Wesel, Germany
Luria-Bertani (LB)-medium	Oxoid, Wesel, Germany
M199 medium	Thermo Fisher Scientific, Schwerte, Germany
2 x M199 medium for PA	Thermo Fisher Scientific, Schwerte, Germany
2-(N-morpholino)ethanesulfonic acid buffer, MES	Thermo Fisher Scientific, Schwerte, Germany
NucliSENS easyMAG Lysis Buffer	BioMérieux, Marcy l´Etoile, France
NucliSENS easyMAG Extraction Buffer 1	BioMérieux, Marcy l´Etoile, France
NucliSENS easyMAG Extraction Buffer 2	BioMérieux, Marcy l´Etoile, France
NucliSENS easyMAG Extraction Buffer 3	BioMérieux, Marcy l´Etoile, France
NucliSENS easyMAG Magnetic Silica	BioMérieux, Marcy l´Etoile, France
SOC-medium	Qiagen, Hilden, Germany
D- phosphate-buffered saline solution, PBS	PAN^{TM} Biotech GmBH, Aidenbach, Germany

Table 10: Self-made buffers and media.

Buffer / medium	Recipe
Agarose solution 1% or 2% for gel electrophoresis	For a small gel: cook 0.4g or 0.8g agarose in 40mL TBE Buffer 1% until agarose is dissolve; add 1µl ethidium bromide
Chloroform/Butanol mixture	Mix chloroform and butanol in proportion of 1:1 (v/v)
HCl, 4M	Mix 37% HCl with aqua dest. in proportion of 1:3 (v/v)
Media solution for cultivation of RAW 264.7 cells / LLC-MKS cells	DMEM / M199 was supplemented with 10% fetal calf serum, 1% glutamine, 1% NEAAs and 1% gentamycine / Gibco™ Antibiotic-Antimycotic
Media solution for PA	2 x MEM /2 x M199 was supplemented with 1.5% low melting agarose, 5% FCS, 1% glutamine and 1% gentamycine gentamycine / Gibco™ Antibiotic-Antimycotic. Cook low melting temperature agarose in warm aqua dest. until powder is dissolved; mix cold buffer solution with hot agarose solution
NaOH, 2M	Dissolve 8g sodium hydroxide in 100ml aqua dest.
5 × PEG/NaCl solution	Dissolve 87g NaCl in 500ml aqua dest; add 250g PEG, dissolve under stirring with gentle heating; add aqua dest. and mix; add 250g PEG and dissolve under stirring with gentle heating; add to 1000ml with aqua dest.
TGBE buffer for ISO method	Dissolve tris base 12.1g, glycine 3.8g, beef extract 10g in 1l aqua dest.. Adjust pH to 9.5 with HCl

4.7. Software

For real time RT-qPCR analysis the software 7500 Software v2.3 (Applied Biosystems, Foster City, CA) was used. The amplified PCR products were detected by fluorescence and the signal was presented in a Ct-value suggesting a positive result if clear enough. Also, the calculations regarding RNA copy concentrations were performed by this program with assistance of the standard curve concentrations. The concentrations of the standard curves were calculated by Microsoft Exel with assistance of molecule concentration in the RNA extracts, product lengths of the respective standard RNAs and Avogadro-constant. During generation of RNA standards, we used the program “MegAlign” from the DNASTAR-software (Lasergene, Madison, USA) to compare the sequences of the generated PCR intermediates along with reference sequences. Also, we used the BLAST search program (http://www.ncbi.nlm.nih.gov/BLAST/, Nation Center for Biotechnology Information) to validate the amplified sequences by mapping them to the respective virus.

The statistical analyses used for comparison of the different methods and food matrices were performed with the SPSS Statistics 21 program (IBM, NewYork, USA) by Mai Dinh-Thran (BfR). They included analysis of variance homogeneity, normal distribution and the Mann-Whitney-U-test.

The NGS raw data was used for RIEMS data analysis outlined in Scheuch et al., 2015 performed by Dr. Dirk Höper (FLI, Insel Riems). Also, after NGS analysis, the BLAST search program (http://www.ncbi.nlm.nih.gov/BLAST/, National Center for Biotechnology Information) was used for genotyping of the found hNV sequences. Alignments with other NoV sequences and construction of a phylogenetic tree were performed using the CLUSTAL W method with the IUB residue weight table and the neighbor joining method implemented in the MEGALIGN module of the DNASTAR software package (Lasergene).

The statistical analyses in the thermal inactivation experiments and generation of the three different heat inactivation models were performed by Carolina Plaza-Rodriguez and Matthias Filter (BfR, Berlin, Germany). They used the open source software KNIME with the PMM-Lab extension (Filter et al., 2013).

5. Methods

5.1. Methods for specific applications

5.1.1. Comparison and optimization of detection methods

5.1.1.1. Artificial contamination of strawberries

The fresh strawberry batches were aliquoted into 25g portions, cut into pieces and transferred into 50mL tubes. The tubes were stored for up to 1h at 4°C until contamination with hNV. For the experiments comparing the different virus extraction protocols, the hNV-containing fecal sample was diluted with PBS to a concentration of 2.16 x 10^5 RNA copies/µl and 10µl of this suspension (containing 2.16 x 10^6 hNV RNA copies) were spread on the fruit surfaces under a sterile bench. The tubes were left open for 45 min for efficient adsorption of hNV to the strawberry surfaces before closing the tubes and storing them at -20°C. The frozen strawberries were divided in 25g portions and contaminated with the same hNV starting concentration shortly before starting an experiment. To avoid increased fruit juice discharge, frozen contaminated strawberries were not completely defrosted, but used directly for the experiment or after 10 min incubation at RT. HNV extraction controls (10µl each contacting the starting concentration of 2.16 x 10^6 hNV RNA copies) were generated from the same contamination solution and stored similarly. They were used as baseline for the following calculation of the recovery rates (RR). For the determination of the detection limit of the selected method, tenfold serial dilutions of the hNV solution were prepared and the 25g samples were contaminated with 10 µl aliquots containing 2.16 x 10^5 RNA copies, 2.16 x 10^4 RNA copies, 2.16 x 10^3 RNA copies, 2.16 x 10^2 RNA copies or 2.16 x 10^1 RNA copies. These samples were prepared in triplicates.

5.1.1.2. Virus extraction according to ISO/TS 15216-2

The protocol according to the revised version of the ISO/TS 15216-2 (ISO, 2013) method was used. Briefly, 25g strawberries were placed in a 400ml Stomacher bag with filter compartment. At this point, 10µl of the MS2 phage suspension were added to samples and incubated at room temperature for 10 min. Thereafter, 40ml of Tris Glycin Beef Extract (TGBE)-Buffer (pH 9.5) and 1,140 units pectinase (*A. aculeatus)*

(Sigma Aldrich, Darmstadt, Germany) were added. The sample was incubated on a horizontal shaker for 10 min at room temperature (RT) under soft tilting. This step was followed by checking the pH value and readjusting to 9.5 with NaOH. Thereafter, the sample was incubated on the horizontal shaker for additional 10 min and the pH was checked again. The procedure was repeated until the pH was stable at 9.5. Then, the buffer solution was transferred to a 50ml tube after passing through the bag filter compartment. The solution was centrifuged at 4°C and 10,000 x *g* for 10 min to remove fruit debris. The cleared solution was transferred into a new tube, the pH was adjusted to 7.0 – 7.3 with HCl and 10ml of 5 × PEG/NaCl solution (500 g/l PEG 8,000, Sigma Aldrich, 1.5mol/l NaCl) were added. The mixture was shaken vigorously for 30sec and incubated for 1h in an over-head rotator at 4°C and 60rpm. This step was followed by centrifugation at 10,000 x *g* and 4°C for 30 min. The PEG formed a pellet and the supernatant was discarded. Another centrifugation at 10,000 x *g* and 4°C for 5 min was performed to compact the PEG pellet followed by removal of liquid residues by pipetting. The pellet was dissolved in 500 µl PBS by vortexing and repeated pipetting. The solution was transferred into a fresh Eppendorf tube and 500µl of a chloroform/butanol mixture (1:1, v/v) were added. After vortexing and incubation for 5min at RT, the sample was centrifuged at 10,000 x *g* and 4°C for 15 min. Thereafter, the upper aqueous phase (400 – 500µl) was transferred to a fresh tube by pipetting. The extract was either stored at -80°C or directly used for nucleic acid extraction.

5.1.1.3. Virus extraction using porcine gastrin mucin (PGM)-coated magnetic beads

This method was based on a protocol described by Tian et al. (2005). Briefly, MagnaBind Carboxyl Derivatized Beads (Thermo Fisher Scientific, Schwerte, Germany) were agitated vigorously before 1ml was transferred into a fresh Eppendorf tube and washed 3 times. Each washing step consisted of adding 1ml PBS, detaching the beads from the tube side by careful pipetting and shaking, magnetic separation on a magnetic rack and subsequent removal of the liquid by pipetting. The PGM (Typ III PGM, Sigma-Aldrich) was dissolved in MES buffer (BupH MES Buffered Saline packs, Thermo Fisher Scientific) to a concentration of 10mg/ml. Afterwards, 1ml of this solution was added to the washed beads followed by soft agitation. Thereafter, 10mg EDC (1-Ethyl-3-(3-dimethylaminopropyl)carbodiimid, Sigma Aldrich), were dissolved in 1ml MES buffer and 100µl of the resulting solution were mixed with the PGM/bead suspension by shaking. After incubation for 30 min at RT, the unbound PGM was

removed by magnetic separation including 3 washing steps. Finally, the PGM-conjugated beads were resuspended in 1ml PBS. The hNV contaminated strawberry samples were washed with TGBE buffer including pectinase treatment and pH adjustment as described above. Thereafter, 200µl of the PGM-conjugated beads were added to 40 mL solution. The sample was incubated on a horizontal shaker for 1h under soft tilting at RT followed by magnetic separation for 30min at RT. The supernatant was aspirated, the bead pellet was dissolved in 1ml PBS and transferred to a fresh Eppendorf tube. After 3 washings, the beads were resuspended in 250µl PBS and either stored at -80°C or used directly for RNA extraction. The nucleic acid extraction protocol was slightly modified to remove the PGM-coated magnetic beads, which may interfere with the magnetic silica beads used for nucleic acid extraction. Therefore, 1ml of the lysis buffer (NucliSENS® easyMAG system, BioMérieux, Marcy l´Etoile, France) was directly added to the PGM-bead-containing samples, mixed by repeated pipetting and vortexing followed by an incubation for 5 min at RT. After magnetic separation for 5min at RT, the supernatant was obtained, magnetic silica were added and the nucleic acid extraction protocol was followed as described below.

5.1.1.4. Virus extraction by direct lysis

This method was based on a protocol published by Perrin et al. (2015). Briefly, 25g of hNV contaminated strawberries were treated with 2ml lysis buffer (NucliSENS® easyMAG system, BioMérieux, Marcy l´Etoile, France) in a 50 ml tube and incubated in an over-head rotator at RT and 60rpm for 10min. Afterwards, large strawberry debris was removed with sterile tweezers and smaller debris was pelleted by centrifugation for 10 min at 10,000 x *g* and 4°C. Finally, 3ml of the cleared supernatant were used for nucleic acid extraction as described below.

5.1.1.5. Virus extraction using TRI®Reagent

This method refers to a publication by Szabo et al. (2015), where it was originally used for analysis of sausages. Therefore, modifications were introduced according to the requirements for soft fruits. Briefly, 25g of hNV contaminated strawberry samples were treated directly with 5ml TRI®Reagent Solution (Life Technologies GmBH, Darmstadt, Germany) in a 50 ml tube followed by an incubation in an over-head rotator at RT and 60rpm for 10 min. The larger debris was removed with sterile tweezers and the smaller

debris was pelleted by centrifugation for 20 min at 10,000 x *g* and 4°C. The supernatant was transferred to a fresh tube and 200µl chloroform were added per 1ml. After vortexing and incubation for 5 min at RT, a centrifugation for 15 min at 10,000 x *g* and 4°C was performed. Subsequently, 1ml of the upper aqueous phase was used for nucleic acid extraction as described below.

5.1.1.6. Virus extraction using ultrafiltration

This method is based on protocols of several publications using ultrafiltration for virus concentration (Cheong et al., 2009; Mäde et al., 2013; Esseili et al., 2015). Briefly, 5ml PBS was added to the 25g portions of frozen hNV contaminated strawberries in a 50ml tube. The tube was incubated in an over-head rotator at RT and 60rpm for 10 min. Thereafter, large strawberry debris was removed with sterile tweezers and smaller debris was pelleted by centrifugation for 10 min at 10,000 x *g* and 4°C. The cleared solution was filtrated through a polyethersulfone (PES) filter system containing one filter with pore size 0.45µm and one with pore size 0.22µm (SARSTED, Nümbrecht, Germany). The filtered solution was transferred into a Vivaspin 20 ultrafiltration device (50.000 MWCO, Sartorius, Göttingen, Germany) and was centrifuged in steps of 15 min at 4,600 x *g* and 4°C until 500µl of the solution remained. The solution was transferred into a fresh Eppendorf tube and the ultrafiltration membrane was rinsed with 500µl PBS, which were added to the remaining solution as well. Finally, 1ml of the solution was used for nucleic acid extraction as described below.

5.1.1.7. Calculation of recovery rates, detection limit and statistical analyses

The RRs were calculated by comparison of the Ct-value of the hNV extraction control (hNV nucleic acid directly extracted from 10µl virus solution with the starting concentration) with the Ct-value of sample (hNV nucleic acid extracted from artificially contaminated strawberries after application of the respective virus extraction method). The recovery rate was calculated by the following formula (Scherer et al., 2009):

RR (%) = 2^(-Δct) x 100, where Δct = ct (sample) – ct (process control).

The detection limit of a method was defined as the lowest virus amount (expressed in RNA copy numbers) used for contamination of berries detectable by the method in at least one of three triplicates. The statistical analyses used for comparison of the

different methods and food matrices was performed by Mai Dinh-Thran and included analysis of variance homogeneity, normal distribution and the Mann-Whitney-U-test and were performed with the SPSS Statistics 21 program (IBM, NewYork, USA).

5.1.2. New methods for virus analysis on outbreak material

5.1.2.1. Phylogenetic analysis

HNV sequences identified by NGS were compared to sequences available in GenBank using the BLASTn analysis tool of NCBI. Alignments with other NoV sequences and construction of a phylogenetic tree were performed using the CLUSTAL W method with the IUB residue weight table and the neighbor joining method implemented in the MEGALIGN module of the DNASTAR software package (Lasergene). Bootstrap analysis of phylogenetic trees was performed with 1000 trials and 111 random seeds.

5.1.2.2. NGS data analysis

The frozen strawberries from the large foodborne hNV outbreak in Germany 2012 (Mäde et al., 2013) were analyzed by new detection methods. Singular berries were used for analysis by dPCR by D.Mäde and 25g for NGS analysis and RT-qPCR. Viruses were extracted according to ISO, 2013 followed by RNA extraction and purification. For metagenomic NGS analysis, we sent the resulting extract to GATC Biotech (Konstanz, Germany) on dry ice. They conducted sequencing by Illumina HiSeq 2500 in 125bp paired-end mode. Due to intellectual property no protocol details can be revealed by GATC. The resulting raw data was used for RIEMS data analysis outlined in Scheuch et al., 2015 by Dr. Dirk Höper (FLI, Insel Riems). During RIEMS analysis two reads were found belonging to the *Caliciviridae* family, species Norwalk virus. These sequences were blasted against the open access NCBI database.

5.1.3. Methods for analysis of thermal inactivation

5.1.3.1. mNV and TV propagation

MNV was propagated in the mouse macrophage cell line RAW 264.7. The cells were cultured in Dulbecco's Modified Eagle Medium (DMEM) supplemented with 10% fetal

calf serum, 1% glutamine, 1% NEAAs and 1% gentamycine at 37°C and a 5% CO_2 atmosphere. The media and supplements were purchased from PAN^{TM} Biotech (Magdeburg, Germany). Virus infection was performed according to Li and Chen (2015). At 48h after mNV inoculation, cells were subjected to three freeze-thaw cycles and the supernatant was stored in aliquots at -80°C. MNV was quantified by plaque assay and real time RT-PCR as described below.

Furthermore, TV was propagated in the monkey kidney cell line LLC-MK2 using M199 Medium (Thermo Fisher Scientific, Schwerte, Germany) supplemented with 10% fetal calf serum, 1% NEAAs and 1% Gibco™ Antibiotic-Antimycotic (Fisher Scientific, Schwerte, Germany) at 37°C in a 5% CO_2 atmosphere. The virus was harvested at 72h after application of three freeze-thaw cycles (Li and Chen, 2015). Thereafter, TV was concentrated 10-fold from the supernatant using Vivaspin 20 ultrafiltration devices (50.000 MWCO, Sartorius, Göttingen, Germany) before it was aliquoted and stored at -80°C. TV was quantified by plaque assay and real time RT-PCR as described below.

5.1.3.2. Inoculation of the samples and heat treatment

Based on the recommendations for heat inactivation studies as suggested by Arthur and Gibson (2015a), temperatures of 50°C, 56°C, 63°C, 72°C and 80°C were selected for the experiments. The applied time intervals (tab.8) were chosen based on results from related studies (Arthur and Gibson 2015a; Bozkurt et al., 2015b; Araud et al., 2016, Croci et al., 2012). All analyses were done in triplicates. The puree samples were inoculated with a solution of 450µl mNV, 450µl TV and 100µl hNV (100µl of a 1:2 dilution containing 2.7 x 10^8 hNV RNA copies). Previous experiments indicated that the addition of 1ml room-tempered virus solution to the 15g preheated strawberry puree induced a large transient temperature decrease. Therefore, the 50 ml tubes containing 15g strawberry puree were preheated in a water bath to 58°C, 65°C, 74°C, 86°C or 90°C, respectively, as measured by a meat thermometer. Thereafter, the tubes were quickly transferred to a heat block with a temperature of 50°C, 56°C, 63°C, 72°C or 80°C, respectively. Immediately, the virus solution (or water control) was added to the puree sample under constant stirring with the pipet tip leading to a quick equilibration at the desired temperatures. These conditions were derived from experiments as described in the results section. After the distinct incubation time was

completed, the reaction was stopped by the addition of 20 ml cold (6°C) Tris Glycin Beef Extract (TGBE) Buffer (pH 9.5) and the tubes were placed on ice for 10 min.

5.1.3.3. Virus extraction from puree

According to the results of previous experiments, a virus extraction protocol combining a PEG precipitation method with an ultrafiltration method was chosen based on published protocols shown in fig.9 (ISO, 2013; Bartsch et al., 2016; Butot et al., 2009; Huang et al., 2016). Briefly, 150µl pectinase (*A. aculeatus)* (Sigma Aldrich, Darmstadt, Germany) were added to the heat-treated samples. Thereafter, the solution was centrifuged at 5,000 x *g* at 4°C for 20 min for removal of debris and the supernatant was separated into two parts of 15 ml each.

For plaque assay analysis, 15ml were transferred to a 20ml syringe attached to a 0.22 µm PES filter (Merck Millipore, Darmstadt, Germany) for sterile-filtration. The filtrate was transferred to a Vivaspin 20 ultrafiltration device (50.000 MWCO, Sartorius, Göttingen, Germany) and centrifuged for 1h to 2h at 4,600 x *g* and 10°C until concentration to 500µl.

For capsid integrity testing, the other 15ml portion was mixed with 4ml of a polyethylene glycol (PEG) solution (500 g/l PEG 8000, 1.5 mol/l NaCl) in a 50ml tube. The solution was incubated and centrifuged as described above resulting in a compacted pellet (Bartsch et al., 2016). The pellet was resuspended in 150µl PBS and subsequently subjected to RNase A treatment (see below).

5.1.3.4. Virus infectivity titration with plaque assay

The plaque assay was performed according to Gonzalez-Hernandez et al. (2012). Briefly, RAW 264.7 cells seeded in six-well plates were inoculated with 10-fold dilutions of the virus extracts (10^{-1} to 10^{-6} dilutions, each 50µl sample in 450µl DMEM without FCS). After infection, the solution was removed, and the cells were overlaid with 2 ml Eagle minimum essential medium (MEM; Lonza, Köln, Germany) containing 1.5% low melting agarose, 5% FCS, 1% glutamine and 1% gentamycine. After incubation for 48h at 37°C and 5% CO_2, 2ml neutral red solution (0.33% w/v in DPBS; Carl Roth GmbH, Karlsruhe, Germany) were added to each well and the cells were incubated for 2 h. The solution was removed, and plaques were counted on a light tablet.

Previous experiments indicated that LLC-MK2 cells could not be infected with TV present in the ultrafiltration concentrate from the virus extraction procedure. Therefore, an additional purification step using PEG precipitation was applied with 400µl of the ultrafiltration concentrate. Briefly, 100µl PEG solution was added, mixed by vortexing for 30sec and incubated in an overhead incubator at 40rpm for 30 min. The samples were centrifuged for 5 min at 10.000 x *g* and RT, the supernatant was discarded, and the pellet was resuspended in 100µl PBS. The plaque-assay was performed with this solution with a similar protocol as described above for mNV; however, LLC-MK2 cells, 2 x M199 medium and Gibco™ Antibiotic-Antimycotic (Thermo Fisher Scientific, Schwerte, Germany) were used. Plaques were counted by holding the plates against daylight, because some small plaques were not visible on the light tablet.

The PFUs in total were calculated based on a common formula for calculation of PFU per mL (Gonzalez-Hernandez et al., 2012): PFU/volume = plaque number/(inoculation volume x dilution). The well with the highest dilution and a plaque number >10 (if available) was used for quantification.

5.1.3.5. RNase A treatment

RNase treatment was performed according to Schielke et al. (2011), with some modifications. Briefly, 5.25µl of a 1:10 dilution of RNAse A (7.000 U/ml, Qiagen) were added to 150µl virus extract. After careful mixing, the sample was incubated for 1 h at 37°C. Thereafter, 27U of QIAGEN RNase Inhibitor (4 U/µl, Qiagen) were added to the sample followed by an incubation for 30 min at RT. After adding 150µl chloroform-butanol (1:1, v/v), the mixture was vortexed and incubated for 5 min at RT. The sample was centrifuged at 10,000 x g and 4°C for 15 min and the upper aqueous phase (150µl) was transferred to a fresh tube. The nucleic acids were extracted as described below. Sample volumes of 150µl were used and the RNA was eluted in 60µl elution buffer. After RNA purification, 75U of Protector RNase Inhibitor (40U/µl, Sigma Aldrich) were added to the RNA followed by incubation for 30 min at room temperature. The samples were stored at -80°C.

5.1.3.6. Mathematical modeling

The statistical analyses and generation of the three different heat inactivation models were performed by Carolina Plaza-Rodriguez and Matthias Filter. Prior to the model

generation process, a data preprocessing step was applied to identify and remove outliers. Thereafter, the applicability of three different linear and non-linear equations (Linear Bigelow, bilinear and Weibull) to the log_{10}-transformed experimental data was assessed. Based on this pre-analysis, primary models were generated for each of the temperatures (50, 56, 63, 72, and 80°C) and each virus/method combination using the Linear Bigelow equation utilizing the free, open source software KNIME with the PMM-Lab extension (Filter et al., 2013). The Bigelow equation was selected, as the data showed log-linear inactivation characteristics at all temperature regimes.

Secondary models were generated that describe the dependency of *D*-value on temperature. For this, a log-linear regression model was generated for each virus strain and experimental approach.

A tertiary predictive model was then generated for hNV by fitting a combined primary-secondary model through all available experimental data from 50°C to 80°C in a so-called one-step fitting procedure, applying the maximum-likelihood-based approach proposed by Lorimer and Kiermeier (2007).

5.2. General methods

5.2.1 Nucleic acid extraction

For nucleic acid extraction, the NucliSENS® easyMAG system (BioMérieux, Marcy l´Etoile, France) was used according to the manufacturer's instructions. The sample volumes amounted between 150µl and 1,000µl, depending on the virus extraction protocol. Elution was done with 60µl or 100µl elution buffer and the extracts were stored at -80°C until real-time RT-PCR analysis.

5.2.2. RNA purification using Mobispin S-400 columns

The MobiSpin S-400 columns (MoBiTec, Göttingen, Germany) were used according to the instructions of the supplier (MoBiTec GmbH, 2012). Briefly, the column was shortly vortexed, the bottom plug removed, and the cap loosened. The column was then placed onto a 1.5ml Eppendorf tube and centrifuged for 1min at 800 x *g* at RT to compact the matrix. The column was placed onto a new 1.5ml Eppendorf tube and 30µl to 50µl of the RNA extract was added to the center of the resin. After centrifugation

for 2min at 800 x *g* at RT, the purified RNA was present at the bottom of the tube. The purified RNA was directly used or stored at -80°C until real-time RT-PCR analysis.

5.2.3. Generation of RNA standards for hNV, MNV and TV

The virus standards were generated according to Kreuzer et al., 2012 . The viral target regions corresponding to genome segments of hNV, MNV or TV were amplified by specific primers in a conventional RT-PCR using the Qiagen One Step RT-PCR kit (Qiagen, Hilden, Germany). The viral target regions, the primers and cycling conditions are described in the following section. The amplified target regions were cloned into the pCR4-TOPO vector using the TOPO TA Cloning Kit (Invitrogen, Karlsruhe, Germany). After Sequencing, the inserts which were now flanked by a T7 promotor by PCR were amplified with primers M13F and M13R (Invitrogen, Karlsruhe, Germany). The resulting PCR products were purified with the QIAquick Gel Extraction Kits (Qiagen, Hilden, Germany) and transcribed to stable RNA *in vitro* using the MEGAscript T7 Kit (Applied Biosystems, Darmstadt, Germany) according to the manufacturer's instructions. After a DNase I (recombinant, RNase free; Roche, Mannheim, Germany) digestion step, in vitro transcripts were purified via High Pure RNA Isolation Kit (Roche, Mannheim, Germany) and the RNA was stored at −80°C. In the last step, RNA concentrations were photo metrically measured by NanoDrop device (Thermo Fisher Scientific, Bonn, Germany) and used to calculate the numbers of RNA molecules per µl. For the generation of the RNA standards, tenfold dilution series of hNV, mNV or TV RNA standards were prepared and validated by real-time RT-PCRs. Afterwards these standard dilution series were used for the quantification of hNV, mNV and TV RNA in our artificial samples and outbreak material.

5.2.4. (Quantitative) real-time RT-PCR

Real-time RT-PCR analyses were performed using 5µl of extracted nucleic acids in 25µl reactions with the QuantiTect Probe RT-PCR Kit (Qiagen, Hilden, Germany) in an ABI Prism 7500 Sequence Detection System (Applied Biosystems, Foster City, CA). Primer sequences and probes are listed in tab.4. HNVGII detection was performed according to Hoehne & Schreier (2006) with primers from Loisy (2005). Also, bacteriophage MS2 was detected by a protocol established by Dreier et al. (2005). Additionally, mNV detection was performed according to Kitajima et al., 2010 with a

primer and probe concentration of 40µM. TV was detected by a protocol from Xu et al., 2015 with a small alteration: The original HEX-BHQ probe was replaced by a FAM-BHQ probe but the probe sequence was not modified. The primers and probe were utilized in a concentration of 20µM. The cycling conditions for the respective viruses were performed as in the mentioned individual sources in accordance with the QuantiTect Probe RT-PCR Kit manual instructions.

In the experiments for determination of the detection limits during method comparison and optimization, hNVGI and hNVGII detection was performed according to ISO/TS 15216-2 protocol including. Therefore, the RNA Ultrasense One Step qRT-PCR System (Thermo Fisher Scientific, Schwerte, Germany) was used here according to the manufactures protocol.

Quantitative real time RT-PCR analyses were performed with standard curves. Since 5µl nucleic acid were used in every reaction the standard curves gave us the number of RNA copies per 5µl. Because the nucleic acids of the relevant samples were extracted in 60µl elution buffer, the number of RNA copies per 5µl had to be multiplied with 12 to receive the total amount of RNA copies for one sample. The RNA copy numbers were calculated using the fixed concentration of the standard dilutions in combination with the 7500 Software v2.3 software (Applied Biosystems, Foster City, CA).

6. Results

6.1. Comparison and optimization of human norovirus detection methods on berries

6.1.1. Testing of different strawberry batches

First, strawberries from different harvest times and with distinct colors were validated regarding their inhibitor level with the same method. Five different batches of strawberries were purchased from different stores, artificially contaminated with hNVGII.3, frozen and subsequently tested using the ISO/TS 15216 method. The batches differed in ripeness and matrix consistency and consisted either of fresh or frozen strawberries (tab.11). As evident from tab. 8, the calculated hNV RRs differed remarkably between the batches despite the use of the identical contamination and detection protocol. Mean hNV RRs between 10.29 ± 6.03% and 0.21 ± 0.13% were evident, which showed a clear correlation with the ripeness and fresh/frozen condition at purchase. A statistical analysis showed that only the differences in the hNV RRs between batch 2 and 3 as well as between batch 4 and 5 were not significant (p=0.955 and p=0.065), whereas the RRs between all other batches were highly significant (p-values between <0.001 and 0.026). The highest hNV RRs were determined for fresh berries showing a light red color, whereas the lowest hNV RRs were found in frozen, dark red colored strawberries.

Table 11: Results of five strawberry batches artificially contaminated with hNVGII.3 using the ISO/TS 15216-2 method. The strawberries were originally purchased in different stores, contaminated with hNV GII.3 and frozen before analysis. The characteristics of the berries from the different batches and the resulting hNV recovery rate (RR) along with the standard deviation (SD) are shown.

	Batch 1	Batch 2	Batch 3	Batch 4	Batch 5
Sample number	6	6	9	6	6
Condition at purchase	fresh	fresh	fresh	frozen	frozen
Harvest time	November	September	May	unknown	unknown
Fruit color	light red	red	red	dark red	dark red
RR mean value ± SD (%)	10.29 ± 6.03	2.95 ± 2.44	2.77 ± 2.39	0.59 ± 0.49	0.21 ± 0.13

6.1.2. Comparison of methods for hNV detection in strawberries

Second, five virus extraction methods were selected from the published literature for direct comparison concerning recovered virus amounts. They were based on ultrafiltration, direct lysis in RNA extraction buffer, lysis with TRI®Reagent or the use of PGM-coated magnetic beads and compared to the ISO/TS 15216-2 method. Strawberries of batches 3 and 4 (at least 3 samples of each) were artificially contaminated with hNVGII.3, frozen and treated with the respective virus extraction protocol. Thereafter, an identical protocol for RNA extraction and real-time RT-PCR was applied in all cases for hNV detection. As evident from tab.12, the hNV RRs differed remarkably between the methods showing mean values from 0.01± 0.03% to 1.71 ± 2.31%. The highest hNV RR was achieved by using the ISO/TS 15216 method.

Table 12: Method comparison for hNVII.3 detection on strawberries. Strawberries of batches 3 and 4 were artificially contaminated with hNV GII.3, frozen and subsequently analyzed by the mentioned methods. At least 3 samples from each batch were analyzed with each method and the mean hNV recovery rates (RRs) along with the standard deviation (SD) are indicated.

Method	RR mean ± SD (%)	Reference
ISO/TS 15216	1.71 ± 2.31	ISO (2014)
Ultrafiltration	0.98 ± 0.95	Esseili *et al.* (2015)
Direct lysis	0.52 ± 0.54	Perrin *et al.* (2015)
PGM magnetic Beads	0.04 ± 0.1	Tian *et al.* (2005)
TriReagent	0.01 ± 0.03	Szabo *et al.* (2015)

6.1.3. Optimization of the ISO/TS 15216 method using MobiSpin S-400 columns

Third, due to fact that the ISO method delivered the best recovery rates we focused on further optimizing this method while reducing the inhibitor level in the RNA extracts. To further purify the RNA extracted from the artificially contaminated strawberries, the use of MobiSpin S-400 columns in addition to the ISO/TS 15216 protocol was tested. Three different batches of strawberries were analyzed, which exhibited different RT-PCR-inhibiting activities as assessed in the first set of experiments. In detail, one half of the RNA extract from one sample was treated with a MobiSpin column and compared to the untreated other half of the RNA extract using real time RT-qPCR. As shown in tab.10, the hNV RRs could be largely improved by using the columns in case of the strawberry batches 3 and 4. For these batches, the improvement also turned out to be highly significant (tab.13). In contrast, no improvement in the hNV RRs could be obtained in case of batch 1.

Table 13: Optimization of the ISO/TS 15216-2 method using MobiSpin S-400 columns. Strawberries of batches 1, 3 and 4 were artificially contaminated with hNV GII.3, frozen and subsequently analyzed by the ISO/TS 15216 method with or without a further purification step of the extracted RNA using MobiSpin S-400 columns. A total of 6 samples were analyzed for each batch and the mean hNV recovery rates (RRs) along with the standard deviation (SD) are indicated. The p-values obtained by Mann-Whitney-U-test indicating the significance of differences between the results of both methods are indicated right.

Batch	ISO/TS 15216 method RR mean ± SD (%)	ISO/TS 15216 method + MobiSpin columns RR mean ± SD (%)	p-value
1	9.85 ± 6.88	9.42 ± 5.22	1.00
3	2.83 ± 2.92	15.28 ± 9.73	0.09
4	0.59 ± 0.49	5.60 ± 1.58	0.02

6.1.4. Determination of detection limits

For the direct comparison of the standard and our extended ISO protocol tenfold dilutions of the hNVGII.3 suspensions were used for artificial contamination of strawberries of batch 2. The amounts of virus RNA copies per sample were calculated in advance for the subsequent determination of the detection limits by one positive RNA detection out of three samples. Afterwards, the samples were tested in triplicate by the ISO/TS 15216-2 method with or without the use of MobiSpin S-400 columns. As shown in tab.14, real time RT-qPCR analysis confirmed that the detection limit was about 10-fold lower after the use of the columns as compared to the original ISO/TS 15216-2 method. The results confirm the better performance of the optimized method and indicate a higher sensitivity of this method for strawberries containing high amounts of RT-PCR inhibitors.

Table 14: Comparison of detection limits for hNV GII.3 on artificially contaminated strawberries using the ISO/TS 15216-2 method with and without using MobiSpin S-400 columns. 1:10 serial dilutions of a quantified hNV GII.3 solution were used for artificial contamination of strawberries from batch 2. The detection limit was defined by real time RT-qPCR as the highest dilution showing a positive detection in at least one of 3 samples.

Inoculation level (hNVII RNA copies/ 25 g strawberries)	ISO/TS 15216 method positive/samples tested	ISO/TS 15216 method + MobiSpin columns positive/samples tested
2.16×10^5	3/3	3/3
2.16×10^4	3/3	3/3
2.16×10^3	1/3	3/3
2.16×10^2	0/3	1/3
2.16×10^1	0/3	0/3

6.1.5. Testing of field samples

Thereafter, the performance of the optimized method on samples naturally contaminated with hNV was assessed. First, a batch of frozen strawberries imported from China involved in a large hNV gastroenteritis outbreak in Germany in 2012 was analyzed. A total of 22 subsamples were derived from the batch and tested with the ISO/TS 15216-2 method with or without the use of MobiSpin S-400 columns before real time RT-PCR analysis. The addition of the MobiSpin S-400 column-based RNA purification increased the detection rate of hNVGI from 22.3% (5 out of 22) to 59.1% (13 out of 22) and for hNVGII from 40.1% (9 out of 22) to 90.9% (20 out of 22) (tab.15). Second, the performance of the methods was also assessed for naturally contaminated frozen raspberry mash, imported from China and involved in a small gastroenteritis outbreak in Germany in 2016 (tab.16). Without RNA purification only 33.3% (2 out of 6) samples were tested positive for hNVGII. In contrast, with RNA purification 66.7% (4 out of 6) samples were hNVGII-positive using the MobiSpin S-400 column-based RNA purification. Furthermore, the RRs for the used process control bacteriophage MS2 were significantly improved by use of the columns. The RRs for MS2 in the strawberries with RNA purification were about 100-fold higher compared to the samples without purification. In raspberry mash, MS2 was not detectable in any of the six samples (0%) without use of the columns. After using of the Sephacryl-based columns MS2 was detectable in all six raspberry samples (100%). However, as the RRs of MS2 were generally very low, they are questioning the use of this bacteriophage as appropriate process control for analysis of berries.

Table 15: Analysis of frozen strawberry field samples involved in a hNV outbreak in Germany 2012 using the ISO/TS 15216-2 method with and without using MobiSpin S-400 columns. 22 sub-samples were analyzed and the detection rates for hNVGI and hNVGII as well as the calculated recovery rate (RR) for the process control (bacteriophage MS2) are shown. NA – not applicable.

Sub-Sample number	hNV GI ISO/TS 15216 method	hNV GI ISO/TS 15216 method+ MobiSpin columns	hNV GII ISO/TS 15216	hNV GII ISO/TS 15216 method+ MobiSpin columns	MS2 RR(%) ISO/TS 15216 method	MS2 RR(%) ISO/TS 15216 method+ MobiSpin columns
1	-	-	-	+	0.0037	0.16
2	+	+	-	-	0.0022	0.15
3	-	-	-	-	0.0026	0.13
4	-	-	+	+	0.0025	0.10
5	-	+	+	+	0.0024	0.16
6	-	+	-	+	0.0023	0.15
7	-	+	+	+	0.0031	0.16
8	-	+	-	+	0.0012	0.08
9	+	-	+	+	0.0001	0.01
10	-	-	-	+	0.0013	0.07
11	+	+	+	+	0.0019	0.10
12	-	+	+	+	0.0034	0.25
13	-	-	-	+	0.0026	0.13
14	-	+	-	+	0.0044	0.36
15	+	+	-	+	0.0027	0.11
16	+	+	+	+	0.0052	0.19
17	-	-	-	+	0.0002	0.02
18	-	-	-	+	0.0002	0.04
19	-	+	+	+	0.0013	0.08
20	-	+	-	+	0.0020	0.22
21	-	+	+	+	0.0017	0.17
22	-	-	-	+	0.0004	0.05
Positive/ samples tested (%)	5/22 (22.3%)	13/22 (59.1%)	9/22 (40.1%)	20/22 (90.9%)	22/22 (100%)	22/22 (100%)
RR mean ± SD (%)	NA	NA	NA	NA	0.0023 ± 0.0013	0.13 ± 0.08

Table 16: Analysis of frozen raspberry mash field samples involved in a hNV outbreak in Germany 2016 using the ISO/TS 15216-2 method with and without using MobiSpin S-400 columns. Six sub-samples were analyzed for hNV GII and for the process control (bacteriophage MS2). For both viruses the calculated detection rates are shown.

Sub-Sample number	hNV GII ISO/TS 15216	hNV GII ISO/TS 15216 method+ MobiSpin columns	MS2 ISO/TS 1 5216 method	MS2 ISO/TS 15216 method+ MobiSpin columns
1	-	+	-	+
2	-	-	-	+
3	-	+	-	+
4	+	+	-	+
5	-	-	-	+
6	+	+	-	+
Positive/ samples tested (%)	2/6 (33.3%)	4/6 (66.7%)	0/6 (0%)	6/6 (100%)

6.2. New methods for virus identification on outbreak material

6.2.1. Virus identification by next generation sequencing

First, it should be assessed if hNV and other viruses on strawberries can be detected by NGS. Therefore, a total of 25 g of frozen strawberries from a lot involved in the hNV gastroenteritis outbreak in Germany 2012 was subjected to RNA isolation followed by NGS using the Illumina HiSeq 2500 device. In total, 28,856,294 sequence reads were generated. The initial metagenomics data analysis performed by GATC did not detect any human-pathogenic gastroenteritis virus sequence. Therefore, all data were analyzed more comprehensively analyzed by Dr. Dirk Höper through the RIEMS 4.0 software. The sequence quality check identified 98,611 reads with low quality, which were not analyzed further. Out of the remaining sequences, 220,802 reads could not be classified leading to 28,536,881 reads, which showed significant homologies to known sequences. The classification of sequences according to the superkingdom resulted in 24,842,819 eukaryotic, 3,690,920 bacterial, 3,064 viral and 56 archaeal sequences.

The results generated by RIEMS analysis including the most abundant microorganisms and most interesting viruses are shown in tab.17 and tab.18 and were validated by us. The most frequent sequence counts belong to bacteria (10,321 – 3,119,912) and eukaryotes (595,163 – 15,346,144) including mostly flowers, strawberries, yeast, fungus and environmental germs. Also, plant-associated pathogenic bacteria were found: *Tatumella citrea* causing pink disease in pineapple and *Kosakonia oryzae* which is associated with rice and has been shown to possess plant growth-promoting properties including the ability to fix atmospheric nitrogen. In addition, 22,1477 counts of *Salmonella enterica* were found.

The smallest unit of the identified microorganisms are archea with only 3 to 6 sequence counts in the top five hits. These are environmental germs with different habitational preferences from peatlands to deserts including methane producers.

The five most frequent viruses (183 – 1,208 counts) identified on the strawberries were bacteriophages or strawberry plant viruses causing severe losses in the cultivated fruits. Considering all identified viruses, bacteriophages were the most abundant species. Also, many plant- and fungus-associated viruses were found. The smallest group was represented by insect, animal and human viruses. In tab.17 we show the

most interesting human pathogens discovered including human immunodeficiency virus (HIV), hepatitis B virus (HBV), Dengue virus, Alphapapillomavirus 9 causing warts up to tumors in humans and monkeys as well as Mamastrovirus 3 inducing infantile gastroenteritis in humans, mammals and vertebrates. Additionally, some animal pathogens were found including porcine type C oncovirus inducing tumors and immunodeficiencies, bat mastadenovirus G causing respiratory diseases, elephantid betaherpesvirus 1 which causes fatal hemorrhagic disease in Asian elephants and sea otter poxvirus which induces small superficially ulcerated skin lesions.

Furthermore, two sequences with similarities to hNV were identified. One of the reads had a length of 151 bp and showed 100% sequence identity to the central part of the ORF1 of a norovirus GII.P16/GII.13 strain. The other read with a length of 146 bp showed 100% identity to the ORF1/ORF2-overlapping region of other hNV GII.P16/GII.13 strains. During the outbreak, several norovirus genotypes have been identified in patients, with a frequent detection of GII.P16/GII.13 strains (Höhne et al., 2015). Also, two genome fragments of a GII.P16/GII.13 strain could be sequenced directly from the involved strawberries (Mäde et al., 2013). A phylogenetic tree set up with the NGS-derived 146 bp sequence together with the most closely related sequences as determined by BLASTn search is shown in fig. 8.

Table 17: Most abundant sequences assigned to specific species as detected by NGS on the strawberry outbreak sample. The five most abundant species per superkingdom and their families, the respective read counts and highest identities with sequences present in the NCBI database are shown. Details on the characteristics of the detected species are given together with respective references.

Organism	Family	Species	counts	Sequence Identity (%)	Details	Reference
Eukaryote	Rosaceae	Sanguisorba sitchensis	15346144	89.8 - 100	Flower	Vivaipriola
	Hydrangeaceae	Jamesia americana	2486369	97.47	Californian shrubs	Calscape
	Rosaceae	Fragaria vesca	2355716	68.0 - 100	Wild strawberry	Urrutia et al., 2017
	Saccharomycetaceae	Saccharomyces cerevisiae	892091	70.0 – 90.0	Yeast	Michel et al., 2017
	Rhizopodaceae	Rhizopus stolonifer	595163	84.91 - 100	Postharvest fungal pathogen	Adriaenssens et al., 2011
Bacteria	Erwiniaceae	Tatumella citrea	3119912	71.43 - 100	Causing pink disease in pineapple	Brady et al., 2010
	Enterobacteriaceae	Salmonella enterica	221477	70.32 - 100	Enteric pathogen or non-pathogenic environmental strains	Altıntaş Kazar et al., 2016
	Enterobacteriaceae	Kosakonia oryzae	107219	74.16 - 90.39	Associated with rice, nitrogen fixation	Meng et al., 2015
	Rhodanobacteraceae	Frateuria aurantia	17074	74.29 - 100	Environmental germ	Joyeux et al., 2015
	Rhodanobacteraceae	uncultured Frateuria sp	10321	97.79 - 100	Environmental germ	Joyeux et al., 2015
Archaea	Methanobacteriaceae	Methanobacterium paludis	6	75.51 - 84.31	Important environmental germ in peatlands	Cadillo-Quiroz etal., 2014
	Unknown	uncultured archaeon	6	81.97 - 93.33	Environmental germ	Auguet et al., 2010
	Unknown	Nanohaloarchaea archaeon SG9	4	90.0 - 92.11	Environmental germ	Crits-Christoph et al., 2016
	Methanosarcinaceae	Methanosarcina sp WWM596	3	77.45 - 83.33	Methane producing environmental germ	Barros et al., 2017
	Methanobacteriaceae	Methanobrevibacter ruminantium	3	88.37 - 90.48	Methane producing environmental germ	Wei et al., 2017
Viruses	Alphaexiviridae	Strawberry mild yellow edge virus	1208	83.5 - 95.15	Causes severe losses in cultivated strawberries	Jelkmann et al., 1990
	Caulimoviridae	Strawberry vein banding virus	292	97.83 - 100	Might cause losses in cultivated strawberries	Mahmoudpour et al., 2003
	Myoviridae	Escherichia phage ESCO13	218	68.97 - 86.0	Bacteriophage infecting E. coli	Trotereau et al., 2017
	Podoviridae	Pantoea virus Limelight	217	68.46 - 91.49	Lytic bacteriophage infecting *Pantoea agglomerans*	Adriaenssens et al., 2011
	Myoviridae	Enterobacteria phage ECGD1	183	68.0 - 97.14	Bacteriophage	UniProt

Table 18: Mammalian virus sequence reads detected by NGS on the strawberry outbreak sample. The assignment of virus species and their families, the respective read counts and highest identities with sequences present in the NCBI database are shown. Details on the characteristics of the detected viruses are given together with respective references.

Family	Species	Counts	Sequence identity (%)	Details	Source
Adenoviridae	Bat mastadenovirus G	1	94.12	Causes respiratory disease in bats	Ogawa et al., 2017
Astroviridae	Mamastrovirus 3	1	98.1	Causes gastroenteritis in humans and animals	Jarchow-Macdonald et al., 2015
Caliciviridae	Norwalk virus	2	100	Causes gastroenteritis in humans	Atmar et al., 2014
Flaviviridae	Dengue virus	1	83.08	Causes hemorrhagic fever in humans	Shihada et al., 2017
Hepadnaviridae	Hepatitis B virus	1	89.13	Causes hepatitis in humans	Haussig et al., 2017
Herpesviridae	Elephantid betaherpesvirus 1	1	80.6	Causes fatal hemorrhagic disease in Asian elephants	Ehlers et al., 2006
Papillomaviridae	Alphapapillomavirus 9	1	87.5	Causes warts and tumors in humans	Fuller et al., 2017
Poxviridae	Sea otter poxvirus	1	85.71	Causes ulcerated skin lesions in sea otters	Tuomi et al., 2014
Retroviridae	Human immunodeficiency virus 1	1	86.28	Causes AIDS in humans	Bätzing-Feigenbaum et al., 2008
	Porcine type C oncovirus	1	98.25	May induce tumors and immunodeficiencies	Denner et al., 2003

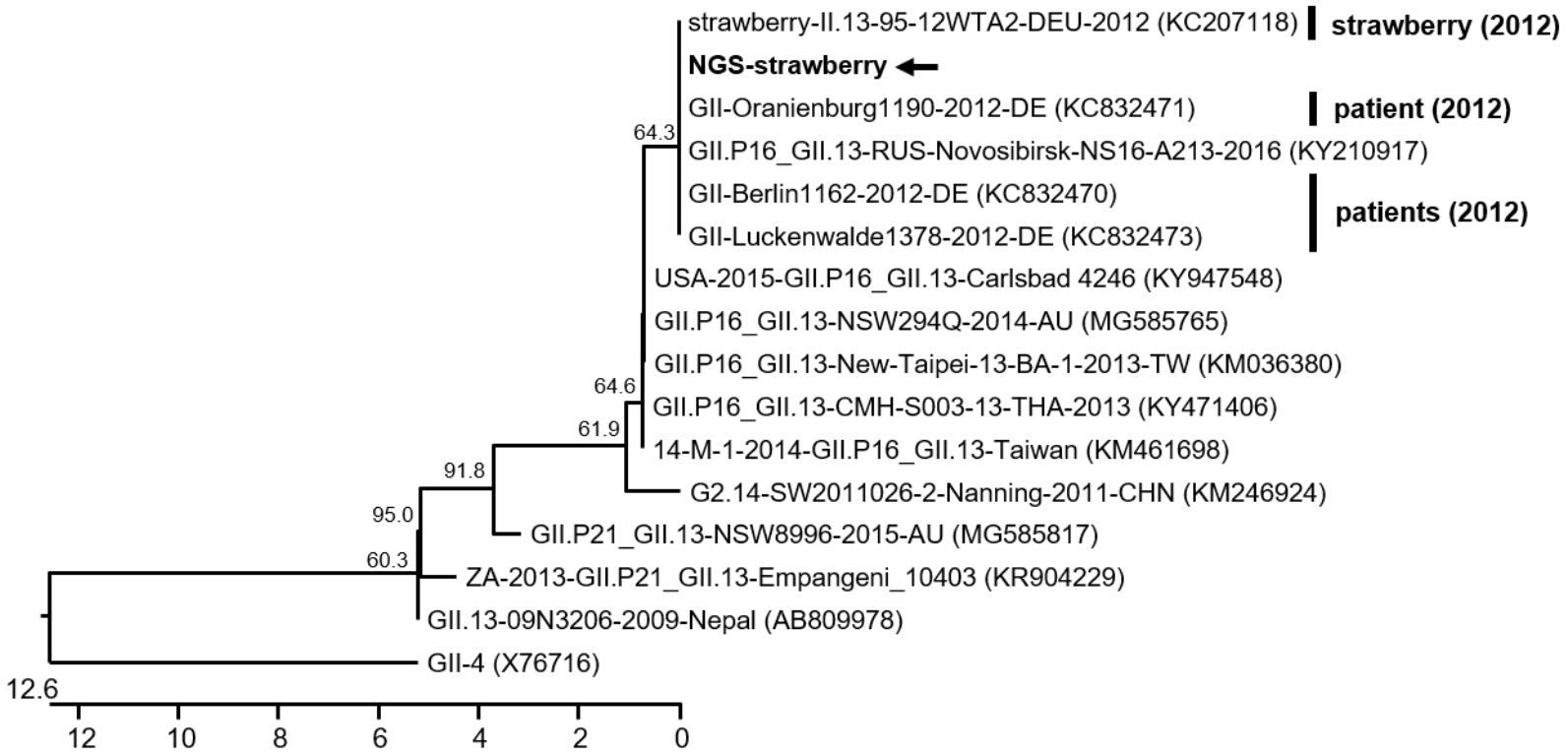

Figure 8: Phylogenetic tree showing the relationship of the 146 bp norovirus sequence detected in the strawberry sample by NGS with other closely related norovirus sequences. Included are the 10 sequences showing the highest identify with the norovirus sequence in a BLASTn search of GenBank as well as four more distantly related sequences; the GII.4 sequence serves as an outgroup. The sequences are labelled with their strain designation, genotype (as available), year of detection, country of origin and the GenBank accession number. The NGS-derived norovirus sequence is marked with an arrow and sequences derived from the outbreak in 2012 in Germany are indicated. The tree was set up using the neighbour-joining method implemented in the MEGALIGN module of the DNASTAR software package (Lasergene). Bootstrap values >50 % are indicated.

6.2.2. hNV quantification by RT-qPCR and dPCR

Second, real time RT-qPCR results were compared to RT-dPCR results generated by Prof. Dietrich Mäde regarding method effectivity and sensitivity. In order to quantify the hNV amount present in the strawberry sample, RT-dPCR and RT-qPCR were applied and compared to each other. The analyses were conducted in different laboratories using different bags from the same lot of strawberries. For dPCR analysis, only one strawberry was used per sample. In total, ten samples were analyzed individually, from which three were tested negative for hNV. The viral load of the other samples ranged from 34 up to 102 RNA copies (tab. 19). For RT-qPCR analysis, samples of 25 g were used. In total, 22 samples were analyzed resulting in a NoV-negative result in one sample. The viral load per 25 g of the other samples ranged from 7 to 1031 RNA copies (tab. 19).

In average, 25 g of the sample corresponded to 4.5 individual strawberries. In order to enable a comparison between the results of RT-dPCR and RT-qPCR, the respective values were therefore calculated using the factor 4.5. By this, an average RNA copy number of 185 and 257 per 25 g were calculated for RT-dPCR and RT-qPCR, respectively. Obviously, RT-dPCR leads to a slightly higher estimation of hNV concentration in the berries as compared to RT-qPCR.

Table 19: hNVII quantification from outbreak material (2012) by RT-qPCR and RT-dPCR. Viruses from 25g or one frozen strawberry were extracted using ISO/TS 15216-2 method. After RNA extraction and and purification by MobiSpin columns **or** 1:10 dilution hNVII was quantified using real time RT-PCR with standard curve or dPCR. * calculated RNA copies for 25g. **calculated RNA copies for one berry.

Sample number	RT-qPCR (hNVII RNA copies per 25g)	RT-dPCR (hNVII RNA copies per berry)
1	102	0
2	145	34
3	0	102
4	492	0
5	227.5	0
6	109	78
7	524.5	58
8	249	28
9	220	72
10	7	38
11	1031	
12	431.5	
13	345	
14	151	
15	205	
16	233	
17	117	
18	271	
19	203	
20	134	
21	35.5	
22	411	
Range per 25 g	0 – 229*	0 - 102
Average per 25 g	57*	41
Range per berry	0 - 1031	0 – 459**
Average per berry	257	185**

6.3. Thermal inactivation of human norovirus in strawberry puree

6.3.1. Method development and optimization

First, an optimized experimental protocol for the performance of a thermal inactivation study had to be developed. Since there are multiple factors influencing result accuracy and comparability many options for experiment design had to be considered. As hNV stability could not be directly assessed due to the lack of reliable cell culture-based infectivity assays, an alternative strategy involving surrogate viruses and molecular assays was developed. As a result, mNV and TV were selected as surrogate viruses and a capsid integrity assay based on RNase I treatment of hNV particles was additionally applied. The thermal treatment involved temperatures between 50°C to 80°C according to the suggestion of Arthur and Gibson (2015a). The applied distinct temperature/time combinations are listed in tab.20.

Table 20: Temperature/time combinations used in the heat treatment study.

Temperature in °C	**Treatment time**				
50	15 min	30 min	45 min	60 min	90 min
56	5 min	10 min	20 min	30 min	40 min
63	1 min	2 min	5 min	12 min	15 min
72	5 sec	10 sec	20 sec	30 sec	40 sec
80	2 sec	4 sec	6 sec	8 sec	-

In the first series of experiments, the three viruses were co-inoculated into strawberry puree and thereafter subjected to heating. However, it became evident that a long time was needed for heating the preparation to the desired temperatures (data not shown). Also, addition of virus solution to pre-heated strawberry puree resulted in significant temperature drops. Therefore, pre-heating of strawberry puree at higher temperatures resulting in the distinct target temperature after adding of the virus solution was applied in the final protocol as described in tab.21.

Table 21: Assessment of temperatures of strawberry puree before and after addition of virus solutions. The strawberry puree was pre-heated in a water bath to the respective temperatures A or B and transferred to a heating block with the indicated target temperature. Thereafter, 1 ml of virus solution (or water) at RT was added water and the temperature drop was measured by a meat thermometer.

Preheat Temp. A [°C]	Temperature drop to (after adding 1ml at RT) [°C]	Preheat Temp. B [°C]	Temperature drop to (after adding 1ml at RT) [°C]			Time until target temp. reached [sec]	Target temp. [°C]
	Sample A		*sample B1*	*sample B2*	*sample B3*		
50	42.6	58	49.1	48.9	48.6	10	50
56	47.1	65	54.3	55.6	53.4	10-30	56
63	52.9	74	61.5	62.3	63.5	0-20	63
72	58.7	86	72.5	71.5	72.6	0-3	72
80	70.2	90	78.6	81.2	82.3	0-2	80

Plaque assays were applied for measurement of residual infectivity of mNV and TV. However, whereas the plaque assay worked well for mNV with the processed strawberry puree samples, no plaques could be derived for TV by applying the same procedure for this virus (data not shown). This problem was solved by adding an additional PEG precipitation step prior to the plaque assay in the case of TV. Also, the capsid integrity assay for hNV, mNV and TV did not work well with the processed strawberry puree samples derived from ultrafiltration (data not shown). Optimization experiments showed that PEG precipitation without prior ultrafiltration solved this problem for hNV and TV, but not for mNV (tab.22). Based on these results, capsid integrity assays were included for hNV and TV, but not for mNV. A schematic presentation of the optimized method applied in this study is given in fig.9.

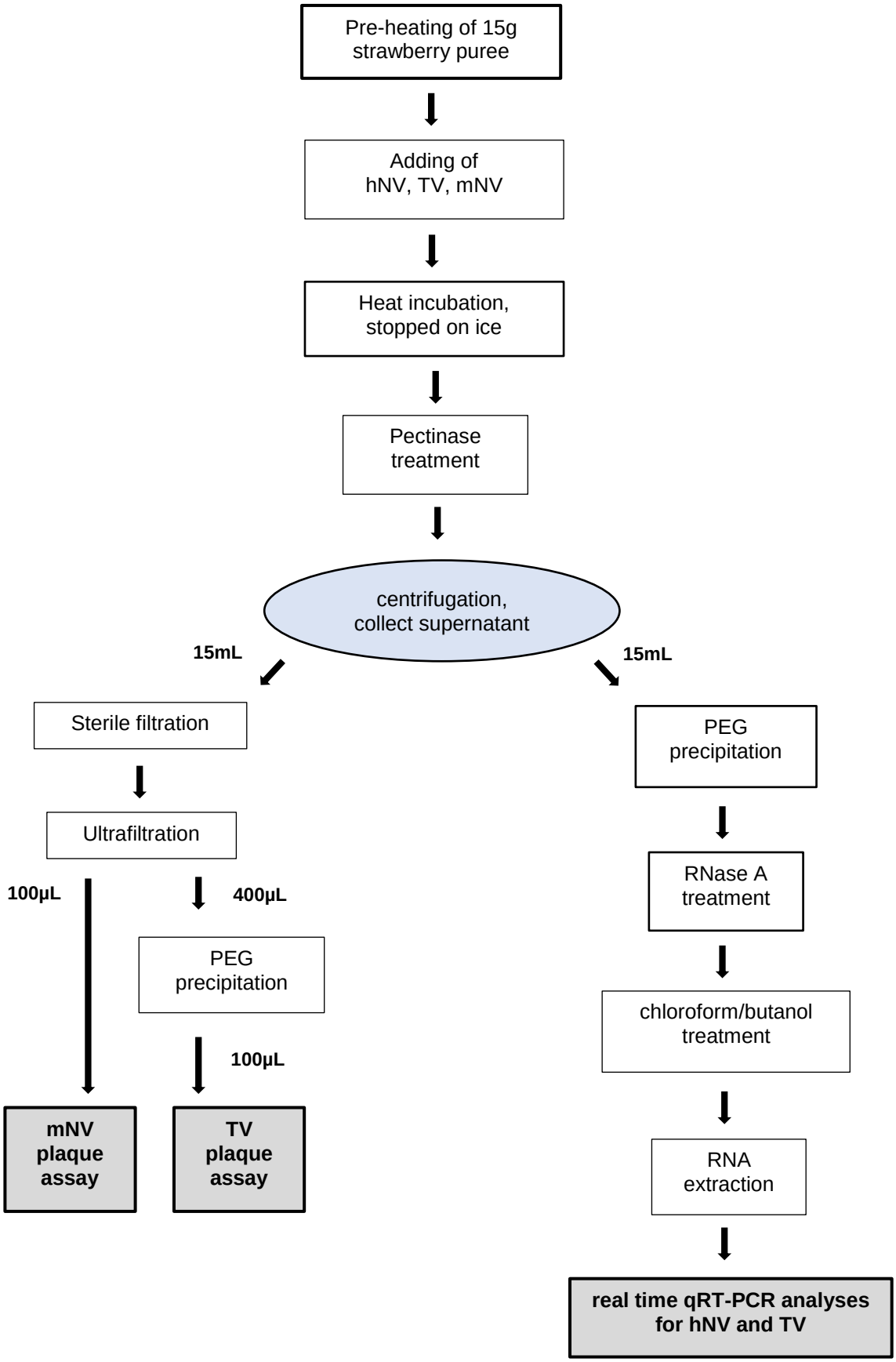

Figure 9: Experimental workflow of thermal virus inactivation. The strawberry puree was simultaneously contaminated with hNV, TV and mNV, heat-treated and subjected to several purification steps before analysis with capsid integrity assays or plaque assays.

Table 22: Performance analysis of the capsid integrity assay using RNase treatment followed by nucleic acid extraction and real time RT-PCR analysis of viral RNA. Virus solutions (undiluted or in 10-fold dilutions) were added to strawberry puree at room temperature (RT) or at 90°C. At the indicated time, the virus was extracted and treated with or without RNase. The log_{10} RNA copy numbers for hNV, TV and mNV as assessed by RT-qPCR are indicated. ND: Not detected; conc.: concentration

	Initial amount in log_{10} RNA copies			Recovered log_{10} RNA copies after treatment without or with RNase					
RT for 0 min	**hNV**	**TV**	**mNV**	**hNV**		**TV**		**mNV**	
				-RNase	+RNase	-RNase	+RNase	-RNase	+RNase
undiluted	7.3	9.2	11.8	6.9	6.4	7.9	7.5	10.9	6.1
10^{-1}	6.3	8.2	10.8	5.8	5.6	6.3	5.9	9.7	ND
10^{-2}	5.3	7.2	9.8	4.8	4.2	5.7	5.3	8.7	ND
10^{-3}	4.3	6.2	8.8	3.7	3.3	4.9	4.7	8.0	ND
10^{-4}	3.3	5.2	7.8	2.9	2.3	3.9	3.1	7.3	ND
10^{-5}	2.3	4.2	6.8	ND	ND	ND	ND	6.5	ND
90°C for 5 min									
undiluted A	7.3	9.2	11.8	4.2	ND	5.7	ND	9.3	ND
undiluted B	7.3	9.2	11.8	4.0	ND	5.7	ND	8.5	ND

The functionality of the capsid integrity assay was tested for each virus by comparing the detected RNA copy numbers of untreated samples (RT for 0min) to that of samples heated at 90°C for 5 min. As evident from tab.21 there was minor loss of RNA copies due to application of the extraction method without RNase A treatment for all three viruses at RT. But, after application of the RNase A treatment a major loss of mNV RNA copies could be observed. The amount of RNase-protected RNA decreased from $10^{6.4}$ RNA copies for the untreated samples to undetectable for the heated sample for hNV, from $10^{7.5}$ to undetectable for TV and from $10^{6.1}$ to undetectable for mNV, generally indicating a good performance of the assay. As describes in the method section RNAse A treatment is combined with PEG precipitation including higher shear and mechanical forces for the target viruses than during ultrafiltration. The sensitivity of the assay was assessed by testing of dilution series of the virus preparations. For hNV and TV, virus dilutions up to 10^{-4} allowed the detection of RNase-protected RNA. Consequently, RNase A treatment can be used for successful analysis of intact hNV and TV particles even at low concentrations of a few hundred (hNV) to a few thousand

(TV) capsids. In contrast, RNase-protected RNA of mNV could not be detected after 10^{-1} dilution of the virus indicating that the capsid integrity assay could not be applied for mNV as already mentioned above. It was also suggested that the mNV RNA copies measured without RNase treatment belonged to already destructed virus capsids.

6.3.2. Method characterization

Second, the optimzed experimental protocol had to be evaluated regarding result efficiency. For characterization of the method performance, two parameters were tested. First, the presence of PCR inhibitors in the analyzed preparations heated to different temperatures was assessed. Respectively, one µl of bacteriophage MS2 RNA was added to 4µl RNA extract of the samples from different heat treatments (or water as control) and analyzed by real-time RT-PCR. As shown in tab.23, the respective Ct values differed only up to 0.5 units indicating the absence of PCR inhibitors in the preparations.

Table 23: Testing the extracted nucleic acids for the presence of PCR inhibitors. One 1 µl of bacteriophage MS2 RNA was added to 4µl RNA extract derived from strawberry puree treated as indicated and analyzed in triplicates by real time RT-qPCR.

Sample	Mean Ct value
MS2 control	23.1
25°C, 0 min	22.8
50°C, 15 min	23.2
63°C, 1 min	23.3
80°C, 2 sec	23.2

Thereafter, the method-based virus reduction was assessed by comparing the virus amounts added to the samples with recovered amounts from the samples after application of the full protocol without heat treatment. As shown in tab.24, the capsid-protected RNA amounts decreased for $10^{0.7}$ (hNV) or $10^{0.8}$ (TV) RNA copies and the infectious virus amount decreased for $10^{1.3}$ (TV) or $10^{0.5}$ (mNV) PFU. The recovered $\log_{10}$ amounts of the viruses in the respective assays (tab.23) represent the starting

concentrations (baselines) for the calculation of heat inactivation modelling. The log_{10} amounts of decreasing virus capsids (qRT-PCR assay) and infectious viruses (plaque assay) were generated by calculating the RNA copy numbers or PFU for every sample (4 virus applications per sample = 2 RNA copy and 2 PFU calculations per sample; 3 baseline samples + 72 heat treated samples = 75 samples; 4 calculation x 75 samples = 300 calculations).

Table 24: Determination of the method-based virus reduction. Strawberry puree was inoculated with defined amounts of viruses at 25°C, extracted after capsid integrity assay using RNase A and analyzed by real time RT-qPCR or plaque assay as described. The log_{10} count refers to log_{10} RNA copies for real time RT-qPCR analysis and log_{10} PFU for plaque assay

Method	Virus	Initial amount	Recovered amount	Reduction
Real time RT-qPCR (log_{10} RNA copies)	hNV	8.1	7.4	0.7
	TV	10.4	9.6	0.8
Plaque assay (log_{10} PFU)	TV	8.5	7.2	1.3
	mNV	9.3	8.8	0.5

6.3.3. Inactivation of mNV and TV as assessed by plaque assay

After preparations and preliminary experiments regarding experimental setup and result efficiency, the actual measurement at specific time/temperature combinations started. Different temperature/time combinations were applied to artificially virus-contaminated strawberry puree and the residual infectious virus was determined by plaque assay. Fig.10 shows the results for TV and mNV. In overall, both viruses showed similar inactivation curves with continuous decline of the virus amounts over time. MNV showed a slightly higher stability as compared to TV. Infectious virus could still be detected after treatment at 50°C for 90 min, with about 4 $\log_{10}$ PFU reductions for TV and 3.3 $\log_{10}$ PFU reductions for mNV. A more rapid decrease in virus infectivity was found at 63°C, with no residual virus detection for TV (>7 $\log_{10}$ PFU reductions) and 5 $\log_{10}$ PFU reduction for mNV after heating for 5min. At 72°C for 40sec, virus reductions of >7 $\log_{10}$ PFU (TV) or 5.5 $\log_{10}$ PFU (mNV) were recorded. Both viruses could no longer be detected (>7 $\log_{10}$ PFU reduction for TV and >9 $\log_{10}$ PFU for mNV) after heating at 80°C for 8sec.

6.3.4. Inactivation of TV and hNV by capsid integrity assay

The same artificially virus-contaminated samples previously subjected to the defined temperature/time combinations were tested using RNase treatment in capsid stability assays for TV and hNV. As shown in fig.11, only marginal changes in the amount of RNase-protected RNA were recorded after treatment at 50°C for up to 90min. In contrast, the RNA amount continuously declined for both viruses when temperatures between 56°C and 80°C were applied. Generally, the amount of RNase-protected TV RNA decreased much faster as compared to hNV. At 56°C for 40min, a 2 $\log_{10}$ decrease in TV RNA copy number was found, whereas only a 0.5 $\log_{10}$ decrease of hNV RNA copy numbers was recorded under these conditions. At 72°C for 40sec, a 5 $\log_{10}$ decrease of TV RNA copies was detected as compared to only a 1 $\log_{10}$ decrease of hNV RNA copies. Similarly, at 80°C for 8 sec, an 8 $\log_{10}$ decrease of TV RNA copies was detected as compared to a 3.5 $\log_{10}$ decrease of hNV RNA copies.

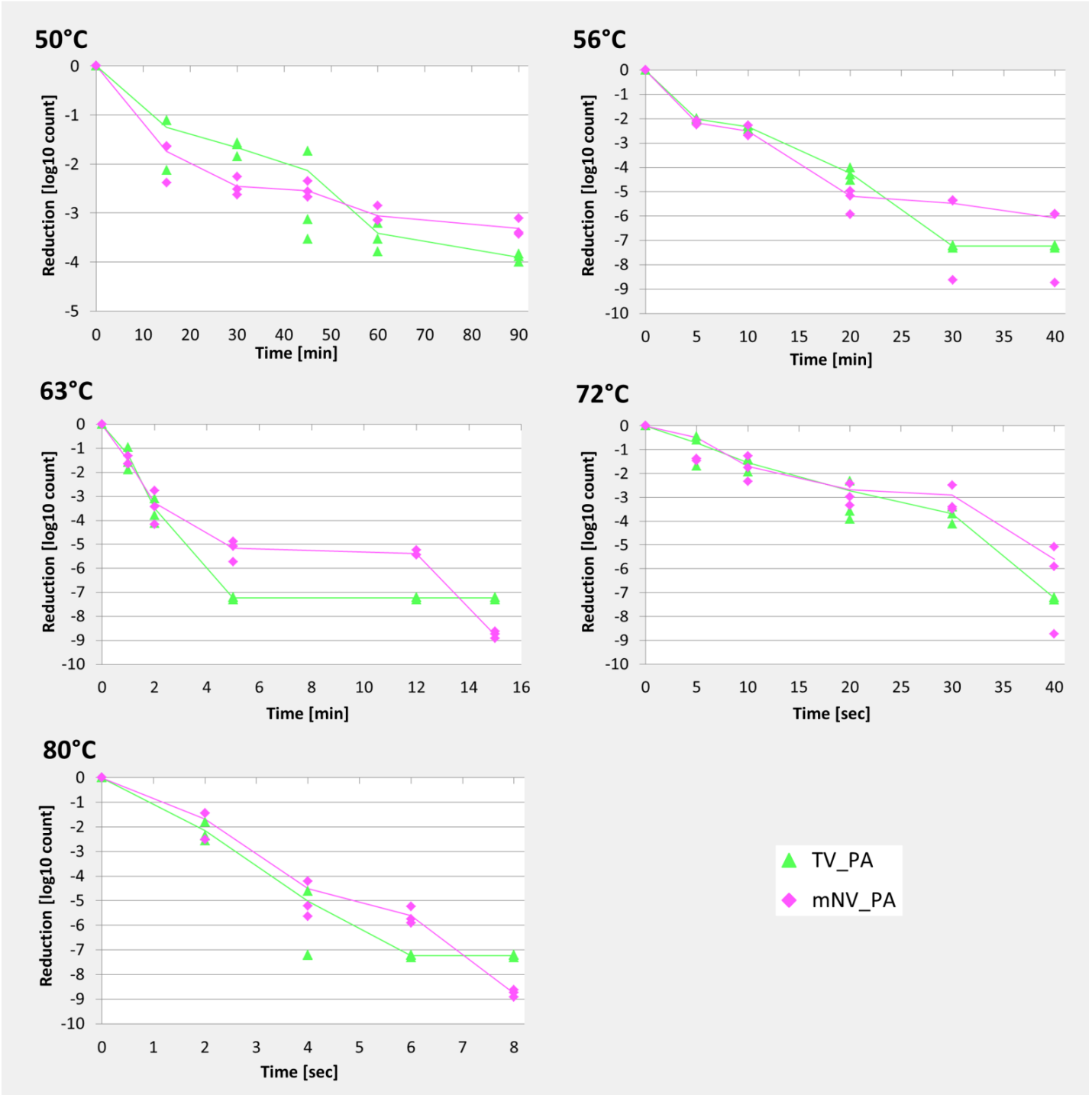

Figure 10: Heat inactivation of mNV and TV in strawberry puree as assayed by plaque assay (PA). Strawberry puree was spiked with the viruses and heated at the presented temperatures for the indicated time intervals. The $\log_{10}$ reduction of plaque forming units (PFU) is plotted against time. Triangle: TV; diamond: mNV.

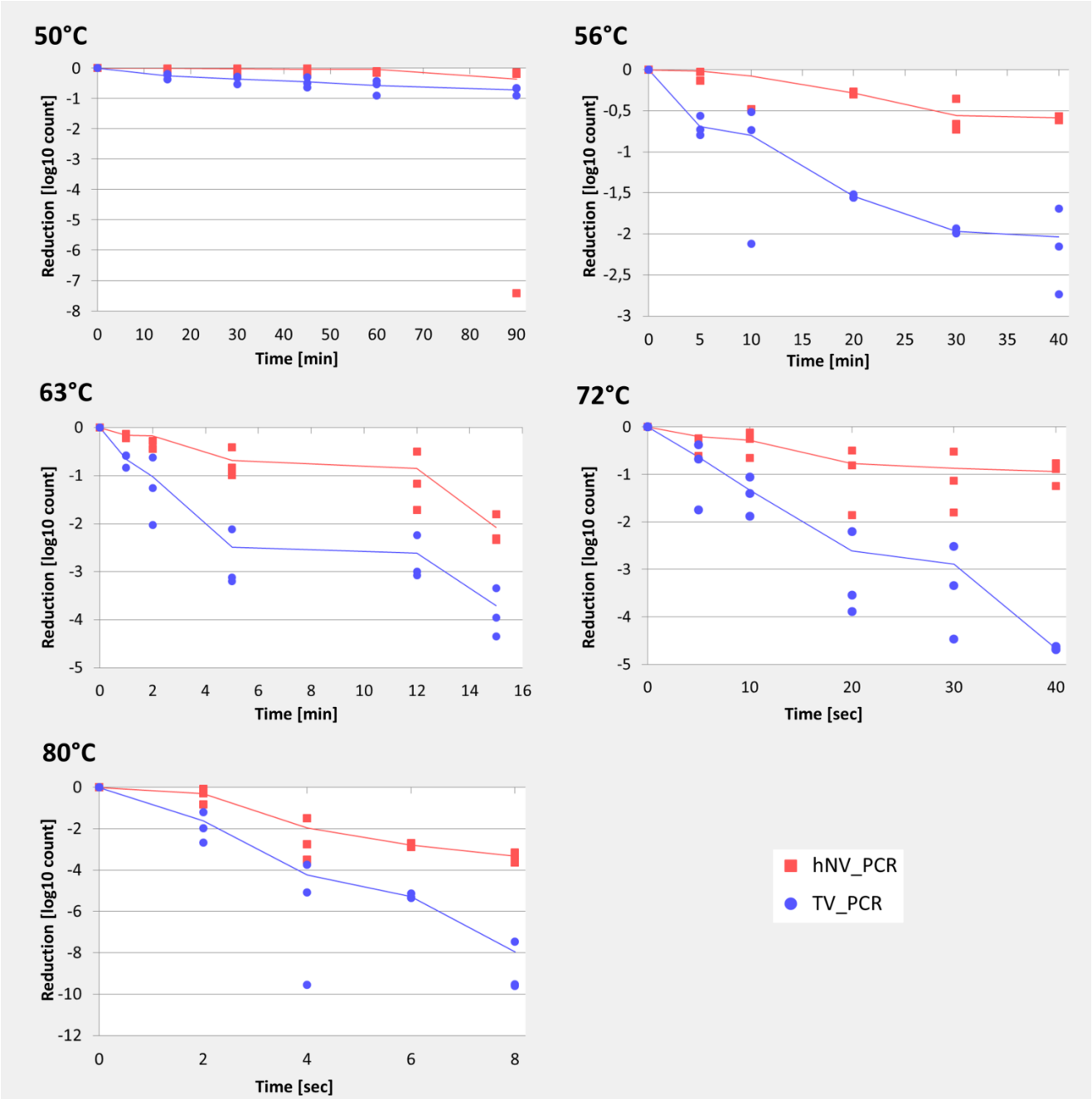

Figure 11: Heat inactivation of TV and hNV in strawberry puree as assayed by capsid integrity assay using RNase A treatment and real time RT-qPCR (PCR). Strawberry puree was spiked with the viruses and heated at the presented temperatures for the indicated time intervals. The log_{10} reduction of virus RNA copies is plotted against time. Circle: TV; square: hNV.

6.3.5. Inactivation models and D- and z-values

From the generated data through the heat inactivation curves predictive mathematical models for the different viruses should be created. The following calculations and modelling were performed by Dr. Carolina Plaza-Rodriquez and Matthias Filter. Thermal inactivation models were calculated for each virus/method/temperature combination. As evident from fig.12, linear Bigelow equation fits well with the observed (log_{10}-transformed) inactivation data. This fig. also shows that the amount of capsid-protected RNA determined by PCR generally decreased slower than that of virus infectivity as assessed by plaque assay.

D-values were calculated for hNV and each of the surrogates for each experimental method (tab.25). The highest *D*-values (in min) correspond to capsid-protected hNV RNA (hNV-PCR) at 50°C. At this temperature, the largest differences were observed between the different virus/method combinations. For example, the *D*-value for hNV-PCR is 4 times higher than for TV-PCR, 25 times higher than for infections TV (TV-PA) and 18 times higher than for infectious mNV (mNV-PA). However, at higher temperatures the differences between the *D*-values were smaller. For example, at 80°C the *D*-value for hNV-PCR was only twice as high as for every other virus/method combination. ʒ-values (in °C) were also calculated for each virus and detection method (tab.26).

The correlation analysis between log_{10} *D*-values from the different virus/detection methods led to the finding that a linear correlation could be established between the log_{10} *D*-values of the different virus/detection methods (fig.13). As our *D*-values were log_{10}-transformed, the assumption of normally distributed residuals of the linear regression models holds, so that the Pearson correlation coefficient can be reported. All correlation coefficients were greater than 0.99 and significantly different from “0”. This means, that between all experimental settings, a strong correlation can be expected with respect to the observed log_{10}-transformed *D*-values. For the relationship between TV-PCR and hNV-PCR (equation 3) as well as TV-PA and TV-PCR (equation 4) this correlation could be expressed in the following model:

$$TV_{(PCR)} = 0{,}9563 * hNV_{(PCR)} - 0{,}3611 \quad (3)$$

$$TV_{(PA)} = 0{,}7907 * TV_{(PCR)} - 0{,}0187 \quad (4)$$

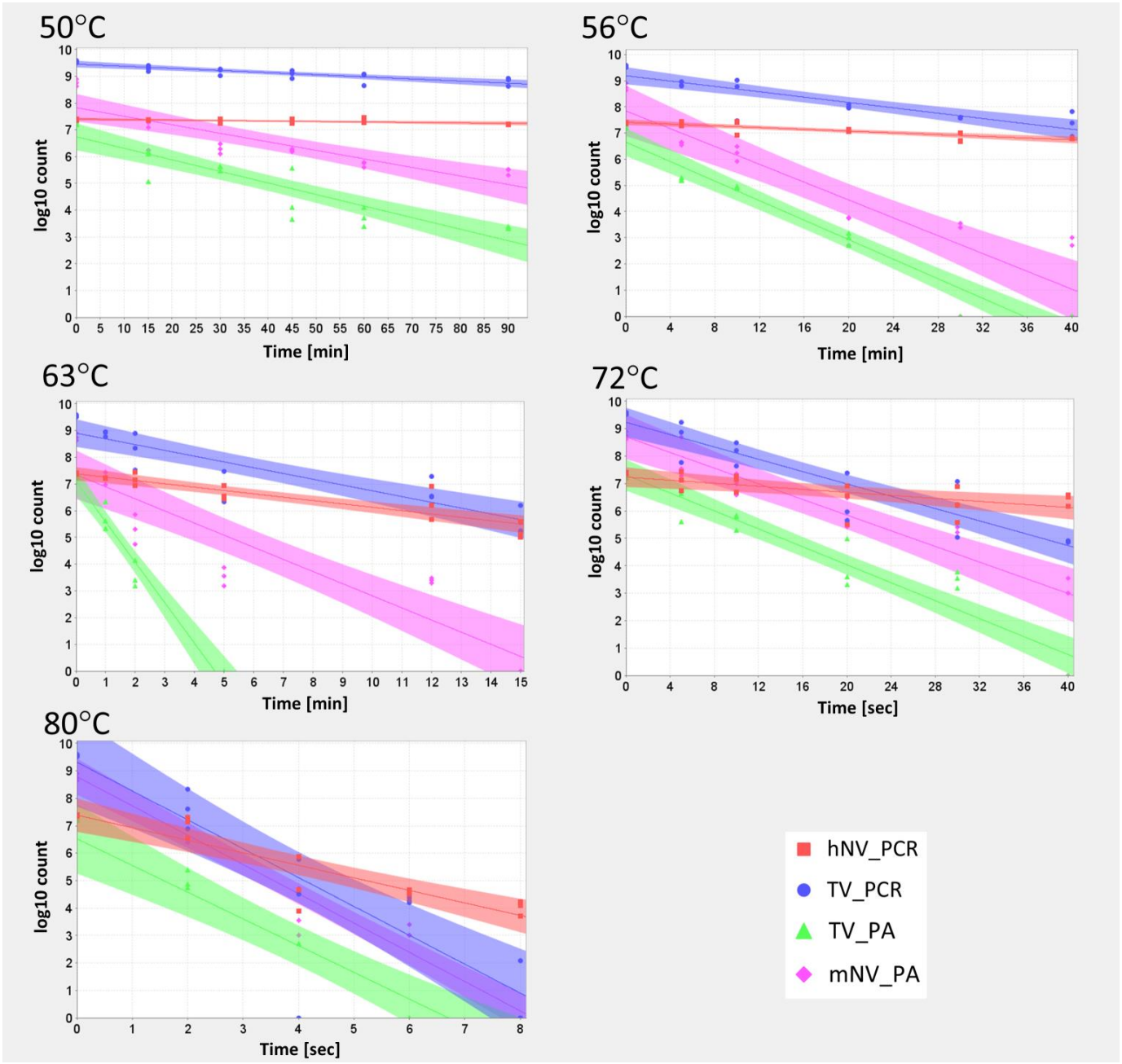

Figure 12: Thermal inactivation models for hNV, TV and mNV. Plot of the Linear Bigelow equation-based primary models generated for the different temperatures and assays. Infectivity was measured by plaque assay (PA) and capsid integrity by RNase treatment and qRT-PCR (PCR). The log_{10} count refers to log_{10} RNA copies for mNV_PCR and TV_PCR and log_{10} plaque-forming units (PFU) for TV_PA and mNV_PA. Each primary model is plotted together with the original experimental data and the confidence interval around the regression line.

Table 25: *D*-values of the primary Linear Bigelow model of hNV, TV and mNV in strawberry puree during their thermal inactivation at different temperatures. *a* – capsid integrity assay using RNase and PCR; *b* – infectivity assay using plaque assay

Virus *(Assay)*	T°C	*D*-value (min)	RMSE	R^2
hNV *(PCR[a])*	50	584.1 ± 189.5	0.1	0.4
	56	59.8 ± 8.1	0.1	0.8
	63	8.0 ± 1.0	0.4	0.8
	72	0.6 ± 0.2	0.5	0.5
	80	0.0 ± 0.0	0.6	0.8
TV *(PCR[a])*	50	126.3 ± 18.8	0.2	0.7
	56	19.5 ± 2.6	0.4	0.8
	63	4.6 ± 0.6	0.7	0.8
	72	0.2 ± 0.0	0.7	0.9
	80	0.0 ± 0.0	1.7	0.8
TV *(PA[b])*	50	23.2 ± 2.6	0.6	0.8
	56	5.4 ± 0.3	0.7	0.9
	63	0.7 ± 0.0	0.5	1.0
	72	0.1 ± 0.0	0.7	0.9
	80	0.0 ± 0.0	1.3	0.8
mNV *(PA[b])*	50	31.4 ± 4.8	0.6	0.7
	56	5.9 ± 0.7	1.2	0.8
	63	2.2 ± 0.3	1.3	0.8
	72	0.1 ± 0.0	1.0	0.8
	80	0.0 ± 0.0	0.7	1.0

Table 26: ʒ-values of the log_{10}-transformed secondary model for the *D*-values for hNV, TV and mNV. *a* – capsid integrity assay using RNase and PCR; *b* – infectivity assay using plaque assay

Virus *(Assay)*	**ʒ-value (°C)**	**RMSE**	**R^2**
hNV *(PCR^a)*	6.1 ± 0.1	2.1	0.9
TV *(PCR^a)*	7.5 ± 0.2	1.9	0.9
TV *(PA^b)*	9.3 ± 0.1	1.0	0.9
mNV *(PA^b)*	8.6 ± 0.6	1.7	0.9

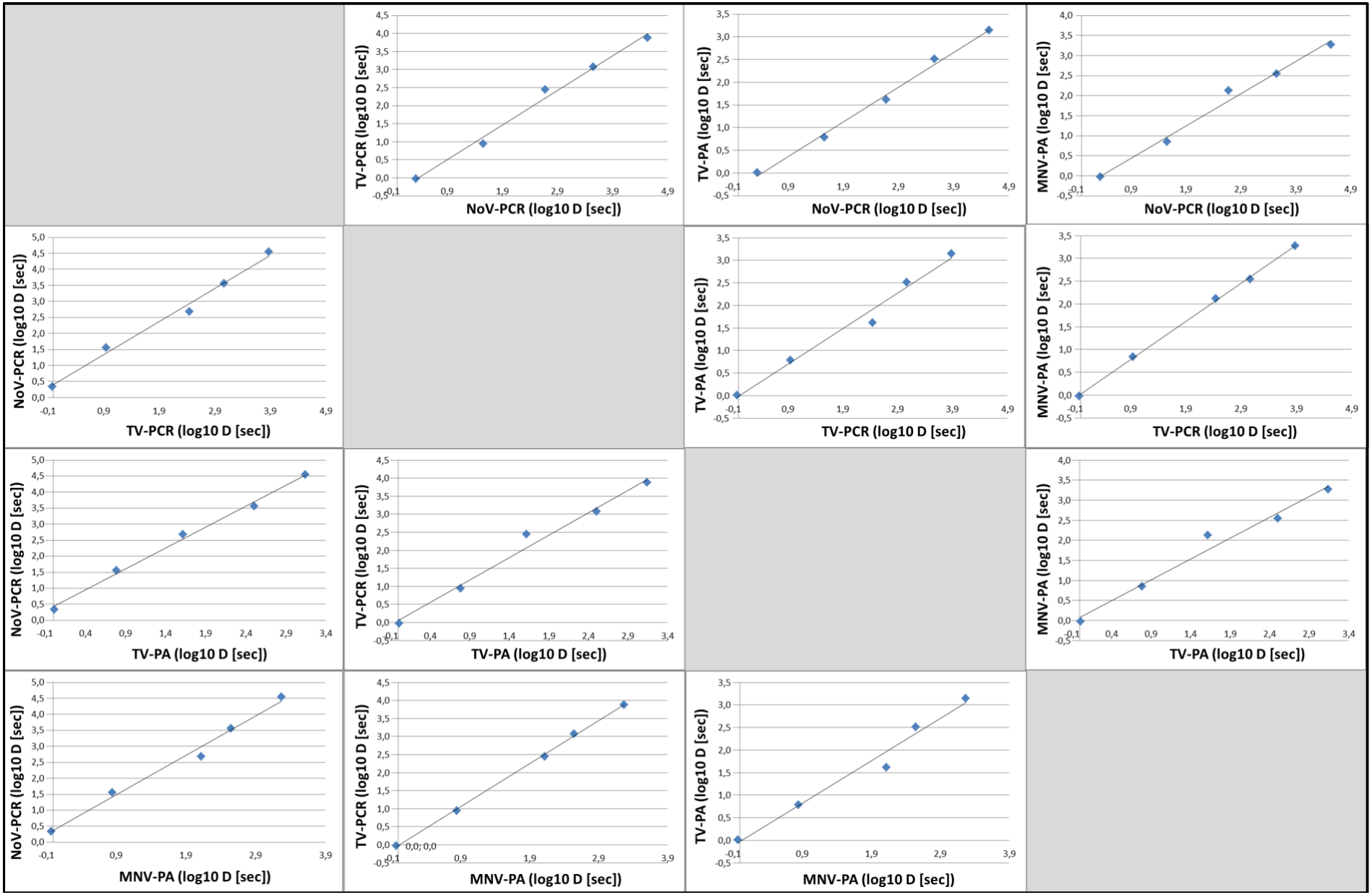

Figure 13: Correlation (scatter) plot illustrating the relationship between the log_{10} D-values (sec) obtained from primary models for the different virus / analysis methods experiments. PCR – capsid integrity assay using RNase and PCR. PA – infectivity assay using plaque assay.

6.3.6. Predictive model for hNV capsid stability

Lastly, a model for the prediction of the inactivation behavior of hNV capsids should be created for a specific virus concentration of 4 log_{10} count reduction. A tertiary model was generated for hNV that could be used to predict the temperature dependent reduction of capsid-protected hNV RNA for any time/temperature combination in the range of 50°C to 80°C and 0 to 1.5 hours (tab.27). All estimated model parameters are provided in detail within PMFX files. The RMSE of 0.365 log_{10} virus counts indicates a good accuracy of the generated model. Thus, this model can be used to predict the reduction of capsid-protected hNV RNA in strawberry puree within the range of temperatures used. In addition, the time needed to achieve a desired reduction can be predicted. For example, to achieve a 4 log_{10} count reduction the model predicts heating the strawberries for several hours at 50°C or 56°C and around half an hour at 63°C. However, at 72°C and 80°C viruses would be inactivated after heat treatment for just 2 min or 10sec respectively.

Table 27: Predictions made by the generated tertiary model for hNV. The log_{10} count refers to predicted average reduction of capsid-protected RNA copies of hNV.

Temperature (°C)	Time	log_{10} count reduction	Time for 4 log_{10} count reduction
50	90 min	0.2 log_{10}	30 h
56	30 min	0.4 log_{10}	5 h
63	15 min	1.8 log_{10}	33 min
72	40 sec	1.4 log_{10}	2 min
80	8 sec	3.6 log_{10}	10 sec

6.4. Publications

Bartsch, C., Szabo, K., Dinh-Thanh, M., Schrader, C., Trojnar, E., Johne, R., 2016. Comparison and optimization of detection methods for noroviruses in frozen strawberries containing different amounts of RT-PCR inhibitors. Food Microbiol. 60, 124–130.

Berg, C., **Bartsch**, C., Johne, R., Schneider, R., Böhm, T., Winkelsett, S., Guder., G., 2017. Smoothies – the new minced meet? - frequent detection of noroviruses in frozen berries. Amtstierärztlicher Dienst und Lebensmittelkontrolle 24 (2), 94-100.

In review process at "Food Microbioloy":

Bartsch, C., Plaza-Rodriguez, C., Trojnar, E., Filter, M., Johne, R., 2018. Predictive models for thermal inactivation of human norovirus and surrogates in strawberry puree.

Bartsch, C., Höper, D., Mäde, D., Johne, R., 2018. Analysis of frozen strawberries involved in a large gastroenteritis outbreak using next generation sequencing and digital PCR.

7. Discussion

7.1. Comparison and optimization of virus detection methods

7.1.1. Different amounts of PCR inhibitors in strawberries

The optimized detection of viruses in berries could provide a powerful tool for screening of batches before marketing or identification of outbreak sources. However, the currently available detection methods offer false-negative results in food, especially in berries. Berries can contain large amounts of real time RT-PCR inhibiting substances (Schrader et al., 2012; Mäde et al., 2013). It may be assumed that the amount of those substances increases during ripening and that repeated freezing and thawing increasingly releases these substances into the analyzed liquid. So far, the distinct substances involved in this process are not known. However, anthocyanins and other aromatic molecules present in berries can partially resemble nucleic acids structures by their aromatic ring structure and may therefore interfere with RT-PCR enzymes (Peist et al., 2011; Seeram et al., 2006; Wei et al., 2008). The differences of the inhibiting activities in different lots should generally be considered during the development of RT-PCR-based detection methods. Consequently, RRs and detection limits reported in different publications and assessed with different lots of berries cannot be directly compared to each other. To enable comparison of detection methods, two strawberry lots were therefore selected here for all the following experiments. As a good detection method should work with all field samples, some of which may contain high amounts of RT-PCR inhibitors, two batches with considerable inhibitor amounts were selected.

7.1.2. Method optimization for norovirus detection

Many extraction methods for viruses are available, but not all are adjustable to the extraction from berries. The ultrafiltration method aims at the virus concentration and removal of inhibiting substances by filtration devices. The results show that the RRs are lower than using the ISO/TS 15216 method, which is in concordance with another study comparing these methods with strawberries involved in a hNV outbreak (Mäde et al., 2013). Either the virus concentration is ineffective by ultrafiltration, or inhibitory substances bind to the filter matrix and are therefore not efficiently removed but also

concentrated. The direct lysis method showed results comparable with the ultrafiltration method. This method is very rapid and easy to perform and has previously been shown to produce good results with frozen raspberries (Perrin et al., 2015). The low RRs determined in our study may be explained by using strawberries containing high amounts of RT-PCR-inhibiting substances, which were presumably not removed by this quick method. The method using PGM-coated magnetic-beads showed only very low recovery rates. PGM was used as binding agent because of its resemblance to HBGAs, which are known interacting partners of hNVs. Indeed, different hNV types have been shown to exhibit different binding activities to HBGAs (Koromyslova et al., 2015). As this method depends on specific binding of hNV particles to sugar residues of the PGM (Tan et al., 2008), an inefficient binding may be supposed. The binding activity of the used hNVGII.3 strain to PGM is not known. Also, the TRI®Reagent protocol showed very low RRs. It is based on rapid denaturation of the viruses in the food sample by a phenol-like substance, which should lead to efficient release of viral RNA. Although this method has previously been shown to be very effective for meat products (Szabo et al., 2015), it seems to be less appropriate for the analysis of berries. Maybe, the absence of thorough purification steps in this protocol leads to inefficient removal of RT-PCR inhibitors present in the berry extracts.

The ISO/TS 15216-2 method is based on a PEG precipitation protocol (Dubois et al. 2002; Butot et al. 2007), which has been optimized during development of the standard method. By application of PEG at a specific pH, the virus particles are efficiently precipitated and concentrated. At a later step, the resuspended virus pellet is treated with chloroform/butanol to remove RT-PCR-inhibiting substances and PEG from the final extracts. Although this protocol is laborious and time-consuming, it seems to be well optimized and efficient for the use with strawberries. Based on the results, we further focused on the optimization of the ISO/TS 15216-2 protocol, because it appeared to be the best-established method for virus detection in strawberries.

The MobiSpin S-400 columns contain a Sephacryl®-based matrix (MoBiTec GmbH, 2012) and can be used in a quick and easy centrifugation procedure. During the purification process, the sample interacts with the Sephacryl®-based matrix (fig14) leading to a binding of small molecules, whereas larger molecules pass the column. Most of the RT-PCR-inhibiting substances are small molecules (Schrader et al., 2012), which should therefore be removed by this purification step, whereas the larger RNA

molecules are not affected by the procedure and pass the through the matrix. Indeed, the results of our experiments show that the hNV RRs could be improved for the batches 3 and 4, which were considered to contain medium and high amounts of RT-PCR inhibitors. This indicates that some RT-PCR-inhibiting substances were still in the RNA preparation after application of the ISO/TS 15216-2 method and RNA extraction, which thereafter could be efficiently removed by using the columns. In contrast, batch 1 contained only low amounts of RT-PCR inhibitors as already suggested by the results of the first experiments. Therefore, removal of inhibitors was not effective, and the use of the columns could not further improve the hNV RR in this case.

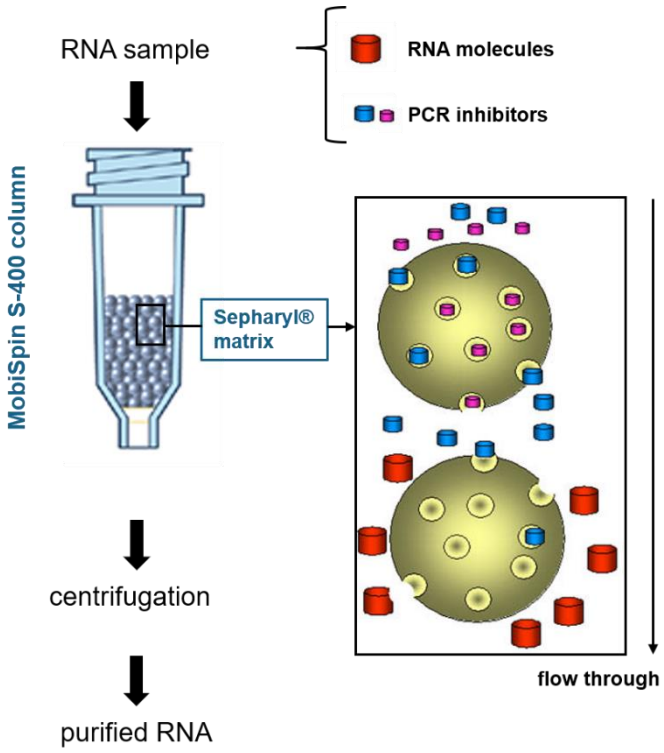

Figure 14: Sephacryl®-based RNA purification with MobiSpin S-400 columns. The inhibitors present in the RNA sample enter the pores of Sephacryl® beads during centrifugation. The smaller the inhibitory substances the better the attachment. The bigger RNA molecules move past the beads in flow through direction.

7.1.3. Testing of field samples

The optimized ISO method was also applied to berries implied in foodborne gastroenteritis outbreaks. The results show that the ISO/TS 15216-2 method is suitable for analysis of field-origin frozen strawberry and raspberry samples and that an additional purification of the extracted RNA can increase the hNV detection rate. The analyzed strawberry batch has been suspected to be contaminated with human sewage explaining the presence of multiple viruses in it (Mäde et al., 2013). In the original analysis of this strawberry batch using a method like ISO/TS 15216, detection rates of 10.7% and 53.6% were reported for hNVGI and hNVGII, respectively (Mäde et al., 2013). The increased hNV detection rates and the increase in the RRs of the process control virus after additional RNA purification argue for the presence of high amounts of RT-PCR inhibitors in strawberry and raspberry field samples. Our results indicate the efficient removal of inhibitors by the extended procedure. Therefore, methods enabling the removal of inhibiting substances should be applied in outbreak investigations and routine monitoring under field conditions to avoid false negative results. Furthermore, both field samples were used in big lunchroom kitchens for the preparation of yoghurt deserts. In both outbreak cases the berries were not heated but only defrosted before adding them to the yoghurt and serving them to people (Mäde et al., 2013; Berg et al., 2017). On the contrary, in another kitchen serving the raspberry yoghurt the berries were heated appropriately before adding them to the yoghurt. People who ate the desert at this kitchen did not suffer from gastroenteritis suggesting a successful inactivation of infectious hNV (Berg et al., 2017). Especially this example points out the importance of adequate heating regimes and the delegacy of these products themselves.

7.2. New methods for virus identification on outbreak material

7.2.1. Identification of hNV and other viruses on outbreak material by NGS

The aim of this analysis was to get more insights in the microbe or pathogen load on the outbreak strawberries from 2012. It should be tested if the hNVII sequences found in diseased patients from the outbreak in 2012 could be detected by NGS. Additionally, we were interested in the presence of other viral pathogens and their possible risks for the consumer. Also, environmental conditions may be reflected by the microbial flora on the berries in the strawberry fields.

When the food-borne outbreak was recognized in 2012 viruses or bacterial toxins present in the frozen strawberries were suspected to be the target pathogens (Bernard et al., 2013). Stool samples of patients were screened and two hNV genotypes GII.P16/GII.13 were found in high amounts. These genotypes were also found by PCR-analysis of packages of the suspected frozen strawberries used for deserts in cafeteria kitchens. The detected recombinant genotype GII.P16/GII.13 had never been reported before in Germany and refers to a strain from Kolkata, India, deposited in the GenBank database (acc.-no.AB592965) (Mäde et al., 2013). Therefore, these genotypes were determined as the diseasing pathogens in the outbreak in 2012 after no pathogenic bacteria or bacterial toxins were found (Bernard et al., 2013; Mäde et al., 2013). From the phylogenetic tree (fig.8), the closest relationship (with 100% nt sequence identity) of the sequence derived by the new NGS analysis with one original sequence from the strawberries and three sequences from patients from the outbreak becomes evident. It can therefore be concluded that the NGS method combined with the RIEMS data analysis was able to identify the aetiological agent within the strawberry sample.

However, the low number of hNV reads in relation to the high number of generated reads either indicates the presence of a low hNV dosage in the sample, or a low sensitivity of the NGS method. Especially, efforts should be made in future to decrease the high number of plant-derived sequences, e.g. by treatment of the sample with DNases before NGS analysis. In addition to the hNV reads, a considerable number of reads with similarities to *Salmonella enterica* sequences were identified by NGS. This bacterium is well-known as a food-associated pathogen, but non-pathogenic strains also exist (Altıntaş Kazar et al., 2016). During the outbreak, the strawberries have been extensively investigated for common foodborne bacteria and viruses, but no other pathogen than norovirus was reported from the respective health departments in

connection with the outbreak (Bernard et al., 2014). Also, specific testing of strawberry samples from the involved did not lead to the identification of salmonella (Dietrich Mäde, personal communication). Either the salmonella type contained in the sample could not be detected by the applied methods or the bacteria were inactivated due to freezing or unknown other treatment of the berries.

The sequence identities of the top five hits from the four different super-kingdoms are indicated in a range (tab.17) because some sequences had a higher base-pair overlap with the microbe species than others. These results give an interesting overview regarding the environment around the strawberry fields and environmental microbes. Unexpected is the presence of sequences from the flower *Jamesia Americana*, an American shrub indigenous in the mountain areas of California. There are two different possibilities how these sequences could be present on strawberries produced in China: First, the food producers might have used products from California during the growing, harvest or packaging processes. Second, there might grow a flower in China very similar to *Jamesia Americana* sharing a sequence overlap. The same hypotheses can be made for *Sanguisorba sitchensis*, also known as *Sanguisorba canadensis*, which is an American garden flower and was also found on the outbreak strawberries.

Most of the identified viral sequences originated from plant-pathogenic viruses or from bacteriophages. The most abundant viruses are known to infect strawberries, which corresponds to the analyzed food matrix. Given the high number of identified bacteria, the presence of bacteriophages is also not surprising. Only 11 reads showed significant sequence similarities to mammalian viruses (tab. 18). Most of them showed sequence identities lower than 95%. Taking into consideration that RIEMS compares the reads to all sequences present in the GenBank database, these reads most likely indicate the presence of viruses somewhat related, but not identical to the respective known virus species. One sequence showed 98.2% identity to a porcine endogenous retrovirus, for which the origin cannot be clarified. Another read showed 98.1% identity to a mammalian astrovirus, which is known as accidental cause of diarrhea in humans and animals (Jarchow-Macdonald et al., 2015). Astroviruses have not been reported in the strawberries or the patients of the outbreak so far; however, it is not known whether specific testing on this pathogen had been performed during the outbreak.

Finally, this analysis gave interesting insights into the microbial community on strawberries. Regular NGS analysis might give an ecological overview regarding

natural risks and environmental conditions and help to organize and optimize food production. As the method represents a non-targeted approach, it is able to detect all pathogens without a preselection and may help to simultaneously identify the range of pathogens possibly involved in an outbreak. In the future it might be also possible to use NGS as investigation tool in outbreak scenarios (fig.15). Food trace-back investigations and sample collections from patients with subsequent standard testing are long, elaborate and expensive processes. If specialized programs for data analyses were established patient material could be screened for containing pathogens and shared food sequences. Reports containing possible foods contaminated with pathogens responsible for an outbreak could be generated in a few days if devices and software are optimized. These reports could be the basis for a more specialized pathogen analysis with standard methods in targeted foods and for specified food surveys for patients. Hence, NGS might contribute to a faster and more reliable outbreak resolution

.

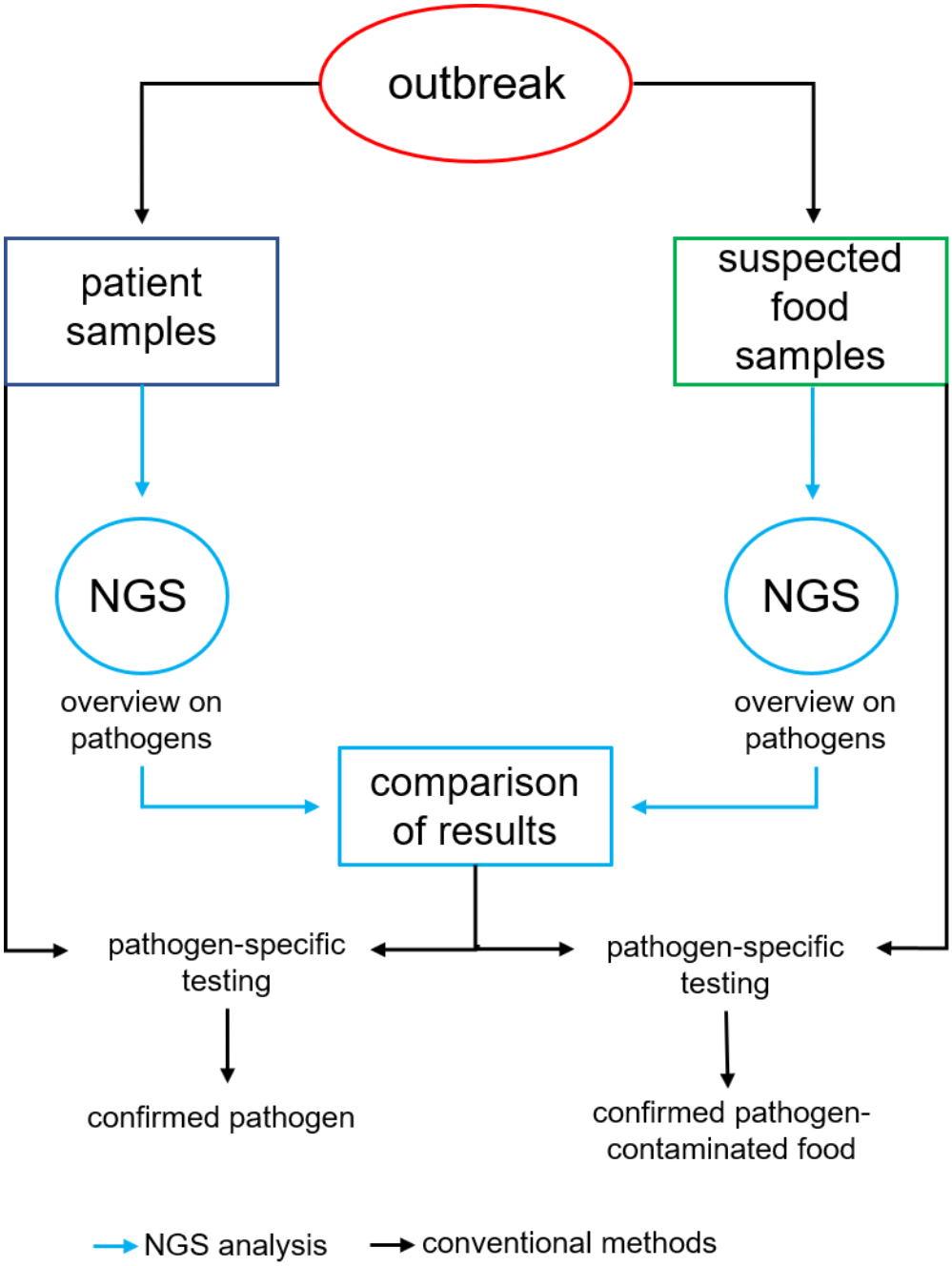

Figure 15: Suggestions for a future application of NGS in an outbreak scenario.

7.2.2. Quantification of viral load on outbreak material with real time RT-qPCR and dPCR

Both methods, RT-qPCR and dPCR, showed a good performance and high sensitivity regarding virus detection on outbreak material. The results for both methods are similar whereas real time RT-qPCR analysis had less negative tested samples maybe due to a higher amount of material used for virus extractions. In the first part of the study about method optimization (chapter 6.1.) the detection limit for the ISO method with our additional RNA purification to 216 RNA copies per 25 g was determined. The reason why we were able to detect 7 and 35.5 RNA copies in 25 g might be due to relative calculations by the PCR software which are based on the Ct value of the sample and standard curves originated from viral reference material. Since most of the 22 samples were contaminated with over 100 RNA copies, the detection of 7 and 35.5 RNA copies can be considered as statistical deviation. Apart from that, the method sensitivities regarding detection minimum and maximum for RT-qPCR and dPCR are similar.

The highest detected viral loads were only 103 (RT-qPCR) and 102 (dPCR) RNA copies per 25 g/per berry. As shown in chapter 6.2. in strawberries with medium amounts of inhibitors the detection limit for the normal ISO method is 2160 RNA copies per 25 g (Bartsch et al., 2016). This method sensitivity does appear sufficient for the successful identification of hNVII particles during outbreak or routine testing. But considering that in the hNV outbreak in 2012 the maximum viral load was around 1000 RNA copies per 25g/per berry it might be critical to successfully identify the source of an outbreak. Both method combinations, ISO + RNA purification + real time RT-qPCR and ISO + dPCR, have a one $\log_{10}$ step higher sensitivity than the standard ISO/TS 15216-2 protocol according to this study. Therefore, both combinations seem to be more suitable for virus testing in berries than the ISO method alone.

In general, a 4 $\log_{10}$ reduction in virus counts is considered as a valid criterion for complete virus inactivation (Gehrke et al., 2004; Tian et al., 2013) because the viral load on outbreak material is usually very low. In this study, the similarities between the virus concentrations per berry and per 4.5 berries suggest a uniform contamination pattern with a low concentration of pathogens. Nevertheless, not every berry seems to be contaminated, but maybe one out of four due to the same detection rates per berry and 25g. This is also suggested by the 30% rate of hNV-negative samples tested by dPCR (tested per berry) compared to a 4.5% rate of hNV-negative samples tested by

real time RT-qPCR (tested per 4-5 berries). Therefore, the application of an inactivation protocol enabling a 4 log_{10} reduction of the viral load might have prevented the outbreak in 2012. On the official BfR homepage, our institute suggests cooking of deep frozen berries before consumption (BfR, 2013) and especially before serving them to high risk groups as children and elderly (BfR, 2017).

7.3. Thermal inactivation

7.3.1. Method development and optimization

As a measure for prevention of gastroenteritis outbreaks, proper heating of frozen berries before consumption has been suggested (BfR 2013a, b, 2017). However, the distinct conditions for efficient hNV inactivation in berries through heating are not known. Only a few studies on virus inactivation in berries have been published so far. In these studies, inactivation by short-term heating was assessed for hepatitis A virus (Deboosere et al., 2004), murine norovirus (Baert et al., 2008b), or feline calicivirus (Butot et al., 2009). Studies on hNV in berries were performed using RT-qPCR detection of the genome, which does not enable distinction between intact and destroyed virus particles (Butot et al., 2009; Verhaelen et al., 2012). Therefore, we aimed on a systematic analysis, which can be used for prediction of hNV inactivation in berries at different temperature/time combinations.

As reliable cell culture methods for infectivity measurement of hNV in berries are not available so far, the experimental setting should include molecular tests on capsid stability of hNV as well as infectivity testing of surrogate viruses. A hNVGII.3 strain present in a human fecal sample was selected due to availability, former successful use in other studies (Mormann et al., 2010; Scherer et al., 2010) and due to frequent involvement of GII.3 strains in foodborne outbreaks (Vega et al., 2014). The mNV was chosen as surrogate as this virus is closely related to hNV and has been already used in many stability studies (Bozkurt et al., 2013; Baert et al., 2008b). TV has been identified more recently, but has been suggested as suitable surrogate to study hNV thermal stability based on experimental data (Arthur and Gibson, 2015b). The applied temperature/time combinations tested were delineated from published stability data of the used viruses (Arthur and Gibson 2015a; Bozkurt et al., 2015b; Araud et al., 2016; Croci et al., 2012) as well as on general requirements for heat stability studies as

delineated by Arthur and Gibson (2015a). The experimental setup using simultaneous contamination of strawberry puree with the three selected viruses should enable us to perform direct comparisons of the inactivation results, which should thereafter be used for generation of inactivation models.

During the development of the experimental procedure, several difficulties aroused, which had to be addressed. In practical settings the inactivating effects of the time-period before and after reaching the desired temperature have also to be considered, which are dependent on the distinctly applied heating method. For example, virus solutions are often added to the food matrix before heating to mimic environmental conditions (Bozkurt et al., 2014; Araud et al., 2016). However, due to the longer heating periods to reach higher temperatures more viruses are inactivated before the actual measuring starts. That means that there might be less intact viruses left for detection systems. Especially, for critical time-temperature combinations after which only a few viruses will be intact, a pre-heating of the sample can help generating a more detailed inactivation model (Arthur and Gibson, 2015b). The procedure for heating of the samples had to be adjusted to pre-heating at higher temperatures to consider the temperature drop due to mixing effects. By this, we were able to exactly measure the effect of heating at a distinct temperature for a distinct time. Somewhat unexpected, we were not able to perform the capsid stability assay with mNV. Even at high virus concentrations (10^{-1} dilution of the cell culture supernatant), the mNV RNA was completely degraded after RNAse treatment of the capsids. Instability of the mNV capsid during the applied treatment procedure used for virus preparation, e.g. PEG treatment, may be considered as the reason, which should be addressed in future method optimization studies. The final protocol included infectivity assessment for mNV and TV and capsid integrity testing for TV and hNV. It was tested regarding functionality, residual inhibitory substances and method-based virus loss as suggested by Arthur and Gibson (2015a), generally showing a good performance.

7.3.2. Comparability between viruses and methods

The results obtained for mNV and TV infectivity assessment were similar, with a slightly higher heat stability of mNV compared to TV. Both viruses could be efficiently inactivated by heating at temperatures ≥63°C for at least 5 min, leading to virus reductions ≥5 $\log_{10}$ PFU. The data obtained for mNV are comparable to published data on its stability in raspberry puree (Baert et al., 2008b), although the investigated

temperature/time combinations are not completely identical. In that study, mNV showed a virus reduction of 1.9 log_{10} PFU after treatment at 65°C for 30sec, whereas we assessed a virus reduction of 1.5 log_{10} PFU after treatment at 63°C for 1min. Similarly, virus reductions of 2.8 log_{10} PFU were determined at 75°C for 15sec (Baert et al., 2008b), compared to 3 log_{10} PFU at 72°C for 20sec in our study. No studies on heat inactivation of TV in berries are available so far.

Comparison of the TV data from the capsid integrity assay with that of infectivity testing showed a clear difference, indicating that the molecular assay predicts a higher heat stability than the infectivity assay. Remarkable differences between capsid integrity assays and infectivity assays have also been recorded for hepatitis E virus (Schielke et al., 2011; Johne et al., 2017). It has been shown for hNV virus-like particles, that structural changes on the particle surface occur at temperatures above 60°C, which stepwise affect secondary-, tertiary-, and quaternary-level protein structural perturbations (Ausar et al., 2006) outlined in fig.16.

According to the model, the first changes due to heat inactivation may affect the capsid protein structures responsible for binding to the cell, thus abolishing infectivity. At the same time, the virus particle can still be intact and protect the viral RNA from RNAse digestion. Only at higher temperatures or longer time-intervals, the particles are increasingly damaged leading to an effect detectable by the capsid integrity assay. However, as no infectivity can be suspected when the capsid integrity assay detects no protected RNA, this assay can be used as a conservative estimation for the loss of infectivity. By applying the capsid integrity assay to hNV, a considerable higher stability as compared to TV was assessed, especially at temperatures ≥72°C. Consequently, this result would suggest a higher heat stability of hNV than TV or mNV.

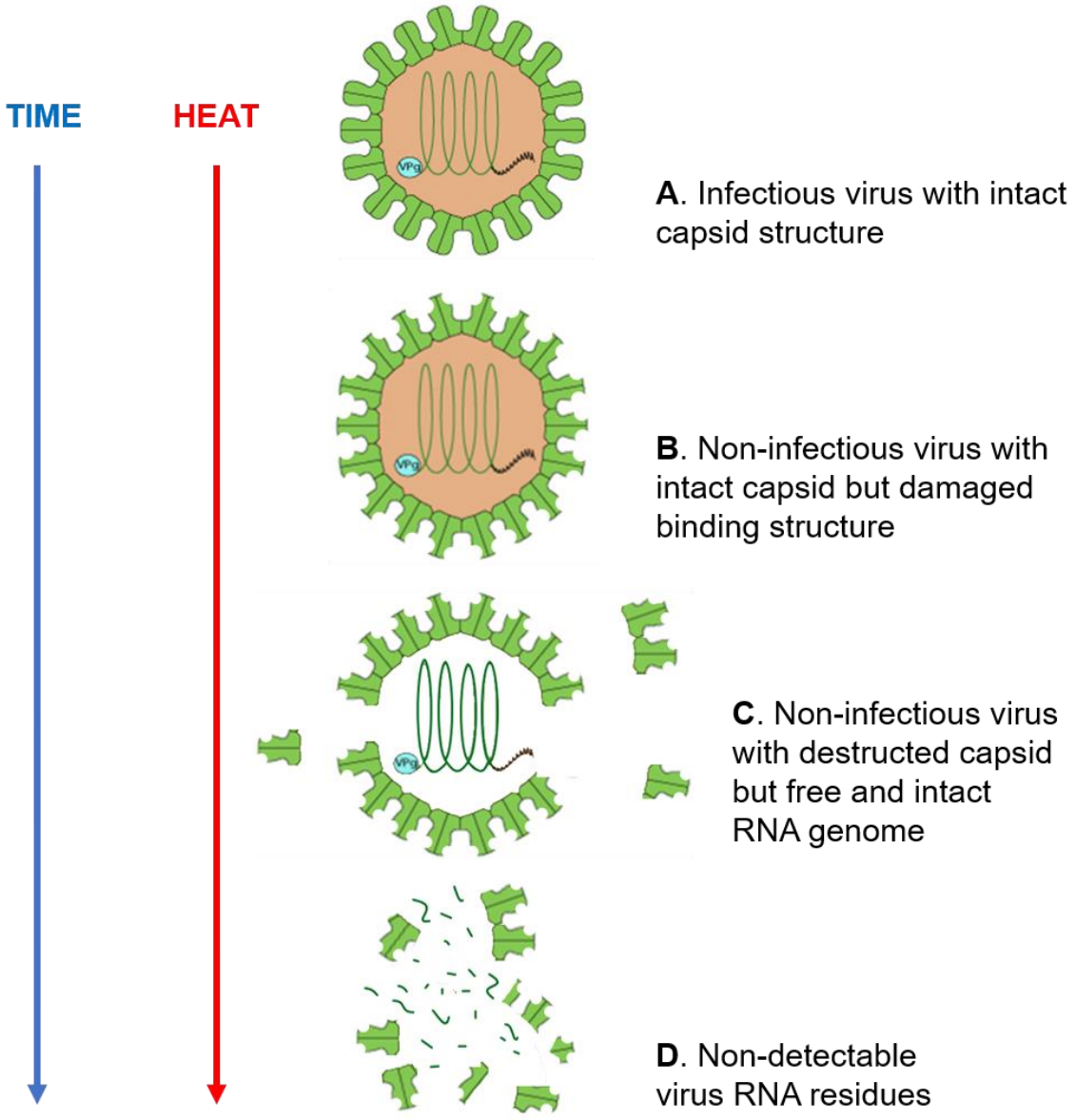

Figure 16: Model of gradual virus degradation. The longer the incubation time and the higher the temperature during thermal inactivation, the more viruses get inactivated and completely degraded. The virus is only infectious if the surface structures are fully intact (A). Intact, but non-infectious viruses enclosing the RNA genome (B) can be measured during capsid integrity assays with RNase A treatment removing all free virus RNA from destructed capsids (C,D). Free virus RNAs can be very stable and still detectable in real time PCR.

7.3.3. Mathematical modelling

For future heating regimes of berries generating a save product but protecting the nutrients in the products, the safety of heating protocols under 90°C were of high interest. Primary models describing the heat inactivation over the whole time-periods at the applied temperatures as well as basic heat resistance parameters (*D* and ϛ values) were calculated for all used viruses/method combinations. By comparison of these data, the large differences between the inactivation rates of mNV and TV in plaque assay, TV in capsid integrity assay and hNV in capsid integrity assay were confirmed, indicating that the results from the surrogate viruses cannot be directly used to describe the inactivation of hNV. However, general correlations were found by comparison of the models, which may enable the use of the surrogate data if infectivity data from hNV will be available in the future.

Using the data from the capsid stability assay, a tertiary model for reduction of hNV was generated, which allows the prediction of hNV inactivation in strawberry puree in the temperature range between 50°C and 80°C and for times ranging from 0 to 1.5 hours. This model may be used to suggest reliable temperature/time combinations to inactivate hNV in berries. Considering a 4 $\log_{10}$ reduction in virus counts as a valid criterion for complete virus inactivation (Gehrke et al., 2004; Tian et al., 2013), the model predicts that treatments at 72°C for 2 min or at 80°C for 10 sec should be sufficient for this purpose, whereas temperatures under 70°C are not reliable (tab.26). As this model is based on an indirect molecular method, a validation with hNV infectivity data should be done in future if possible.

8. Conclusions

8.1. Method comparison and optimization

This study offers new perspectives for virus extraction from berries suggesting a correlation between inhibitor levels and ripeness of the fruits. The results show large differences between the hNV RRs of artificially contaminated strawberries with different degrees of ripeness and matrix conditions. Consequently, the distinct sample type has a strong impact on the results of analytical tests. This should be taken into consideration when method performances and detection limits of methods are compared to each other in the future.

The recently standardized method for hNV detection in soft fruit as laid down in ISO/TS 15216-2 could be shown to be better suited for the analysis of frozen strawberries than any of the other virus extraction methods tested here. However, it could be further improved for frozen strawberries and raspberries containing high amounts of RT-PCR inhibitors by inclusion of an additional RNA purification step. This optimized method should be tested in other laboratories and its suitability for other matrices, e.g. food types with high amounts of RT-PCR inhibitors, should be assessed in future. Considering that the presence or absence of inhibitory substances is usually not known when samples are analyzed under field conditions, a method efficiently removing such substances should generally be applied to avoid false negative results.

8.2. New methods for virus identification on outbreak material

In this study we made first attempts to compare the method sensitivity of RT-qPCR and dPCR which were similar and sufficient to detect hNV in outbreak material. Studies suggest that dPCR might be a promising tool for a fast detection of small virus amounts and for an easy quantification without a standard curve and with a method-based inhibitor reduction (Zhang et al., 2016). After amplification, the total number of target molecules can be calculated apart from external reference standards and the subsampling may also decrease the impact of inhibitors associated with matrix-type components. Nevertheless, this method is still very expensive and not evaluated for many food matrices.

NGS analysis might be a promising tool to identify unknown microbial species and genotypes in the future. The analysis of food products gives interesting insights in the growing and environmental conditions as well as in associated plant-viruses, human pathogens or viruses with zoonotic potential. If used as routine monitoring tool, science and companies might be able to observe changes in the environment or emerging risks for public health based on microbial patterns or the presence of unusual microbes. It can also enhance the awareness regarding hygienic standards during food harvest and packaging because of the diversity of potential human pathogens on products. In the future, NGS analyses my therefore give a comprehensive view on the food chain and will help to improve food safety. However, the technique is still expensive, time-consuming and may have a low sensitivity for viruses.

8.3. Thermal inactivation

The study assessed the thermal stability of hNV and surrogates in strawberry puree using an optimized experimental approach. The generated primary inactivation models indicated that the results for the surrogate viruses cannot be directly used to predict hNV stability. A tertiary model generated for hNV based on a capsid integrity assay enables the prediction of hNV inactivation in a large range of different temperature/time combinations. The model can be used to suggest effective heat treatment procedures for frozen berries. It should be validated against infectivity data as soon as reliable infectivity assays for hNV are available.

9. Future perspectives

In general, frozen berries represent healthy products contributing to a balanced diet with lots of vitamins and minerals. Unfortunately, they also represent a high-risk food due to frequent contamination with human pathogens leading to virus outbreaks. Therefore, the diligent compliance of hygienic standards during harvest as well as the application of evolved virus detection methods and heating regimes are important to ensure food safety. Regarding food safety, the presented study showed solutions for problems of virus identification, detection and inactivation, but areas of future research have also been identified.

First, this study might help to prevent false negative results in virus detection during outbreak or routine testing. The influence of different amounts of PCR-inhibitors associated with ripeness of the fruits should be also investigated in other studies. Additionally, the influence of Sephacryl®-based RNA purification on other viruses in berries and other food matrices regarding detection limits and RRs should be evaluated.

Second, the comparison of two PCR-based identification and quantification systems (RT-qPCR and dPCR) revealed a similar efficiency in RNA detection. Other studies suggest that dPCR might have a better future prospective in food control because of the method-based reduction of PCR inhibitors and the independence from reference RNAs during virus identification and quantification. These properties may simplify the currently used complicated and time-consuming protocols and accelerate experiments. Therefore, the method potential of dPCR should be further investigated in future studies and optimized products should be developed and standardized for distinct food matrices.

Third, due to immature NGS analytical systems the identification of hNV in the outbreak material from 2012 was very difficult. By the application of the RIEMS data analysis system it was possible to verify the presence of hNV RNA with genotypes from patients. In the future development of better NGS devices and data analysis systems are needed to simplify and standardize the method for commercial use. Also, efforts should be made to improve the method sensitivity for human pathogenic viruses in food samples. By NGS only two hNV reads were found in the entire 20 million reads. When NGS analyses are more adapted to viral material in the future they might

become important tools for studies regarding evaluation of the food environment, irrigation water and packaging processes as well as identification of new viruses or viruses with zoonotic potential.

Lastly, we investigated the thermal inactivation behavior of hNV in strawberry puree. Due to extension of the virus extraction protocol by the addition of an RNase A treatment we were able to distinguish between intact and destroyed virus capsids. Since the number of intact capsids contained infectious and non-infectious particles our time-temperature predictions for thermal hNV inactivation in strawberry puree are safe. Heating at lower temperatures around 72°C might protect important vitamins in berries from denaturation. Therefore, our results may help to retain the food value and improve food safety by giving advices for effective food treatment and thermal inactivation conditions. Heat inactivation kinetics of hNV capsids should be investigated by PCR experiments including RNase A treatment in future studies involving different foods. Also, studies should focus on the adaption of hNV cell culture systems to food microbiology and development of infectivity assays. Only the availability of those cell culture systems will enable a solid validation of the results obtained with surrogate viruses or capsid integrity tests.

10.References

Adriaenssens, E.M., Ceyssens, P.-J., Dunon, V., Ackermann, H.-W., van Vaerenbergh, J., Maes, M., Proft, M. de, Lavigne, R., 2011. Bacteriophages LIMElight and LIMEzero of Pantoea agglomerans, belonging to the "phiKMV-like viruses". Appl Environl Microbiol. 77 (10), 3443–3450.

Ahn, J.Y., Chung, J-W., Chang, K-J., You, M.H., Chai, J.S., Kang, Y.A., Kim, S-H., Jeoung, H., Cheon, D., Jeoung, A., Choi, E.S., 2011. Clinical characteristics and etiology of travelers' diarrhea among Korean travelers visiting South-East Asia. J Kor Med Sci. 26, 196–200.

Altıntaş Kazar, G., Şen, E., 2016. Investigation of antitumorigenic effects of food-borne non-pathogenic and pathogenic Salmonella enterica strains on MEF, DU145 and HeLa cell lines. Mikrobiyol Bul. 50 (3), 382–391.

Araud, E., DiCaprio, E., Ma, Y., Lou, F., Gao, Y., Kingsley, D., Hughes, J.H., Li, J., 2016. Thermal Inactivation of Enteric Viruses and Bioaccumulation of Enteric Foodborne Viruses in Live Oysters (Crassostrea virginica). Appl Environ Microbiol. 82 (7), 2086–2099.

Arthur, S.E., Gibson, K.E., 2015a. Comparison of methods for evaluating the thermal stability of human enteric viruses. Food Environ Virol. 7 (1), 14–26.

Arthur, S.E., Gibson, K.E., 2015b. Physicochemical stability profile of Tulane virus: A human norovirus surrogate. J Appl Microbiol. 119 (3), 868–875.

Atmar, R.L., Estes, M.K., 2006. The epidemiologic and clinical importance of norovirus infection. Gastroen Clin North Am. 35, 275–290.

Atmar, R.L., Opekun, A.R., Gilger, M.A., Estes, M.K, Crawford, S.E., Neill, F.H., Graham, D.Y., 2008. Norwalk virus shedding after experimental human infection. Emer Infect Dis.14, 1553–1557.

Auguet, J.-C., Barberan, A., Casamayor, E.O., 2010. Global ecological patterns in uncultured Archaea. ISME J. 4 (2), 182–190.

Ausar, S. F., Foubert, T. R., Hudson, M. H., Vedvick, T. S., Middaugh, C. R., 2006. Conformational stability and disassembly of Norwalk virus–like particles: effect of pH and temperature. J Biol Chem. 281, 19478–19488.

Aw, T.G., Wengert, S., Rose, J.B., 2016. Metagenomic analysis of viruses associated with field-grown and retail lettuce identifies human and animal viruses. Int J Food Microbiol. 223, 50–56.

Baert, L., Uyttendaele, M., Debevere, J., 2008a. Evaluation of viral extraction methods on a broad range of Ready-To-Eat foods with conventional and real-time RT-PCR for Norovirus GII detection. Int J Food Microbiol. 123,101–108.

Baert, L., Uyttendaele, M., van Coillie, E., Debevere, J., 2008b. The reduction of murine norovirus 1, B. fragilis HSP40 infecting phage B40-8 and E. coli after a mild thermal pasteurization process of raspberry puree. Food Microbiol. 25 (7), 871–874.

Bartsch, C., Szabo, K., Dinh-Thanh, M., Schrader, C., Trojnar, E., Johne, R., 2016. Comparison and optimization of detection methods for noroviruses in frozen strawberries containing different amounts of RT-PCR inhibitors. Food Microbiol. 60, 124–130.

Barrabeig, I., Rovira, A., Buesa, J., Bartolomé, R., Pintó, R., Prellezo, H., Domínguez, A., 2010. Foodborne norovirus outbreak: The role of an asymptomatic food handler. BMC Infect Dis. 10, 269.

Barros, V.G., Duda, R.M., Vantini, J.D.S., Omori, W.P., Ferro, M.I.T., Oliveira, R.A., 2017. Improved methane production from sugarcane vinasse with filter cake in thermophilic UASB reactors, with predominance of Methanothermobacter and Methanosarcina archaea and Thermotogae bacteria. Bioresour Technol. 244, 371–381.

Bätzing-Feigenbaum, J., Loschen, S., Gohlke-Micknis, S., Zimmermann, R., Hermann, A., Kamga Wambo, G.O., Kücherer, C., Hamouda, O., 2008. Country-wide HIV incidence study complementing HIV surveillance in Germany. Euro Surveill. 13, 36.

Berg, C., Bartsch, C., Johne, R., Schneider, R., Böhm, T., Winkelsett, S., Guder., G., 2017. Smoothies – the new minced meet? - frequent detection of noroviruses in frozen berries. Amtstierärztlicher Dienst und Lebensmittelkontrolle. 24 (2), 94-100.

Bernard, H., Faber, M., Wilking, H., Haller, S., Höhle, M., Schielke, A., Ducomble, T., Siffczyk, C., Merbecks, S.S., Fricke, G., Hamouda, O., Stark, K., Werber, D., Investiga, o.b.o.t.O., 2014. Large multistate outbreak of norovirus gastroenteritis associated with frozen strawberries, Germany, 2012. Euro Surveill.19 (8).

BfR, 2013a. http://www.bfr.bund.de/en/press_information/2013/05/deep_frozen_berries_are_better_thoroughly_cooked_before_consumption-133016.html

BfR, 2013b. http://www.bfr.bund.de/cm/350/verbrauchertipps-schutz-vor-viralen-lebensmittelinfektionen.pdf

BfR, 2017. http://www.bfr.bund.de/cm/364/safe-food-especially-vulnerable-groups-in-community-institutions.pdf

Boonham, N., Kreuze, J., Winter, S., van der Vlugt, R., Bergervoet, J., Tomlinson, J., Mumford, R., 2014. Methods in virus diagnostics: From ELISA to next generation sequencing. Virus Research. 186, 20–31.

Bovo, S., Mazzoni, G., Ribani, A., Utzeri, V.J., Bertolini, F., Schiavo, G., Fontanesi, L., 2017. A viral metagenomic approach on a non-metagenomic experiment: Mining next generation sequencing datasets from pig DNA identified several porcine parvoviruses for a retrospective evaluation of viral infections. PloS one. 12 (6), e0179462.

Bozkurt, H., D'Souza, D.H., Davidson, P.M., 2013. Determination of the thermal inactivation kinetics of the human norovirus surrogates, murine norovirus and feline calicivirus. J Food ProtecT. 76 (1), 79–84.

Bozkurt, H., D'souza, D.H., Davidson, P.M., 2014. Thermal inactivation of human norovirus surrogates in spinach and measurement of its uncertainty. J Food Protect. 77 (2), 276–283.

Bozkurt, H., D'Souza, D.H., Davidson, P.M., 2015a. Thermal Inactivation Kinetics of Human Norovirus Surrogates and Hepatitis A Virus in Turkey Deli Meat. Appl Environ Microbiol. 81 (14), 4850–4859.

Bozkurt, H., D'Souza, D.H., Davidson, P.M., 2015b. Thermal Inactivation of Foodborne Enteric Viruses and Their Viral Surrogates in Foods. J Food Protect. 78 (8), 1597–1617.

Brady, C.L., Venter, S.N., Cleenwerck, I., Vandemeulebroecke, K., Vos, P. de, Coutinho, T.A., 2010. Transfer of Pantoea citrea, Pantoea punctata and Pantoea terrea to the genus Tatumella emend. as Tatumella citrea comb. nov., Tatumella punctata comb. nov. and Tatumella terrea comb. nov. and description of Tatumella morbirosei sp. nov. Int J Sys Evol Microbiol. 60 (Pt 3), 484–494.

Brassard, J., Gagné, M.J., Généreux, M., Côté, C., 2012. Detection of human food-borne and zoonotic viruses on irrigated, field-grown strawberries. Appl Environ Microbiol. 78, 3763–3766.

Butot, S., Putallaz, T., Sánchez, G., 2007. Procedure for rapid concentration and detection of enteric viruses from berries and vegetables. Appl Environ Microbiol. 73, 186–192.

Butot, S., Putallaz, T., Amoroso, R., Sánchez, G., 2009. Inactivation of enteric viruses in minimally processed berries and herbs. Appl Environ Microbiol. 75 (12), 4155–4161.

Cadillo-Quiroz, H., Bräuer, S.L., Goodson, N., Yavitt, J.B., Zinder, S.H., 2014. Methanobacterium paludis sp. nov. and a novel strain of Methanobacterium lacus isolated from northern peatlands. Int J Sys Evol Microbiol. 64 (5), 1473–1480.

Calscape. http://calscape.org/Jamesia-americana-().

Caul, E.O., 1996. Viral gastroenteritis: small round structured viruses, caliciviruses and astroviruses. Part II. The epidemiological perspective. J Clin Pathol. 49, 959–964.

Chapin, A.R., Carpenter, C.M., Dudley, W.C., Gibson, L.C., Pratdesaba, R., Torres, O., Sanchez, D., Belkind-Gerson, J., Nyquist, I., Kärnell, A., Gustafsson, B., Halpern, J.L., Bourgeois, A.L., Schwab, K.J., 2005. Prevalence of norovirus among visitors from the United States to Mexico and Guatemala who experience traveler's diarrhea. J Clin Microbiol. 43, 1112–1117.

Cheesbrough, J.S., Barkess-Jones, L., Brown, D.W., 1997. Possible prolonged environmental survival of small round structured viruses. J Hosp Infect. 35, 325–326.

Cheong, S., Lee, C., Choi, W.C., Lee, C.H., Kim, S.J., 2009. Concentration method for the detection of enteric viruses from large volumes of foods. J Food Prot. 72, 2001–2005.

Chiapponi, C., Pavoni, E., Bertasi, B., Baioni, L., Scaltriti, E., Chiesa, E., Cianti, L., Losio, M.N., Pongolini, S., 2014. Isolation and genomic sequence of hepatitis A virus from mixed frozen berries in Italy. Food Environ Virol. 6 (3), 202–206.

Codex Alimentarius, 2012. Guidelines on the application of general principles of food hygiene to the control of viruses in food. CAC/GL 79.

Collier, M.G., Khudyakov, Y.E., Selvage, D., Adams-Cameron, M., Epson, E., Cronquist, A., Jervis, R.H., Lamba, K., Kimura, A.C., Sowadsky, R., Hassan, R., Park, S.Y., Garza, E., Elliott, A.J., Rotstein, D.S., Beal, J., Kuntz, T., Lance, S.E., Dreisch, R., Wise, M.E., Nelson, N.P., Suryaprasad, A., Drobeniuc, J., Holmberg, S.D., Xu, F., 2014. Outbreak of hepatitis A in the USA associated with frozen pomegranate arils imported from Turkey: An epidemiological case study. Lancet Infect Dis. 14 (10), 976–981.

Compton, S.R., 2008. Prevention of murine norovirus infection in neonatal mice by fostering. J Am Assoc Lab Anim Sci. 47(3), 25-30.

Cook, N., Knight, A., Richards, G.P., 2016. Persistence and Elimination of Human Norovirus in Food and on Food Contact Surfaces: A Critical Review. J Food Protect. 79 (7), 1273–1294.

Coudray-Meunier, C., Fraisse, A., Martin-Latil, S., Guillier, L., Delannoy, S., Fach, P., Perelle, S., 2015. A comparative study of digital RT-PCR and RT-qPCR for quantification of Hepatitis A virus and Norovirus in lettuce and water samples. Int J Food Microbiol. 201, 17–26.

Crits-Christoph, A., Gelsinger, D.R., Ma, B., Wierzchos, J., Ravel, J., Davila, A., Casero, M.C., DiRuggiero, J., 2016. Functional interactions of archaea, bacteria and viruses in a hypersaline endolithic community. Environ Microbiol. 18 (6), 2064–2277.

Croci, L., Suffredini, E., Di Pasquale, S., Cozzi, L., 2012. Detection of norovirus and feline calicivirus in spiked molluscs subjected to heat treatments. Food Control. 25, 17–22.

Cromeans, T., Park, G.W., Costantini, V., Lee, D., Wang, Q., Farkas, T., Lee, A., Vinjé, J., 2014. Comprehensive comparison of cultivable norovirus surrogates in response to different inactivation and disinfection treatments. Appl Environ Microbiol. 80 (18), 5743–5751.

da Silva, A.K., Le Saux, J.C., Parnaudeau, S., Pommepuy, M., Elimelech, M., Le Guyader, F.S., 2007. Evaluation of removal of noroviruses during wastewater treatment, using Real-Time Reverse Transcription-PCR: different behaviors of genogroups I and II. Appl Environ Microbiol. 73(24), 7891–7897.

de Wit, M.A., Koopmans, M.P., Kortbeek, L.M., Wannet, W.J., Vinjé, J., van Leusden, F., Bartelds, A.I., van Duynhoven, Y.T., 2001. Sensor, a population-based cohort study on gastroenteritis in the Netherlands: incidence and etiology. Am J Epidemiol. 154, 666–674.

Deboosere, N., Legeay, O., Caudrelier, Y., Lange, M., 2004. Modelling effect of physical and chemical parameters on heat inactivation kinetics of hepatitis A virus in a fruit model system. Int J Food Microbiol. 93, 73–85.

Denner, J., Specke, V., Thiesen, U., Karlas, A., Kurth, R., 2003. Genetic alterations of the long terminal repeat of an ecotropic porcine endogenous retrovirus during passage in human cells. Virology. 314 (1), 125–133.

Dolin, R., Blacklow, N.R., DuPont, H., Buscho, R.F., Wyatt, R.G., Kasel, J.A., Hornick, R., Chanock, R.M., 1972. Biological properties of Norwalk agent of acute infectious nonbacterial gastroenteritis. Proc Soc Exp Biol Med. 140 (2), 578–583.

Dreier, J., Störmer, M., Kleesiek, K., 2005. Use of bacteriophage MS2 as an internal control in viral reverse transcription-PCR assays. J Clin Microbiol. 43, 4551–4557.

Drouaz, N., Schaeffer, J., Farkas, T., Le Pendu, J., Le Guyader, F.S., 2015. Tulane Virus as a Potential Surrogate To Mimic Norovirus Behavior in Oysters. Appl Environ Microbiol. 81 (15), 5249–5256.

Dubois, E., Agier, C., Traoré, O., Hennechart, C., Merle, G., Crucière, C., Laveran, H., 2002. Modified concentration method for the detection of enteric viruses on fruits and vegetables by reverse transcriptase-polymerase chain reaction or cell culture. J Food Prot. 65, 1962–1969.

Duret, S., Pouillot, R., Fanaselle, W., Papafragkou, E., Liggans, G., Williams, L., van Doren, J.M., 2017. Quantitative Risk Assessment of Norovirus Transmission in Food Establishments: Evaluating the Impact of Intervention Strategies and Food Employee Behavior on the Risk Associated with Norovirus in Foods. Risk analysis. Off Pub Societ Risk Anal. 37 (11), 2080–2106.

Ehlers, B., Dural, G., Marschall, M., Schregel, V., Goltz, M., Hentschke, J., 2006. Endotheliotropic elephant herpesvirus, the first betaherpesvirus with a thymidine kinase gene. J Gen Virol. 87 (Pt 10), 2781–2789.

Esseili, M.A., Saif, L.J., Farkas, T., Wang, Q., 2015. Feline Calicivirus, Murine Norovirus, Porcine Sapovirus, and Tulane Virus Survival on Postharvest Lettuce. Appl Environ Microbiol. 81, 5085–5092.

Ettayebi, K., Crawford, S.E., Murakami, K., Broughman, J.R., Karandikar, U., Tenge, V.R., Neill, F.H., Blutt, S.E., Zeng, X.-L., Qu, L., Kou, B., Opekun, A.R., Burrin, D., Graham, D.Y., Ramani, S., Atmar, R.L., Estes, M.K., 2016. Replication of human noroviruses in stem cell-derived human enteroids. Science. 353 (6306), 1387–1393.

Farkas, K., Hassard, F., McDonald, J.E., Malham, S.K., Jones, D.L., 2017. Evaluation of Molecular Methods for the Detection and Quantification of Pathogen-Derived Nucleic Acids in Sediment. Frontiers Microbiol. 8, 53.

Farkas, T., Sestak, K., Wei, C., Jiang, X., 2008. Characterization of a rhesus monkey calicivirus representing a new genus of Caliciviridae. J Virol. 82, 5408–5416.

Farkas, T., Cross, R. W., Hargitt, E., Lerche, N. W., Morrow, A. L., Sestak, K., 2010. Genetic diversity and histo-blood group antigen interactions of rhesus enteric caliciviruses. J Virol. 84, 8617–8625.

Fell, G., Boyens, M., Baumgarte, S., 2007. Frozen berries as a risk factor for outbreaks of norovirus gastroenteritis. Results of an outbreak investigation in the summer of 2005 in Hamburg. Bundesgesundheitsblatt, Gesundheitsforschung, Gesundheitsschutz 50, 230–236.

Filter, M., Thöns, C., Brandt, J., Weiser, A., Falenski, A., Appel, B., Käsbohrer, A., 2013. A community resource for integrated predictive microbial modelling (PMM-Lab), 5th International Workshop Cold Chain Management. http://ccm.ytally.com/index.php?id=176 Bonn, Germany.

Fraenkel, C.J., Inghammar, M., Söderlund-Strand, A., Johansson, P.J.H., Böttiger, B., 2018. Risk factors for hospital norovirus outbreaks: Impact of vomiting, genotype and multioccupancy rooms. J Hosp Infect. pii: S0195-6701(18)30054-9.

Fraisse, A., Coudray-Meunier, C., Martin-Latil, S., Hennechart-Collette, C., Delannoy, S., Fach, P., Perelle, S. Digital RT-PCR method for hepatitis A virus and norovirus quantification in soft berries, 2017. Int J Food Microbiol. 243, 36–45.

Fuller, C., Hudgins, E., Finelt, N., 2017. Human-papillomavirus-related disease in pediatrics. Curr Opin Pediatr. EPub, doi: 10.1097/MOP.0000000000000561.

Gehrke, C., Steinmann, J., Goroncy-Bermes, P. 2004. Inactivation of feline calicivirus, a surrogate of norovirus (formerly Norwalk-like viruses), by different types of alcohol in vitro and in vivo. J Hosp Infect. 56, 49–55.

Glass, P.J., White, L.J., Ball, J.M., Leparc-Goffart, I., Hardy, M.E., Estes, M.K., 2000. Norwalk virus open reading frame 3 encodes a minor structural protein. J Virol. 74(14), 6581–6591.

Glass, R.I., Parashar, U.D., Estes, M.K., 2009. Norovirus gastroenteritis. New England J Med. 361(1), 1776–1785.

Gonzalez-Hernandez, M.B., Bragazzi Cunha, J., Wobus, C.E., 2012. Plaque assay for murine norovirus. Journal of visualized experiments. JoVE (66), e4297.

Green, K.Y., Knipe, D.M., Howley P.M., 2013. Caliciviridae: the noroviruses. Book: Fields Virology (Lippincott/Williams and Wilkins: Philadelphia). 1 (6), 582–608.

Grote, U., Schleenvoigt, B.T., Happle, C., Dopfer, C., Wetzke, M., Ahrenstorf, G., Holst, H., Pletz, M.W., Schmidt, R.E., Behrens, G.M., Jablonka, A., 2017. Norovirus outbreaks in german refugee camps in 2015. Z Gastroenterol. 55 (10), 997–1003.

Guzman-Herrador, B., Jensvoll, L., Einöder-Moreno, M., Lange, H., Myking, S., Nygård, K., Stene-Johansen, K., Vold, L., 2014. Ongoing hepatitis A outbreak in Europe 2013 to 2014- imported berry mix cake suspected to be the source of infection in Norway. Euro Surveill. 19 (15).

Haussig, J.M., Nielsen, S., Gassowski, M., Bremer, V., Marcus, U., Wenz, B., Bannert, N., Bock, C.T., Zimmermann, R., Kücherer. C., Santos-Hövener, C., 2017. Large proportion of people who inject drugs are susceptible to hepatitis B – results from a bio-behavioural study in eight German cities. Int J Infect. Epub, doi: 10.1016/j.ijid.2017.10.008.

Hoehne, M., Schreier, E., 2006. Detection of Norovirus genogroup I and II by multiplex real-time RT- PCR using a 3'-minor groove binder-DNA probe. BMC Infect Dis. 10, 69.

Huang, R., Ye, M., Li, X., Ji, L., Karwe, M., Chen, H., 2016. Evaluation of high hydrostatic pressure inactivation of human norovirus on strawberries, blueberries, raspberries and in their purees. Int J Food Microbiol. 223, 17–24.

Hull, R.N., Cherry, W.R., Tritch, O.J., 1962. Growth characteristics of monkey kidney cell strains LLC-MK1, LLC-MK2, and LLC-MK2(NCTC-3196) and their utility in virus research. J Exp Med. 115, 903–918.

Imamura, S., Kanezashi, H., Goshima, T., Haruna, M., Okada, T., Inagaki, N., Uema, M., Noda, M., Akimoto, K., 2017. Next-Generation Sequencing Analysis of the Diversity of Human Noroviruses in Japanese Oysters. Foodborne Pathogens Dis. 14 (8), 465–471.

ISO, 2013. Microbiology of the food chain — Horizontal method for determination of hepatitis A virus and norovirus in food using real-time RT-PCR. ISO/TS 15216-2:2013.

Jarchow-Macdonald, A.A., Halley, S., Chandler, D., Gunson, R., Shepherd, S.J., Parcell, B.J., 2015. First report of an astrovirus type 5 gastroenteritis outbreak in a residential elderly care home identified by sequencing. J Clin Virol. 73,115–119.

Jelkmann, W., Martin, R.R., Lesemann, D.-E., Vetten. H.J., Skelton, F., 1990. A new potexvirus associated with strawberry mild yellow edge disease. J Gen Virol. 71, 1251–1258.

Jiang, X., Wang, M., Wang, K., Estes, M.K., 1993. Sequence and genomic organization of Norwalk virus. Virology. 195, 51–61

Joensen, K.G., Engsbro, A.L.Ø., Lukjancenko, O., Kaas, R.S., Lund, O., Westh, H., Aarestrup, F.M., 2017. Evaluating next-generation sequencing for direct clinical diagnostics in diarrhoeal disease. European journal of clinical microbiology & infectious diseases. Europ Society Clin Microbiol. 36 (7), 1325–1338.

Johne, R., Trojnar, E., Filter, M., Hofmann, J., 2017. Thermal stability of hepatitis E virus estimated by a cell culture method. Appl Environ Microbiol. 82, 4225–4231.

Jones, M.K., Watanabe, M., Zhu, S., Graves, C.L., Keyes, L.R., Grau, K.R., Gonzalez-Hernandez, M.B., Iovine, N.M., Wobus, C.E., Vinje, J., Tibbetts, S.A., Wallet, S.M.,

Karst, S.M., 2014. Enteric bacteria promote human and mouse norovirus infection of B cells. Science. 346, 755–759

Joyeux, C., Fouchard, S., Llopiz, P., Neunlist, S., 2004. Influence of the temperature and the growth phase on the hopanoids and fatty acids content of Frateuria aurantia (DSMZ 6220). FEMS Microbiol Ecol. 47 (3), 371–379.

Karst, S. M., Wobus, C. E., Lay, M., Davidson, J., Virgin, IV H. W., 2003. STAT1-dependent innate immunity to a Norwalk-like virus. Science. 299, 175–1578.

Karst, S.M., Zhu, S., Goodfellow, I.G., 2015. The molecular pathology of noroviruses. J Pathol. 235, 206–216.

Kageyama, T., Kojima, S., Shinohara, M., Uchida, K., Fukushi, S., Hoshino, F.B., Takeda, N., Katayama, K., 2003. Broadly reactive and highly sensitive assay for Norwalk-like viruses based on real-time quantitative reverse transcription-PCR. J Clin Microbiol. 41 (4), 1548–1557.

Kato, K., Ishiwa, A., 2015. The role of carbohydrates in infection strategies of enteric pathogens. Trop Med Health. 43, 41–52.

Kirkwood, C.D., Streitberg, R., 2008. Calicivirus shedding in children after recovery from diarrhoeal disease. J Clin Virol. 43, 346–348.

Kitajima, M., Oka, T., Takagi, H., Tohya, Y., Katayama, H., Takeda, N., Katayama, K., 2010. Development and application of a broadly reactive real-time reverse transcription-PCR assay for detection of murine noroviruses. J Virol Meth. 169 (2), 269–273.

Koo, H.L., Ajami, N., Atmar, R.L., DuPont, H.L., 2010. Noroviruses: the leading cause of gastroenteritis worldwide. Discov Med.10, 61–70.

Koromyslova, A.D., Leuthold, M.M., Bowler, M.W., Hansman, G.S., 2015. The sweet quartet: Binding of fucose to the norovirus capsid. Virology. 483, 203–208.

Kreuzer, S., Machnowska, P., Aßmus, J., Sieber, M., Pieper, R., Schmidt, M.F., Brockmann, G.A., Scharek-Tedin, L., Johne, R., 2012. Feeding of the probiotic bacterium Enterococcus faecium NCIMB 10415 differentially affects shedding of enteric viruses in pigs. Vet Res. 27, 43–58.

Kroneman, A., Vega, E., Vennema, H., Vinje, J., White, P.A., Hansman, G., Green, K., Martella, V., Katayama, K., Koopmans, M., 2013. Proposal for a unified norovirus nomenclature and genotyping. Arch Virol. 158, 2059–2068.

Kulkarni, P., Frommolt, P., 2017. Challenges in the Setup of Large-scale Next-Generation Sequencing Analysis Workflows. Comput Struct Biotech J. 15, 471–477.

Lambden, P.R., Caul, E.O., Ashley, C.R., Clarke, I.N., 1993. Sequence and genome organization of a human small round-structured (Norwalk-like) virus. Science. 259 (5094), 516–519.

Li, X., Chen, H., 2015. Evaluation of the porcine gastric mucin binding assay for high-pressure-inactivation studies using murine norovirus and tulane virus. Appl Environ Microbiol. 81 (2), 515–521.

Loisy, F., Atmar, R.L., Guillon, P., Le Cann, P., Pommepuy, M., Le Guyader, F.S., 2005. Real-time RT-PCR for norovirus screening in shellfish. J Virol Methods. 123 (1) 1–7.

Lopman, B., 2011. Air sickness: vomiting and environmental transmission of norovirus on aircraft. Clin Infect Dis. 53, 521–522.

Lorimer, M.F., Kiermeier, A., 2007. Analysing microbiological data: Tobit or not Tobit?. Int J Food Microbiol. 116, 313–318.

Mahmoudpour, A., 2003. Infectivity of recombinant strawberry vein banding virus DNA. J Gen Virol. 84 (6), 1377–1381.

Maunula, L., Kaupke, A., Vasickova, P., Söderberg, K., Kozyra, I., Lazic, S., van der Poel, W.H., Bouwknegt, M., Rutjes, S., Willems, K.A., Moloney, R., D'Agostino, M., de Roda Husman, A.M., von Bonsdorff, C.H., Rzeżutka, A., Pavlik, I., Petrovic, T., Cook, N., 2013 Tracing enteric viruses in the European berry fruit supply chain. Int J Food Microbiol. 167, 177–185.

Mäde, D., Trübner, K., Neubert, E., Höhne, M., Johne, R., 2013. Detection and Typing of Norovirus from Frozen Strawberries Involved in a Large-Scale Gastroenteritis Outbreak in Germany. Food Environ Virol. 5, 162–168.

Mattison, K., Shukla, A., Cook, A., Pollari, F., Friendship, R., Kelton, D., Bidawid, S., M. Farber, J.M., 2007. Human Noroviruses in Swine and Cattle. Emer Infect Dis. 13 (8), 1184–1188.

Meeroff, J.C., Schreiber, D.S., Trier, J.S., Blacklow, N.R., 1980. Abnormal gastric motor function in viral gastroenteritis. Annals Int Med. 92, 370–373.

Meng, X., Bertani, I., Abbruscato, P., Piffanelli, P., Licastro, D., Wang, C., Venturi, V., 2015. Draft Genome Sequence of Rice Endophyte-Associated Isolate Kosakonia oryzae KO348. Genome announcements. 3 (3).

Meyer, M., Kircher, M., 2010. Illumina Sequencing Library Preparation for Highly Multiplexed Target Capture and Sequencing. Cold Springs Harb Prot. Epub, doi: 10.1101/pdb.prot5448.

Michel, C.J., Ngoune, V.N., Poch, O., Ripp, R., Thompson, J.D., 2017. Enrichment of Circular Code Motifs in the Genes of the Yeast Saccharomyces cerevisiae. Life (Basel, Switzerland). 7 (4).

MoBiTec GmbH, 2012. MobiSpin Columns, S-400, Standard Protocol, p. 7.

Monteiro, S., Santos, R., 2017. Nanofluidic digital PCR for the quantification of Norovirus for water quality assessment. PloS one. 12 (7), e0179985.

Morin, G., Robinson, B.A., Rogers, K.S., Wong, S.W., 2015. A Rhesus Rhadinovirus Viral Interferon (IFN) Regulatory Factor Is Virion Associated and Inhibits the Early IFN Antiviral Response. J Virol. 89 (15), 7707–7721.

Mormann, S., Dabisch, M., Becker, B., 2010. Effects of technological processes on the tenacity and inactivation of norovirus genogroup II in experimentally contaminated foods. Appl Environ Microbiol. 76 (2), 536–545.

Mouchtouri, V.A., Verykouki, E., Zamfir, D., Hadjipetris, C., Lewis, H.C., Hadjichristodoulou, C., The Eu Shipsan Act Partnership, 2017. Gastroenteritis outbreaks on cruise ships: contributing factors and thresholds for early outbreak detection. Euro Surveill. 22 (45).

Mui, U.N., Haley, C.T., Tyring, S.K., 2017. Viral Oncology: Molecular Biology and Pathogenesis. J Clin Med. 6 (12).

Murata, T., Katsushima, N., Mizuta, K., Muraki, Y., Hongo, S., Matsuzaki, Y., 2007. Prolonged norovirus shedding in infants under 6 months of age with gastroenteritis. Pediatr Infect Dis J. 26, 46–49.

Nasheri, N., Petronella, N., Ronholm, J., Bidawid, S., Corneau, N., 2017. Characterization of the Genomic Diversity of Norovirus in Linked Patients Using a Metagenomic Deep Sequencing Approach. Frontiers Microbiol. 8, 73.

Nyakarahuka, L., Ayebare, S., Mosomtai, G., Kankya, C., Lutwama, J., Mwiine, F.N., Skjerve, E., 2017. Ecological Niche Modeling for Filoviruses: A Risk Map for Ebola and Marburg Virus Disease Outbreaks in Uganda. PLoS Curr. 5, 9.

Ogawa, H., Kajihara, M., Nao, N., Shigeno, A., Fujikura, D., Hang'ombe, B.M., Mweene, A.S., Mutemwa, A., Squarre, D., Yamada, M., Higashi, H., Sawa, H., Takada, A., 2017. Characterization of a Novel Bat Adenovirus Isolated from Straw-Colored Fruit Bat (Eidolon helvum). Viruses. 9 (12).

Park, S.Y., Bae, S.-C., Ha, S.-D., 2015. Heat inactivation of a norovirus surrogate in cell culture lysate, abalone meat, and abalone viscera. Food Environ Virol. 7 (1), 58–66.

Peist, R., Honsel, D., Twieling, G., Löffert, D., 2001. PCR inhibitors in plant DNA preparations. QIAGEN News. 3, 7–9.

Perrin, A., Loutreul, J., Boudaud, N., Bertrand, I., Gantzer, C., 2015. Rapid, simple and efficient method for detection of viral genomes on raspberries. J Virol Methods. 224, 95–101.

Phillips, G., Tam, C.C., Conti, S., Rodrigues, L.C., Brown, D., Iturriza-Gomara, M., Gray, J., Lopman, B., 2010. Community incidence of norovirus-associated infectious intestinal disease in England: improved estimates using viral load for norovirus diagnosis. Am J Epidemiol. 171, 1014–1022.

Polo, D., Schaeffer, J., Fournet, N., Le Saux, J.-C., Parnaudeau, S., McLeod, C., Le Guyader, F.S., 2016. Digital PCR for Quantifying Norovirus in Oysters Implicated in Outbreaks, France. Emer Infect Dis. 22 (12), 2189–2191.

Prompiboon, P., Lietze, V.-U., Denton, J.S.S., Geden, C.J., Steenberg, T., Boucias, D.G., 2010. Musca domestica salivary gland hypertrophy virus, a globally distributed

insect virus that infects and sterilizes female houseflies. Appl Environ Microbiol. 76 (4), 994–998.

Raschke, W.C., Baird, S., Ralph, P., Nakoinz, I., 1978. Functional macrophage cell lines transformed by Abelson leukemia virus. Cell. 15, 261–267.

Sachsenröder, J., Twardziok, S.O., Scheuch, M., Johne, R., 2014. The general composition of the faecal virome of pigs depends on age, but not on feeding with a probiotic bacterium. PloS one. 9 (2), e88888.

Sarvikivi, E., Roivainen, M., Maunula, L., Niskanen, T., Korhonen, T., Lappalainen, M., 2012. Multiple norovirus outbreaks linked to imported frozen raspberries. Epidemiol Infect. 140, 260–267.

Sattar, S.A., Tetro, J., Springthorpe, V.S., Giulivi, A., 2001. Preventing the spread of hepatitis B and C viruses: where are germicides relevant? Am J Infect Control. 29, 187–197.

Scherer, K., Mäde, D., Ellerbroek, L., Schulenburg, J., Johne, R., Klein, G., 2009. Application of a Swab Sampling Method for the Detection of Norovirus and Rotavirus on Artificially Contaminated Food and Environmental Surfaces. Food Environ Virol. 1, 42–49.

Scherer, K., Johne, R., Schrader, C., Ellerbroek, L., Schulenburg, J., Klein, G., 2010. Comparison of two extraction methods for viruses in food and application in a norovirus gastroenteritis outbreak. J Virol Methods. 169, 22–27.

Scheuch, M., Höper, D., Beer, M., 2015. RIEMS: A software pipeline for sensitive and comprehensive taxonomic classification of reads from metagenomics datasets. BMC bioinformat. 16, 69.

Schielke, A., Filter, M., Appel, B., Johne, R., 2011. Thermal stability of hepatitis E virus assessed by a molecular biological approach. Virol J. 8, 487.

Schrader, C., Schielke, A., Ellerbroek, L., Johne, R., 2012. PCR inhibitors - occurrence, properties and removal. J Appl Microbiol. 113, 1014–1026.

Schreiber, D.S., Blacklow, N.R., Trier, J.S., 1973. The mucosal lesion of the proximal small intestine in acute infectious nonbacterial gastroenteritis. New Eng J Med. 288, 1318–1323.

Seeram, N.P., Adams, L.S., Zhang, Y., Lee, R., Sand, D., Scheuller, H.S., Heber, D., 2006. Blackberry, black raspberry, blueberry, cranberry, red raspberry, and strawberry extracts inhibit growth and stimulate apoptosis of human cancer cells in vitro. J Agric Food Chem. 54, 9329–9339.

Seo, K., Lee, J.E., Lim, M.Y., Ko, G., 2012. Effect of temperature, pH, and NaCl on the inactivation kinetics of murine norovirus. J Food Protect. 75 (3), 533–540.

Shihada, S., Emmerich, P., Thomé-Bolduan, C., Jansen, S., Günther, S., Frank, C., 2017. Genetic diversity and new lineages of Dengue virus serotypes 3 and 4 in returning travelers, Germany, 2006–2015. Emerg. Infect. Dis. 23 (2), 272–275.

Somura, Y., Kimoto, K., Oda, M., Okutsu, Y., Kato, R., Suzuki, Y., Siki, D., Hirai, A., Akiba, T., Shinkai, T., Sadamasu, K., 2017. Serial Food Poisoning Outbreaks Caused by Norovirus-Contaminated Shredded Dried Laver Seaweed Provided at School Lunch, Tokyo, 2017. Shokuhin Eiseigaku Zasshi. 58 (6), 260–267.

Subba-Reddy, C.V., Goodfellow, I., Cheng Kao, C., 2011. VPg-Primed RNA Synthesis of Norovirus RNA-Dependent RNA Polymerases by Using a Novel Cell-Based Assay. J Virol. 85 (24), 13027–13037.

Svraka, S., Duizer, E., Vennema, H., de Bruin, E., van der Veer, B., Dorresteijn, B., Koopmans, M., 2007. Etiological role of viruses in outbreaks of acute gastroenteritis in The Netherlands from 1994 through 2005. J Clin Microbiol. 45 (5), 1389–1394.

Szabo, K., Trojnar, E., Anheyer-Behmenburg, H3., Binder, A., Schotte, U., Ellerbroek, L., Klein, G., Johne, R., 2015. Detection of hepatitis E virus RNA in raw sausages and liver sausages from retail in Germany using an optimized method. Int J Food Microbiol. 215, 149–56.

Tan, M., Jiang, X., 2008. Association of histo-blood group antigens with susceptibility to norovirus infection may be strain-specific rather than genogroup dependent. J Infect Dis. 198, 940–941.

Tavoschi, L., Severi, E., Niskanen, T., Boelaert, F., Rizzi, V., Liebana, E., Gomes Dias, J., Nichols, G., Takkinen, J., Coulombier, D., 2015. Food-borne diseases associated with frozen berries consumption: a historical perspective, European Union, 1983 to 2013. Euro Surveill. 20 (29), 21193.

Tian, P., Brandl, M., Mandrell, R., 2005. Porcine gastric mucin binds to recombinant norovirus particles and competitively inhibits their binding to histo-blood group antigens and Caco-2 cells. Lett Appl Microbiol. 41, 315–320.

Tian, P., Yang, D., Quigley, C., Chou, M., Jiang, X., 2013. Inactivation of the Tulane Virus, a Novel Surrogate for the Human Norovirus. J Food Prot. 76 (4), 712–718.

Thompson, J.R., Leone, G., Lindner, J.L., Jelkmann, W., Schoen, C.D., 2002. Characterization and complete nucleotide sequence of Strawberry mottle virus: a tentative member of a new family of bipartite plant picorna-like viruses. J Gen Virol. 83, 229–239.

Trotereau, A., Gonnet, M., Viardot, A., Lalmanach, A.C., Guabiraba, R., Chanteloup, N.K., Schouler, C., 2017. Complete Genome Sequences of Two Escherichia coli Phages, vB_EcoM_ ESCO5 and vB_EcoM_ESCO13, Which Are Related to phAPEC8. Genome Announc. 5 (13), pii: e01337-16.

Tuomi, P.A., Murray, M.J., Garner, M.M., Goertz, C.E., Nordhausen, R.W., Burek-Huntington, K.A., Getzy, D.M., Nielsen, O., Archer, L.L., Maness, H.T., Wellehan, J.F. Jr., Waltzek, T.B., 2014. Novel poxvirus infection in northern and southern sea otters (Enhydra lutris kenyoni and Enhydra lutris neiris), Alaska and California, USA. J Wildl Dis. 50 (3), 607–615.

UniProt. Enterobacteria phage ECGD1. http://www.uniprot.org/taxonomy/1784948.

Urrutia, M., Rambla, J.L., Alexiou, K.G., Granell, A., Monfort, A., 2017. Genetic analysis of the wild strawberry (Fragaria vesca) volatile composition. Plant Phys Biochem. 121, 99–117.

Vega, E., Barclay, L., Gregoricus, N., Shirley, S.H., Lee, D., Vinje, J., 2014. Genotypic and epidemiologic trends of norovirus outbreaks in the United States, 2009 to 2013. J Clin Microbiol. 52, 147–155.

Verhaelen, K., Bouwknegt, M., Lodder-Verschoor, F., Rutjes, S.A., de Roda Husman, A. M., 2012. Persistence of human norovirus GII.4 and GI.4, murine norovirus, and human adenovirus on soft berries as compared with PBS at commonly applied storage conditions. Int J Food Microbiol. 160, 137–144.

Vinjé, J., 2015. Advances in laboratory methods for detection and typing of norovirus. J Clin Microbiol. 53 (2), 373–381.

Vivaipriola. Sanguisorba Sitchensis. http://www.vivaipriola.com/sanguisorba-sitchensis/.

Watzinger, F., Ebner, K., Lion, T., 2006. Detection and monitoring of virus infections by real-time PCR. Mol Aspects Med. 27 (2-3), 254–298.

Wei, T., Lu, G., Clover, G., 2008. Novel approaches to mitigate primer interaction and eliminate inhibitors in multiplex PCR, demonstrated using an assay for detection of three strawberry viruses. J Virol Methods. 151, 132–139.

Wei, Y.-Q., Yang, H.-J., Long, R.-J., Wang, Z.-Y., Cao, B.-B., Ren, Q.-C., Wu, T.-T., 2017. Characterization of natural co-cultures of Piromyces with Methanobrevibacter ruminantium from yaks grazing on the Qinghai-Tibetan Plateau: A microbial consortium with high potential in plant biomass degradation. AMB Express. 7 (1), 160.

Wobus, C. E., L. B. Thackray, and H. W. Virgin. 2006. Murine norovirus: a model system to study norovirus biology and pathogenesis. J Virol. 80, 5104–5112.

Xu, S., Wang, D., Yang, D., Liu, H., Tian, P., 2015. Alternative methods to determine infectivity of Tulane virus: A surrogate for human nororvirus. Food Microbiol. 48, 22–27.

Yang, Z., Mammel, M., Papafragkou, E., Hida, K., Elkins, C.A., Kulka, M., 2017. Application of next generation sequencing toward sensitive detection of enteric viruses isolated from celery samples as an example of produce. Int J Food Microbiol. 261, 73–81.

Zagordi, O., Klein, R., Däumer, M., Beerenwinkel, N., 2010. Error correction of next-generation sequencing data and reliable estimation of HIV quasispecies. Nucl Acids Res. 38 (21), 7400–7409.

Zahorsky, J., 1929. Hyperemesis hiemis or the winter vomiting disease. Arch Pediatr. 46, 391–395.

Zhang, Y., Jiang, H-R. A review on continuous-flow microfluidic PCR in droplets: advances, challenges and future, 2016. Analytica Chimica Acta. 7–16.

11.Danksagung

Ich bedanke mich ganz herzlich bei

meinem Verlobten Alejandro ♥	für seine liebevolle Unterstützung, seine Geduld und motivierenden Zuspruch sowie fachlichen Austausch.
seiner Mutter Dr. Gabriele Müller de Cornejo	die uns in den letzten Jahren immer und besonders beim Umzug nach Berlin unterstützt hat.
meinen Freunden Jennifer Hansen, Max Boßeler und Dr. Mira Woitok	für ihre offenen Ohren und liebevollen Zuspruch.
meiner Kollegin Dr. Eva Trojnar,	auf die ich immer zählen konnte und die mir in den letzten 3 Jahren stets mit Rat und Tat zur Seite stand.
meinem Onkel Dr. Olaf Bartsch und seiner Frau Dr. Sabine Langheinrich-Bartsch	die mir während des Studiums unter die Arme gegriffen und mich beruflich inspiriert haben.
meinem Betreuer Prof. Dr. Reimar Johne	für seine wissenschaftliche Anleitung während der Etablierung unserer Methoden, gute Zusammenarbeit, das geduldige Lesen und Korrigieren meiner Publikationen, Präsentationen und Doktorarbeit sowie für eine großartige wissenschaftliche Ausbildung.
meinem ehemaligen Vorgesetzten Prof. Dr. Lüppo Ellerbroek	für sein positives Feedback und motivierenden Worte und dafür mir wissenschaftliches Arbeiten außerhalb des Labors ermöglicht zu haben.
meinen aktuellen und ehemaligen Kollegen/-innen, Silke Apelt, Anja Schlosser, Dr. Carolina Plaza-Rodriguez, Matthias Filter, Dr. Christina Schrader, Dr. Kathrin Szabo, Dr. Michael Buhrwinkel und Mai Dinh-Tran,	für eine hervorragende Zusammenarbeit, für ihren methodischen und wissenschaftlichen Beitrag, für die Aufwertung und Auswertung meiner Forschungsergebnisse durch mathematische Analysen, für die zur Verfügungstellung von interessantem Testmaterial und für die Zusammenarbeit bei unseren Publikationen.
sowie bei den weiteren Beteiligten an unseren Veröffentlichungen, Dr. Dirk Höper, Prof. Dr. Dietrich Mäde, Dr. Christiane Berg, Prof. Dr. Rupert Mutzel	
meinem Arbeitgeber, dem Bundesinstitut für Risikobewertung	dafür mir den Besuch von Konferenzen ermöglicht und meine wissenschaftliche Ausbildung vorangetrieben zu haben.

12. Eidesstattliche Erklärung

Hiermit erkläre ich, dass ich diese Arbeit selbst verfasst habe sowie keine anderen als die angegebenen Quellen und Hilfsmittel in Anspruch genommen habe. Ich versichere, dass diese Arbeit in dieser oder einer anderen Form keiner anderen Prüfungsbehörde vorgelegt wurde.

Christina Bartsch, Berlin Juni 2018

13.Curriculum Vitae

Der Lebenslauf ist in der Online-Version aus Gründen des Datenschutzes nicht enthalten.

Der Lebenslauf ist in der Online-Version aus Gründen des Datenschutzes nicht enthalten.